Liquid Crystal Polymer Brushes and their Application as Alignment Layers in Liquid Crystal Cells

Dissertation

zur Erlangung des akademischen Grades

"Doktor der Naturwissenschaften"

im Fachbereich

Chemie und Pharmazie der

Johannes Gutenberg-Universität Mainz

vorgelegt von

Bin Peng

geboren in Yiyang, China

Mainz 2000

Contents

List of Abbreviations and Symbols

6PB7	(4-hexanoxy)benzoic acid-4´-heptanoxyphenyl ester
A6	4-(6-propenoyloxy)-hexanoxybenzoic acid-4´-methoxyphenyl ester
A6PB4	4-(6-propenoyloxy)-hexanoxybenzoic acid-4´-butanoxyphenyl ester
A6PB6	4-(6-propenoyloxy)-hexanoxybenzoic acid-4´-hexanoxyphenyl ester
ADCS	“azodichlorosilane”, 4,4´-azobis-[4-cyanopentanic acid-(3´-chloro-dimethylsilyl) propylester]
AIBN	4,4´-azobis(isobuytronile)
AMCS	“azomonochlorosilane”, 2´,4-azo-(2´-cyanopropyl)-[4-cyanopentanic acid -(3´´-chlorodimethylsilyl)propylester]
a. u.	arbitrary unit
c, C	crystal(line)
ca.	circa
CRS	crystal rotation setup
d	film thickness
deg.	Degree (°C)
DMOAP	dimethyloctadecyl [3-(trimethoxysilyl) propyl] ammonium chloride
DP	degree of polymerization
DSC	differential scanning calorimetry
d_{theo}	theoretically calculated film thickness
f	initiator coefficient
Fig.	Figure
FTIR	Fourier transformation infrared spectroscopy
g	glass
g	gram
GPC	gel permeation chromatography
h	hour(s)
i, I	isotropic

[I]	initiator concentration
IR	infrared
k_d	rate constant of initiator decomposition
k_p	rate constant of chain propagation
k_t	rate constant of chain termination
L	liter(s)
LC	liquid crystal(line)
LCP	liquid crystalline polymer(s)
Lit.	Literature
LMW	low molecular weight
[M]	monomer concentration
M6	4-[6-(2-methyl-propenoyloxy)-hexanoxy]benzoic acid-4´-methoxyphenyl ester
min	minute(s)
ml	milliliter(s)
M_n	number-average molecular weight
MPI-P	Max-Planck-Institute for Polymer Research in Mainz
mW	milliwatt
M_w	weight-average molecular weight
n, N	nematic
n	refractive index
N_A	Avogadro constant
n_e	extraordinary index of refraction
NEt_3	triethylamine
NMR	nuclear magnetic resonance
n_o	ordinary index of refraction
p	p-polarization (parallel to the incidental plane)
PA6	polymer of A6
PM6	polymer of M6
PMMA	poly(methyl methacrylate)
ppm	part(s) per million

rpm	rotation per minute
s, S	smectic
s	s-polarization (perpendicular to the incidental plane)
SPS	surface plasmon spectroscopy
t	time
T	temperature
tech.	technical (purity grad)
T_g	glass transition temperature
TGA	thermal gravitivity analysis
THF	tetrahydrofuran
T_{NI}	nematic-isotropic transition temperature
T_{SN}	smectic-nematic transition temperature
ZLI	code for liquid crystals from the company Merck

α	pretilt angle of LC molecules
δ	chemical shift
ρ	number density of disclination
Γ_D	grafting density
γ	surface tension
γ_S	surface tension of substrate
γ_{LC}	surface tension of liquid crystal
ξ_d	average domain size of nematic texture
ρ	polymer density
ψ	angle of incidental beam

List of Figures

1 Introduction

1.1 Liquid Crystals and Liquid Crystalline Polymers

Liquid crystals

Liquids and crystals are the most abundant condensed matter phases in nature. The essential difference between these phases is that the molecules in a crystal possess long-range three dimensional order whereas in a liquid they do not. The molecules in a crystal are usually ordered concerning both their positions and orientations. The molecules in liquids, in contrast, diffuse throughout the sample with the molecular axes tumbling randomly. There are several phases, nevertheless, which show more order than present in liquids but less order than typical of crystals. These phases are called liquid crystalline (LC) phases since they share properties normally associated with both liquids and crystals. Another name for this phenomenon is mesomorphic phases where *mesos* is a Greek word meaning “middle” [Coll97].

The molecules in the LC phases diffuse about much like the molecules in a liquid, but they maintain some degree of orientational order and sometimes some positional order as well. There are three types of liquid crystalline phases: *nematic*, *smectic* and *columnar* phases [deGe93]. In a nematic phase the molecules have a high degree of long range orientational order, but no long range transitional order. The molecular axes tend to point along a preferred direction as the molecules undergo diffusion. This preferred direction is called the director or the easy axis of the molecules in the nematic phase. A smectic phase can be viewed as a set of two-dimensional liquid layers stacked on each other with a well defined spacing. A columnar phase can be described as a two-dimensional array of liquid tubes. Many monographs on liquid crystals have been published [Chan92, deGe93, Coll97].

Liquid crystalline molecules have typically a rod-like shape (i.e. one molecular axis is much longer than the other two). The axis along the rod is called the “long axis” of the molecule, while the other two are called “short axes”. The molecules are therefore symbolized as oval objects as those depicted Fig. 1-1. In the nematic phase the molecules are randomly positioned, but their long axes tend to point to a preferred direction (Fig. 1-1a). If we look at such a single nematic molecule, there are three refractive indices depending on the directions with respect to the long axis of the

molecule (Fig. 1-1b): the extraordinary refractive index n_e is that which is parallel to the long axis of the molecule and the ordinary refractive index n_o is that which is perpendicular to the long axis. The two ordinary refractive indices are the same due to the symmetry of the molecule in the direction which is perpendicular to the long axis (Fig. 1-1b). This kind of liquid crystalline substance at which two of the three refractive indices are the same is called uniaxial liquid crystal.

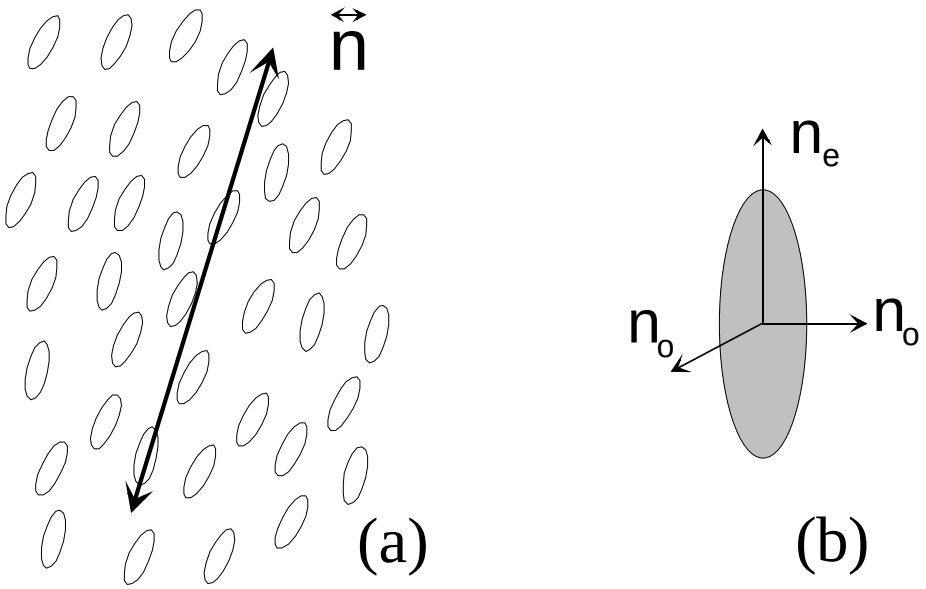

Fig. 1-1: *Schematic depiction of (a) the arrangement of nematic liquid crystalline molecules with a preferred direction n of the molecular long axis. (b) The three refractive indices of the LC molecules: the extraordinary index n_e which is parallel to the long axis and the two ordinary indices n_o which are perpendicular to the long axis.*

Many LC substances can exhibit more than one LC phase. Beginning at low temperature at which an LC substance is in the crystalline state, the substance will pass through the liquid crystalline phase(s), and finally the isotropic phase where the substance is a liquid. For substances that exhibit more than one LC phases, the smectic phase shows up at lower temperatures because it is more ordered than a nematic phase. The temperatures at which two phases are in equilibrium are called phase transition temperatures which are important physical parameters for the LC substance.

To denote a phase transition temperature, the letter T together with an index indicating which two phases are in equilibrium is used. For example, T_{NI} is a nematic-isotropic transition temperature. An alternative description of the phase transition temperatures is to use a one letter abbreviation for the phases involved and with the phase transition

temperature between them. The latter expression creates a way to indicate the comprehensive transition temperatures in a brief way. An example of such a transition sequence of an LC substance can be described as:

c 30.8 s 97.3 n 123.0 i,

which is for a polymer that will be described in detail in §4.3. In the transition sequence, c stands for crystalline, s for smectic, n for nematic and i for isotropic phases. The numbers between two phase states are the phase transition temperatures in degree centigrade of these two neiborning phases.

Liquid crystalline polymers

Liquid crystalline polymers (LCP) are high molecular mass materials which exhibit mesomorphic phases. There are traditionally two major classes of LCP, the so-called main chain and side chain types, depending on whether the mesogenic units are in the main chain or side chain, respectively [Demu98]. These two types of LC polymers are schematically drawn in Fig. 1-2.

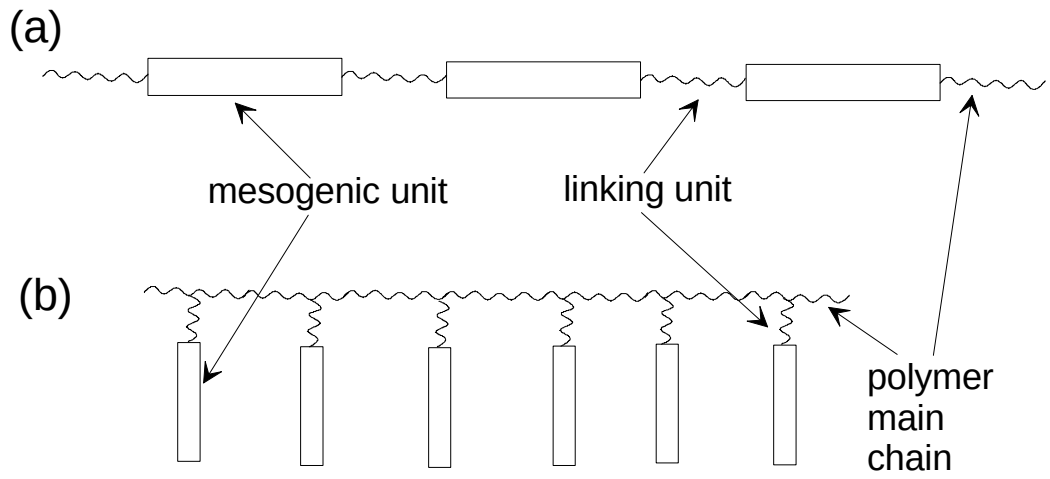

Fig. 1-2: *Schematic drawing of the main chain (a) and the side chain (b) liquid crystalline polymers with the mesogenic units in different locations.*

Although there exists a large variety of possibilities to select the mesogenic groups, the flexible linking units and their combinations, most of the thermotropic main chain LC polymers actually investigated are polyethers [Skor93, Grei98, Chie98]. The primary method of their synthesis is polycondensation, in some cases polyaddition. The presence of the mesogenic units composed of usually unsubstituted benzene rings directly in the main chain gives rise to strong intermolecular interactions among the polymer chains. The melting point of the main chain LC polymers is therefore very high and their LC

states can only be observed at even higher temperatures. The solubility of these polymer substances is usually poor, and becomes worse with increasing length of the polymer chains. The main chain LC polymers have found their commercial applications in the production of strong fibers, for example Kevlar (Du Pont) [Chie98].

In side chain LC polymers, the flexible polymer backbone has a strong tendency to adopt a random, coiled conformation, while arrangement of the mesogenic units can result in an LC phase. When the mesogenic units are attached to the polymer backbone directly, however, the dynamics of the backbone usually dominate the tendency for the mesogenic groups to orient anisotropically. Accordingly, mesomorphic behavior is not generated for these polymers. Earlier work on side chain LC polymers were mainly carried out on these kinds of substances [Blum78]. In the next subsection, a concept with a spacer between the side chain and the main chain will be introduced and discussed.

Side chain liquid crystalline polymers

Systematic investigations on side chain LC polymers began to flourish only after Ringdorf and co-workers proposed that a flexible spacer should be inserted between the polymeric main chain and the mesogenic side groups to decouple the random motions of the polymer backbones due to statistical chain conformation and the anisotropic orientation of the side chains owing to their liquid crystalline features [Fink78]. The presence of the spacer makes it possible to restrict or hinder the influence of the main chains so that mesophases generated from arrangements of the LC units in the side chains can be exhibited [McAr89].

A general chemical structure of the side chain LC polymer molecules can be drawn in Fig. 1-3. The polymer backbones usually consist of substituted carbon-carbon chains (acrylates or methacrylates), although much work on polysiloxanes as the backbones has also been carried out [Gray89]. The mesogenic unit composes of two benzene rings which are connected to form rigid rod-like conformation. The LC unit is linked to the polymer backbones through a flexible alkyl chain, the spacer, whose decoupling behavior enables the exhibition of arrangement of the mesogenic units under certain circumstances (e.g. temperature) into LC phases. Examples for the linking groups and symbols in Fig. 1-3 can be the following:

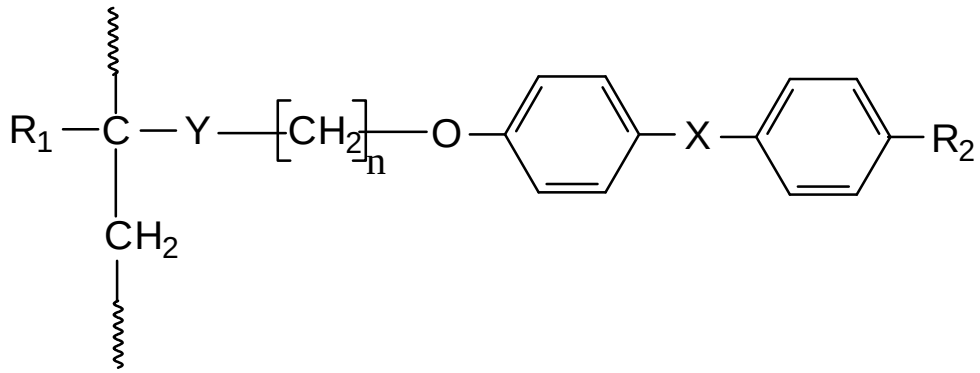

Fig. 1-3: *General chemical structure of the side chain liquid crystalline polymers. The mesogenic unit consists of two benzene rings connected together to form a rigid rod-like conformation. Details on the groups R_1, R_2, X and Y are explained in the text.*

R_1 = H, CH_3;

Y = — COO —, — OOC —, — CONH —, — O —;

n = 0 — 20;

X = — COO —, — OOC —, — N=N —, — N(O)=N —, — CH=N —, — (direct connection);

R_2 = — C_nH_{2n+1}, — OC_nH_{2n+1}, — C_6H_5, — C_6H_4 — O — CH_3, — CN.

Side chain liquid crystalline polymers: two examples

Two kinds of side chain LC polymers have been intensively investigated since the introduction of the spacer concept [Fink84, Shib84]. Figure 1-4 depicts the general chemical structures. Both polymers have (meth)acrylate esters as the main chains. The corresponding monomers undergo readily radical-chain polymerization to give the LC polymers, the mechanism of which has been very well investigated [Mark85].

For the LC units, the two benzene rings are either connected by an ester group, resulting in a phenyl benzoate (Fig. 1-4a), or directly connected to each other forming a biphenyl (Fig. 1-4b). The mesogenic side groups are linked to the polymer main chain through a flexible alkyl chain consisting of several methylene units. Most of the derivatives that have the phenyl benzoate group as the mesogenic core as depicted in Fig. 1-4a exhibit mesophases in spite of the large variations of *p*-and *p´*-substituents [Fink84]. The end group in Fig. 1-4a can be varied finely to tune the properties such as the LC temperature range of the substances. LC polymers with cyano-biphenyl side chains as depicted in Fig.1-4b show a pronounced birefringence (Δn) due to the cyano group attached to the

benzene ring as the end group. This type of side chain LC polymers, therefore, possesses specific electro-optical properties [Shib84].

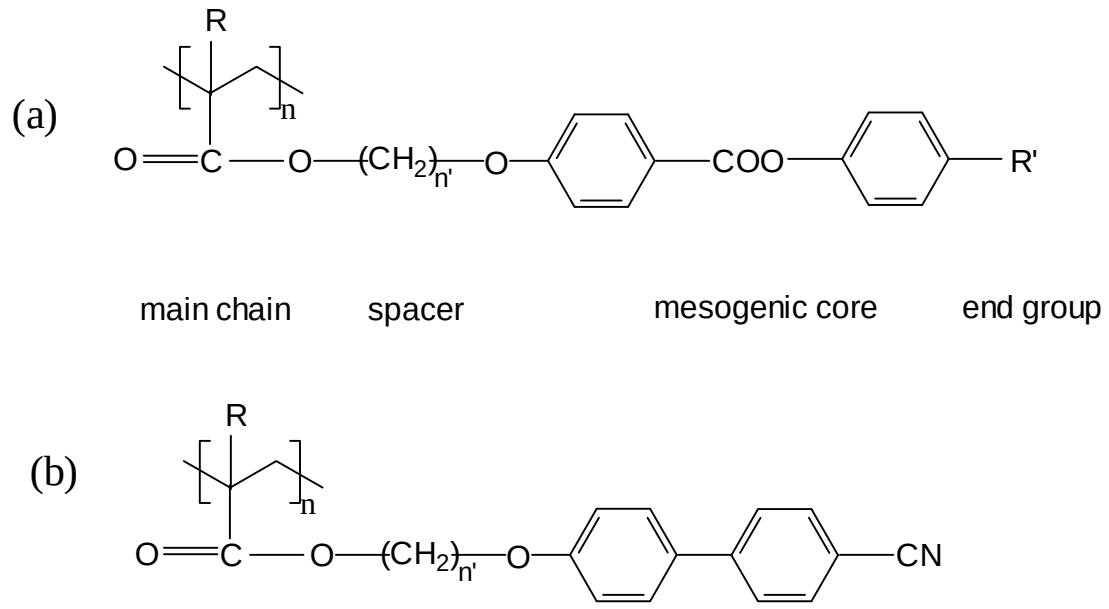

Fig. 1-4: *Side chain liquid crystalline polymers with (meth)acrylate main chain and mesogenic cores of a) phenyl benzoate, b) cyano-biphenyl in the side chains. R = H or CH_3; n' = 2 - 11, R´= OC_mH_{2m+1} or C_mH_{2m+1}, m = 1 - 9.*

The molecular weights of the side chain LC polymers depicted in Fig. 1-4a have been reported to be as high as 400 000 [Port81]. The nematic as well as the smectic LC phases have been observed for these polymers. Usually, the transition temperatures T_{CS} (crystal-smectic), T_{SN} (smectic-nematic), and T_{NI} (nematic-isotropic) increase with increasing molecular weight. When the molecular weight exceeds a certain critical value, however, this effect levels off and increasing the molecular weight does not further influence the transition temperature any more [Kost82].

Phase behavior of side chain LC polymers mixed with low molecular weight (LMW) nematic LC of similar structures

The miscibility of binary mixtures from low molecular weight (LMW) liquid crystals have been extensively studied [Kelk80]. The results of these investigations always obey the rule of Arnold and Sackmann [Arno60], according to which LC substances which have similar structures are miscible over the whole range of concentration.

Finkelmann and co-worker studied the phase behavior of side chain LC polymers mixed with LMW nematics of similar structures [Fink82, Bent85]. They have found that the presence of the LMW component reduces the glass transition temperature of the pure polymer (plasticizing effect), and that the addition of the LC polymer suppresses the crystallization of the LMW nematic. Both effects broaden the nematic phase region [Fink82]. Phase separation in the isotropic and in the nematic phases has also been observed in spite of the fact that the LC side chain polymer contains the same mesogenic moiety as the LMW component. The appearance of such miscibility gaps strongly depends on the chemical structures of the LMW nematic molecules. Increasing the alkyl chain length in the end groups of the LMW component, for example, reduces the miscibility with the LC polymer. The authors have concluded that not only the chemical constitution but also sensitive packing effects of the components determine the miscibility behavior [Bent85].

1.2 Surface Anchoring and Alignment of Nematic Liquid Crystals

1.2.1 Anchoring of Liquid Crystals at the Interface

Anchoring and alignment of nematic liquid crystals at an interface

When a nematic liquid crystal is placed in contact with another phase, an interface is created. The presence of this interface induces a perturbation of the nematic order close to it and results in certain orientations of the surface molecules. The orientation behavior of the molecules right at the interface might be different from that in the bulk and an interfacial region can be characterized in such cases (Fig. 1-5) [Jérô98].

At a distance away from the surface larger than the thickness of the interface, nematic order is recovered. The space symmetry is broken due to the presence of the surface and the orientation of the nematic phase can no longer be arbitrary. Its orientation is determined by the surface. The phenomenon that the macroscopic orientation of a nematic liquid crystal is determined by a surface is called surface anchoring of the nematic LC at the interface (Fig. 1-5).

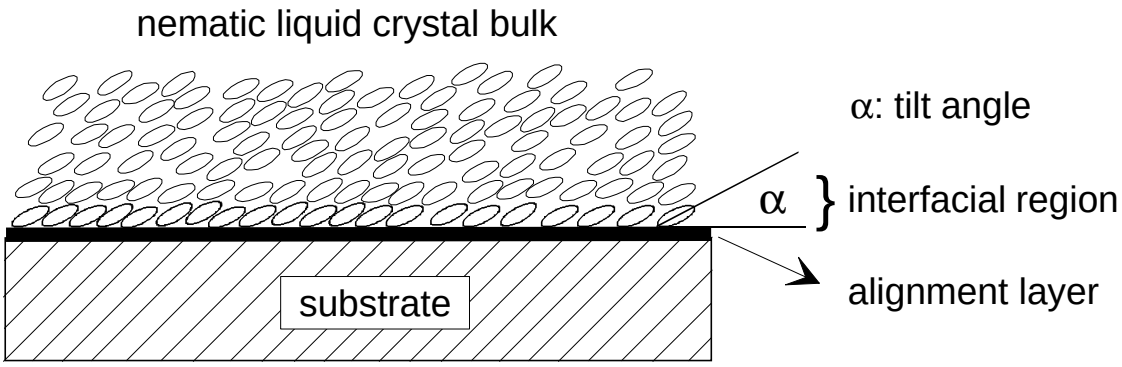

Fig. 1-5: *Schematic drawing of the anchoring and the alignment of nematic liquid crystals in contact with a substrate. The orientation of the first monolayer(s) at the surface determines the alignment of the nematic molecules in the bulk (surface anchoring with a tilt angle of a).*

Alignment of LC molecules

A uniform orientation of the nematic molecules is a prerequisite to build high-contrast LC-displays. The electro-optical performance of the majority of the LC-displays such as twisted nematic, supertwisted nematic, and ferroelectric liquid crystal displays depend strongly on the surface alignment of the LC molecules [Baha90]. As a matter of fact, one of the criteria for optimal performances of such displays is the homogeneous, defect-free alignment of the LC molecules. Great attention has been devoted to the development of techniques to get such homogeneous alignment of the nematic molecules and to the investigation of the anchoring mechanism of various alignment-assisting layers. Many reviews have appeared on this topic [Cogn82, Yoko88, Faet91, Jérô91, Uchi92, Jérô98].

At a nematic/substrate interface as depicted in Fig. 1-5, the tilt angle α is defined as the angle between the easy axis of the nematic molecules and the plane of the substrate surface. Depending on the tilt angle, the alignment of the nematics can be categorized in three major groups:

a) planar (parallel) alignment, when the easy axis is parallel to the plane of the surface. The tilt angle is $\alpha = 0°$ in this case.

b) perpendicular (homeotropic) alignment, where the easy axis is vertical to the surface. The tilt angle is $\alpha = 90°$ in this case.

c) tilted (pretilt) alignment, when the easy axis is at any angle between the two extremes ($0° < \alpha < 90°$).

For optimum operation of LC displays, non-zero, non-vertical tilt angles of the LC director are needed [Baha90]. This is particularly important for super-twisted nematic LC displays where pretilt angles of more than 10° are required. Although parallel and homeotropic alignments of nematic molecules ($\alpha = 0°$ and 90°, respectively) with good reproducibility have been successfully realized by various alignment assisting layers [Cogn82], the introduction and the control of high pretilt angles ($\alpha > 10°$) remains a challenge for further research [Jérô98].

1.2.2 Methods for Homogeneous Alignments of Liquid Crystals

General methods to generate homogeneous alignments

The first attempt to align LC molecules goes back to the early years of the last century. Mauguin [Maug11] produced an aligned liquid crystal layer by sandwiching a *p*-azoxyanisole nematic between two glass plates, the surfaces of which had been rubbed in one direction with a piece of paper. Since then, scientists have been attempting to understand the methods and the mechanism of alignment and orientation of liquid crystalline molecules.

Broadly speaking, there are two ways to orient liquid crystals. One way is to treat the surface of the substrate in a certain way and then bring the LC into contact with the substrate, and the other way is to apply an external field (electrical or magnetic field, flow, etc.) on the bulk LC. Surface treatments can be further divided into two major groups: mechanical treatment (e.g. rubbing) and deposition of molecules that assist alignment (e.g. surfactants, polymers) on the substrate. These two techniques of treatment are also applied together [Soni95].

Mechanical treatments of surfaces

Mechanical treatment of a substrate is often used to obtain a homogeneous planar or tilted orientation of liquid crystals. Many different techniques were tested such as: rubbing, high-speed buffing, mechanical abrasion, chemical milling, ion milling, high vacuum sublimation at oblique angles, and laser milling. The types of materials used to create the effects include such substances as polyesters, cellulose, cellulose acetate, nylon, alumina, diamond, silicon monoxide, magnesium fluoride, and silicon carbide [Cast83].

One of the most prominent techniques for the mechanical treatment of surfaces is rubbing the substrate in one direction in a homogeneous way. Materials such as pieces of cloth, paper and other textile materials [Cogn82], or Teflon [Witt91, Lest95] have been used to rub the substrates.

Organic alignment layers: surfactants

Another way to treat the surface to produce desirable anchoring properties is to cover the substrate with certain organic substances. A large variety of substances such as surfactants and polymers have been deposited on glass substrates to investigate their orienting properties. The techniques to create these alignment layers include spraying, roller coating, spin-coating, dipping, Langmuir-Blodgett films, offset printing, sputtering, high-vacuum sublimation (evaporation), and even chemical reaction at the surface.

The covering of a surface with a layer of surfactant is a very effective way to achieve homogeneous alignment for LC molecules [Cogn82]. A typical surfactant molecule consists of two parts: a hydrophilic (often polar) head and a hydrophobic hydrocarbon tail. These substances are called amphiphilic due to the different relations of the parts of their molecules to water. Among the great number of surfactants, there are two samples that are often used [Cogn82, Feat91]:

a) DMOAP (dimethyloctadecyl-[3-(trimethoxysilyl)-propyl] ammonium chloride);

b) lecithin of natural egg.

Organic alignment layers: polymers

In the literature, mainly in patents, almost all basic types of polymers have been suggested as special layers for liquid crystal orientation in LC displays. The most popular method to obtain such layers is to spread a polymer solution on a surface, evaporate the solvent, cross-link the polymer, if needed, and finally rub the polymer layer. Various polymer films have been prepared in this way. For instance, polystyrene and its derivatives, polyvinyl alcohol, polyarylates, esters and ethers of cellulose, polyesters, epoxide resins, polyurethanes, polysilicones and — most often — polyimides. Among the polymers investigated, rubbed polyimide polymer films have been studied most intensively for decades because the system has the advantages of simplicity in the thin film preparation, high chemical and thermal resistance, very good adhesion to glass and oxide surfaces, and the wide possibilities of influencing the alignment parameters by modification of the chemical structures [Chen89]. Cognard gave an extensive review of the alignment techniques for nematic LC molecules and

their mixtures, in which the anchoring properties of various polymer layers were also discussed [Cogn82].

Both main chain and side chain LC polymers have been spin-coated on substrates to investigate their alignment-assisting effects for LC molecules [Mura93, Raja96]. Results from scanning electron microscopy and atomic force microscopy observations revealed that the surface roughness of the main chain LC polymer film increased drastically after annealing because of recrystallization. Uniform orientation of nematic LC along the rubbing direction was observed on such films [Mura93]. Surfaces that generate high pretilt angles were realized by rubbing unidirectionally films of side chain LC polymer. It was also found that the morphology of these surfaces changed greatly at elevated temperatures, probably due to the interaction between the LMW nematic molecules and the polymers at high temperatures [Raja96].

Practical methods to generate desired LC alignments in industry and in research laboratories

Based on a literature review, Cognard has recommended some practical procedures to create reproducible, uniform parallel and homeotropic alignments of nematic liquid crystals and their mixtures for LC cells [Cogn82].

To generate a parallel alignment, the substrates are rubbed with a textile material. Firstly, a thin layer of polymers such as poly(vinyl alcohol) or polyimide is deposited on the substrate. Rubbed polyimide surfaces as alignment layers have been very often applied both in the industry and in research laboratories. The thickness of the film is typically around 100 nm. A diluted monomer solution of an acid anhydride and a polyamine is spin coated on a substrate and the resulting sample is dried at 80°C for 30 minutes. The soft pre-polymer is then rubbed with a soft material. Polymerization is carried out by curing in two steps: 130°C for 30 minutes followed by 200°C for 30 minutes.

Sandwiching nematic molecules between two DMOAP coated substrates is the easiest way to obtain a homeotropic aligned LC layer. A solution of DMOAP in a volatile solvent (e.g. alcohol) is used and the substrates are either spin-coated or dipped in the solution. The concentration is less important but the use of a dilute (1%) solution avoids the formation of spots. After the coating the substrates are treated at 80°C for 30 min. Uniform alignment is achieved with this technique for most liquid crystals. The LC molecules orient in a direction perpendicular to the substrate plane without any tilt (α = 90°). The alignment is thermally stable. With the same technique lecithin gives similar results.

1.2.3 Anchoring Mechanism

Anchoring mechanism of surfactants treated substrates

Creagh et al. investigated the mechanism of molecular alignment of nematic liquid crystals on solid substrates [Crea73]. They have found that the basic parameters which determine the alignment of the molecules are the surface tension of the substrate γ_S and that of the liquid crystal γ_{LC}. They called this observation the Friedel-Creagh-Kmetz (FCK) rule which simply states:

a): $\gamma_S < \gamma_{LC} \rightarrow$ homeotropic alignment

b): $\gamma_S > \gamma_{LC} \rightarrow$ parallel alignment

This simple semi-empirical rule has been widely supported by experimental data, although exceptions have also been observed [Cogn82, Faet91, Uchi92]. The criteria which determine the alignment types can be understood in the following way:

a) When the surface energy of the substrate is relative low, and the inter-molecular forces among the LC molecules are stronger than the forces across the interface, the longer axis of the nematic molecules is aligned perpendicular to the surface so as to maximize their intermolecular interactions.

b) In the case that the surface tension of the substrate is greater than that of the nematic, the forces across the interface dominates. Therefore, the surface free energy is minimized if the LC molecules are packed flat, that is, aligned parallel to the substrate.

A typical example of case (a) described above is the anchoring behavior at a substrate covered with a layer of surfactant molecules. In such a system, the hydrophilic head of the amphiphilic molecules are attached on the surface which has a relatively higher surface tension, and the hydrophobic hydrocarbon tails point towards the outside. Such a assembly of surfactant molecules dramatically lowers the surface tension of the substrate, which gives $\gamma_S < \gamma_{LC}$, and, therefore, homeotropic alignments [Cogn82].

Anchoring mechanism of rubbed surfaces

Rubbing can be carried out directly on a glass substrate or after deposition of a thin polymer film (e.g. polyimide). The purpose of rubbing is to break the in-plane isotropy of the substrate surface. Depending on the materials and the procedures applied for the

rubbing, different mechanisms may be operative in the alignment [Berr72, Cogn82, Faet91], which are:

a) shear induced crystallization of near-surface polymer regions;
b) formation of macroscopic grooves which induce an orientation along the grooves due to a minimization of the nematic bending energy;
c) transfer of elongated polymer chains or fibrils from the rubbing material to the substrate.

The three mechanisms have one point in common, that is, the presence of an anisotropy in the interface induced by the rubbing. The uniform alignment of the LC molecule is the result of the molecular arrangement according to this anisotropy on the substrate, be it the polymer crystalline regions, the grooves, or the elongated fibrils along the rubbing direction. Evidences related to the three mechanisms have been found by means of various experimental techniques like photomicrography and electron microscopy [Berr73].

1.3 Terminally Attached Liquid Crystalline Polymer Films as Alignment Layers

Alignment layers with adjustable pretilt angle

Alignment layers are key components for the production of LC displays. Designing alignment layers capable of generating any kind of bulk orientation is a formidable challenge for molecular engineering. The surfaces must not only themselves have a well-defined anisotropy according to which the LC molecules are oriented, in addition, they must be able to transfer this orientation into the adjacent nematic fluid and introduce uniform alignment.

Williams and Halperin have suggested to use LC polymers which are terminally attached on the surface of the substrate as alignment layers to induce orientation of LMW nematic LC molecules with adjustable, high pretilted angles [Halp93, Halp94, Will96]. In such systems, the LC polymer chains are covalently bound to the surface and the grafting density of the surface-attached chains is high enough, so that the overlapping between neighboring chains results in chain stretching away from the surface to a brush-like conformation. When such polymer chains are swollen in the LMW nematic medium, the chain conformation of the polymer molecules will induce a

certain orientation of the adjacent bulk liquid crystal phase. Interestingly, this orientation could be tilted because there might exist a competition between the orienting properties of the stretched polymer chains and those of the uncovered fraction of the substrate (Fig. 1-6).

Williams and Halperin considered main-chain LCP brushes on a polar substrate (e.g. glass). Figure 1-6 gives a schematic illustration of the situation. In this case, the bare substrate induces an alignment of the LC molecules parallel to the surface due to the high surface tension of the substrate. The polymer chains stretched away from the surface, on the other hand, favor perpendicular (homeotropic) orientation. The competition between these two effects could result in a tilt orientation of the bulk LMW nematic molecules and the pretilt angle can be tuned via the surface fraction uncovered by the polymer chains (grafting density of the polymer chains).

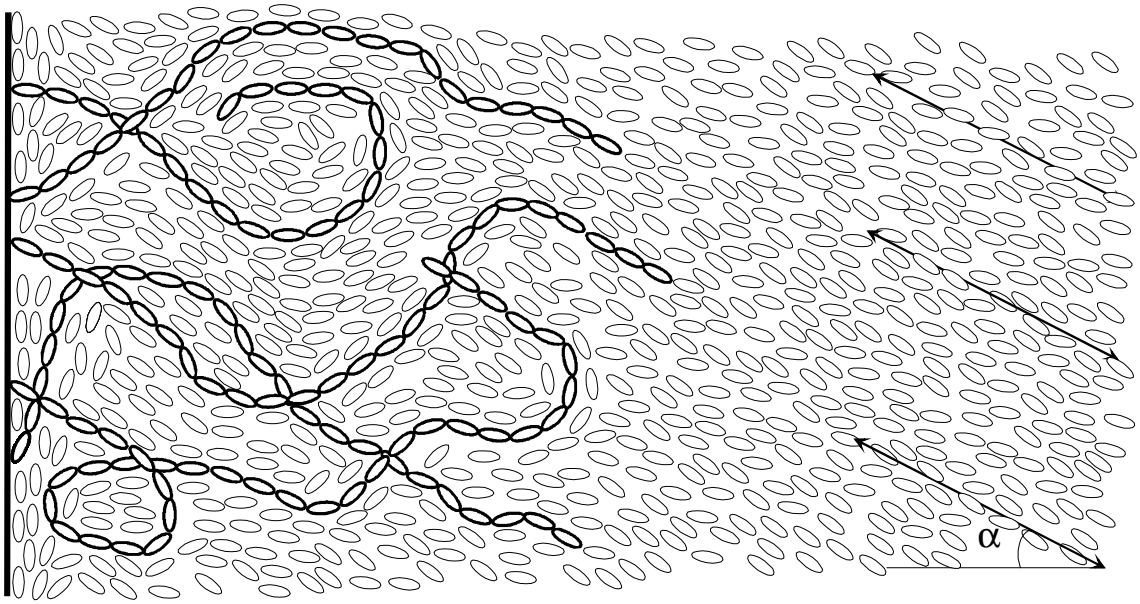

Fig. 1-6: *Schematic drawing of the adjustable alignment of low molar mass nematic molecules (thin ovals) by chemically-attached main chain liquid crystal polymer chains (connected thick ovals). The competition between the polymer chain stretching which brings about homeotropic alignment and the uncovered substrate surface which gives priority to planar alignment could result in an alignment of the bulk nematics with a tilt angle α which could be regulated by the grafting density of the polymer chains.*

Conformation of terminally attached polymer chains

Depending on the grafting density and the absorption enthalpy of the polymer with the surface, the conformation of polymer chains chemically bound on the substrate can be divided into three groups whose names have been coined by de Gennes [deGe76, Alex77, deGe80]:

a) "pancake" conformation, when the grafting density is low and the absorption enthalpy of the polymer chains to the surface is high;

b) "mushroom" conformation, when both the grafting density and the absorption enthalpy are low;

c) "brush" conformation, when the grafting density is high so that the distance between the attached polymer chains is smaller than the space needed for the polymer coils. Overlapping of the polymer chains results in a diffusion of the segments away from the surface and thus the chains stretch perpendicular to the surface. The stronger a chain is stretched, the smaller is the number of possible conformations, and the higher is the loss of entropy. The conformation of the brush chains depends strongly on the grafting density and the polymer molecular weight.

For the system suggested by Williams and Haperin, a pre-requisite for the use of surface-attached polymer films as alignment layers is that the grafting density should be high enough so that the stretching of the polymer chains can happen and induce the corresponding alignment of the adjoining LMW nematic molecules, that is, the attached polymer chains must have the brush conformations. A general introduction to the concept of polymer brushes and their preparation will be given in the following section.

1.4 Polymer Brushes: Terminally Attached Polymer Monolayers

Chemically attached polymer monolayers

Polymer films that are covalently attached on the surface of a substrate are highly desirable both in academic research and in industrial applications, not only because of their long-term stability against desorption, but also due to the fact that they can be treated with solvents and other reagents in order to study their swelling behavior without damaging the films [Rühe94].

In principle there are two major methods to create polymers which are chemically bound to the surface. One is the so-called “grafting to” technique which is based on reactions between (end) groups of polymer chains and functional groups on the substrate surface. The other method is to grow polymer chains *in situ* from initiators that are chemically attached to the surface. This technique is called “grafting from”.

For the “grafting to” technique there exist two major limitations. One of them lays in the low reactivity of long polymer chains so that only polymers with relative low molar mass must be used for the reaction. The other limitation is that when the surface is already covered with polymers, it becomes very difficult for other polymer chains to diffuse through the already attached polymer layer to the substrate for further reaction. Therefore, only relative thin films (8-10 nanometers) have been prepared by the “grafting to” technique [Flee93].

To overcome these intrinsic limitations, the “grafting from” technique has been developed [Laib75, Bove91, Pruc95], in which it is no more the reaction of the polymer itself but rather the polymerization from radicals generated from an initiator layer that is immobilized on the substrate. No diffusion problems will be encountered because only monomers have to diffuse for continuous reaction.

The first report on the “grafting from” system was by Hamann and Laible [Laib75], where terminally attached polystyrene was synthesized by radical polymerization *in-situ* from a layer of on the surface bound azo-initiator. Boven *et al* simplified the system by preparing the bound initiator layer in only two steps [Bove91]. Rühe and co-workers have systematically developed the “grafting from” concept, the essential details of which are given in the following subsection.

The “grafting from” technique

The “grafting from” technique bases on the idea to grow polymer chains from immobilized initiator molecules [Rühe94, Pruc95, Pruck98]. The concept is schematically drawn in Fig. 1-7.

The initiator molecule consists of three parts (Fig. 1-7): the anchoring group for the immobilization of the molecule on the surface; the cleavable group so that the formed chains can later be cleaved off for further analyses (e.g. determination of the molecular weight and the molecular weight distribution); and the initiating group from which radicals are formed to start the polymerization.

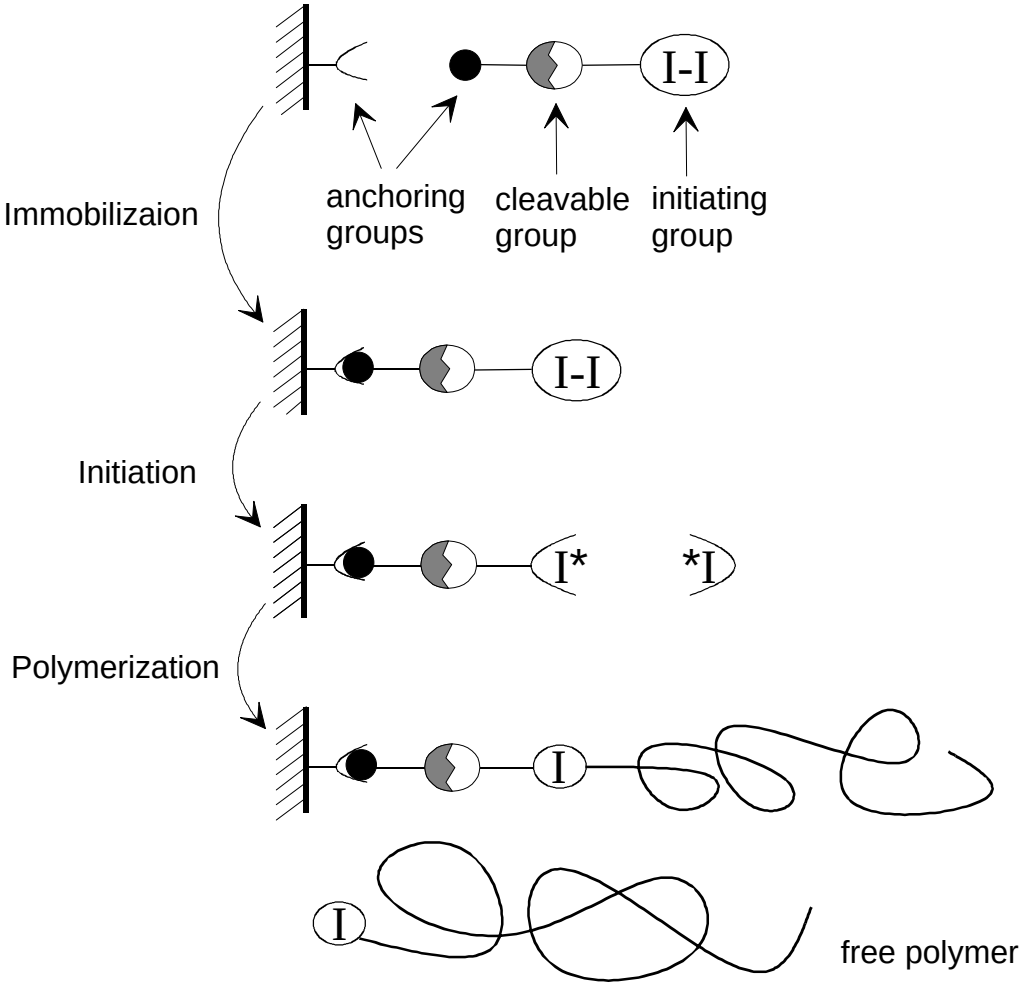

Fig. 1-7: *Schematic drawing of the concept of "grafting from" technique with which terminally attached polymers are prepared by in situ radical-chain polymerization using self-assembled monolayers of initiators covalently bound to the substrate surface. From the other half of a decomposed initiator molecule a polymer chain called a "free polymer" is generated at the same time during the polymerization in the solution.*

The propagation of a polymer chain takes place *in situ* from the immobilized radicals, which results in a brush chain that is covalently bound on the surface via the rest of the initiator molecule. The other half of the initiator can form a chain in the solution which is called a "free polymer". Usually, a solvent extraction is carried out after the reaction to wash away the free polymers that are physisorbed on the substrate in order to get pure samples.

Based on the “grafting from” technique, various polymer monolayers have been prepared and characterized [Rühe00]: polystyrene [Pruc95, Pruc98, Habi98], poly(methyl methacrylate) [Schi95, Schi98], polyelectrolytes [Bies99], and functional polymers based on active esters [Mura00].

Mechanistic studies of the “grafting from” systems showed that the radical-chain polymerization reaction induced by an initiator monolayer attached to a solid surface is comparable to radical-chain polymerization in solution. It has been concluded that the formation of the covalently attached polymer chains with high molecular weight and high grafting density can be achieved with this technique [Pruc98].

Although the brushes are monolayers, polymer films as thick as 2.2 µm have been obtained, the molecular weight of the attached chains can be as high as several millions gram per mole [Schi95, Sch98]. The thickness of the polymer films can be controlled by many parameters such as polymerization temperature, reaction time, monomer concentration, addition of additives, solvent types, and viscosity of the solution [Schi95].

2 General Goal

The goal of this work was to prepare polymer brushes with liquid crystalline side chains on planar glass substrates and to investigate their properties in the dry and swollen states. Subsequently to this, the homogeneity of the nematic textures and the alignment properties of the obtained monolayers were to be studied.

2.1 Polymer Brushes with Liquid Crystalline Side Chains as Alignment Layers

Chemically attached LC polymer films as alignment layers

In comparison to the conventional techniques such as rubbed polyimide layers, chemically attached films from LC polymers as alignment layers have a series of advantages:

a) The polymer chains are covalently bound on the substrate and show therefore superior stability as compared to polymer films which are physisorbed on the surface, especially at elevated temperatures.

b) The polymer brushes can be systematically modified by various parameters such as the grafting density, the molecular weight, copolymerization and a variety of different side chain groups.

c) The orientation of the mesogenic units in the polymer side chains can be influenced to obtain the desired arrangements by means of external fields (e.g. magnetic field, mechanical forces), anisotropy on the substrate surface, or cross-linking of the polymer backbones.

d) A single polymer chain is in contact with many LC molecules, the anchoring behavior is therefore supposed to depend more on the chain conformation than on molecular details. This property makes it possible to investigate the system with regard to theoretical aspects based on previous theoretical work on the conformation of attached polymer chains.

Although spin-coated films from main chain and side chain LC polymers have been used as alignment layers for nematic liquid crystals [Mura93, Raja96], a literature

survey showed that no attempts had been made to use terminally attached LC polymer films as alignment layers owing to the following reasons:

a) synthesis of the terminally attached LC polymer monolayers had not be so well developed;

b) polydomain textures have been observed from spin-coated films both with main chain and side chain LC polymers. The domain size is typically in the micrometer range, which is far away from the demands for the LC polymer films to be used as alignment layers, at which well reproducible LC polymer films with uniform alignment (monodomains) are required.

It has been reported that homogeneous domains were obtained by careful annealing of spin-coated LC polymer films [Noël98], they are nevertheless unsuited for the alignment due to the fact that the films peel off or could be otherwise damaged when being mixed with LMW nematic molecules, especially at elevated temperatures [Raja96]. This motivated the investigation and the use of chemically attached LC polymer films as alignment layers.

Side chain liquid crystalline polymer brushes as the alignment layers

Instead of the main chain LC polymer brushes proposed by Williams and Haperin [Halp93, Halp94], we considered to use side chain LC polymer brushes as the alignment layers because the latter have some key advantages over main chain LC polymer brushes in the following aspects:

a) The miscibility of side chain LC polymers with the corresponding LMW nematic is generally much better than that of main chain LC polymers. Due to the strong intermolecular interactions generated both from the possibility of alignment and the presence of polar groups, many main chain LC polymers tend to aggregate and pack tightly along the polymer chain direction. Many of them are crystals at room temperature and have very poor miscibility and solubility in LMW nematics, especially when the polymers have high molecular weight.

b) The synthesis of side chain LC polymer brushes is simpler. The synthesis of main chain LC polymers brushes are based on condensation reactions, while the side chain LC polymers brushes can be synthesized with the “grafting from” technique with which polymer brushes with high molecular weight and high grafting density have been obtained.

Profile at the brush/nematic interface

The use of side chain LC polymer brushes to generate tilt alignment of LMW nematics again relies on the competition of the alignment properties of the brush molecules and the underlying substrate. This time the mesogenic units are in the side chains, and the stretching of the main chain away from the surface will result in a parallel, not homeotropic, alignment of the nematic molecules. The bare substrate surface, as discussed before, favors a parallel alignment, too. Both parameters are expected to give rise to planar alignments. Therefore, the substrate has to be treated beforehand in a way so that after the treatment the surface will yield the property for a homeotropic orientation instead.

This idea was to pre-treat the substrate with a mixed solution of a surfactant and the initiator. The surfactant and initiator molecules are immobilized on the surface at the same time. Polymer chains can be grown from the initiator molecules. The surface fraction, where there are no polymer chains, is then covered with the surfactant molecules, with the hydrophobic tail pointing towards the outside. This kind of surface, as discussed in §1.2.3, greatly favors perpendicular alignment of the LMW nematic molecules. Therefore, an interface with competing alignment properties is created which is schematically illustrated in Fig. 2-1.

The grafting density of the polymer chains, or the surface fraction covered by the surfactant molecules, can be easily controlled through the surfactant to initiator ratio in the solution with which the substrate is modified previous to the brush growth. Theoretically, the bulk pretilt angle of the LMW nematic is expected to be adjustable by the grafting density.

2.2 Synthesis of Polymer Brushes with Liquid Crystalline Side Chains

The side chain LC polymer brushes were prepared according to the “grafting from” technique. Rühe and co-workers have prepared polymer brushes from various monomers based on this method. Side chain LC polymer brushes, nevertheless, had not been synthesized so far. The synthesis was carried out with very similar procedures, except for the new monomer in the polymerization step. Several parameters and elements related to the synthesis of the side chain LC polymer brushes are given in the following.

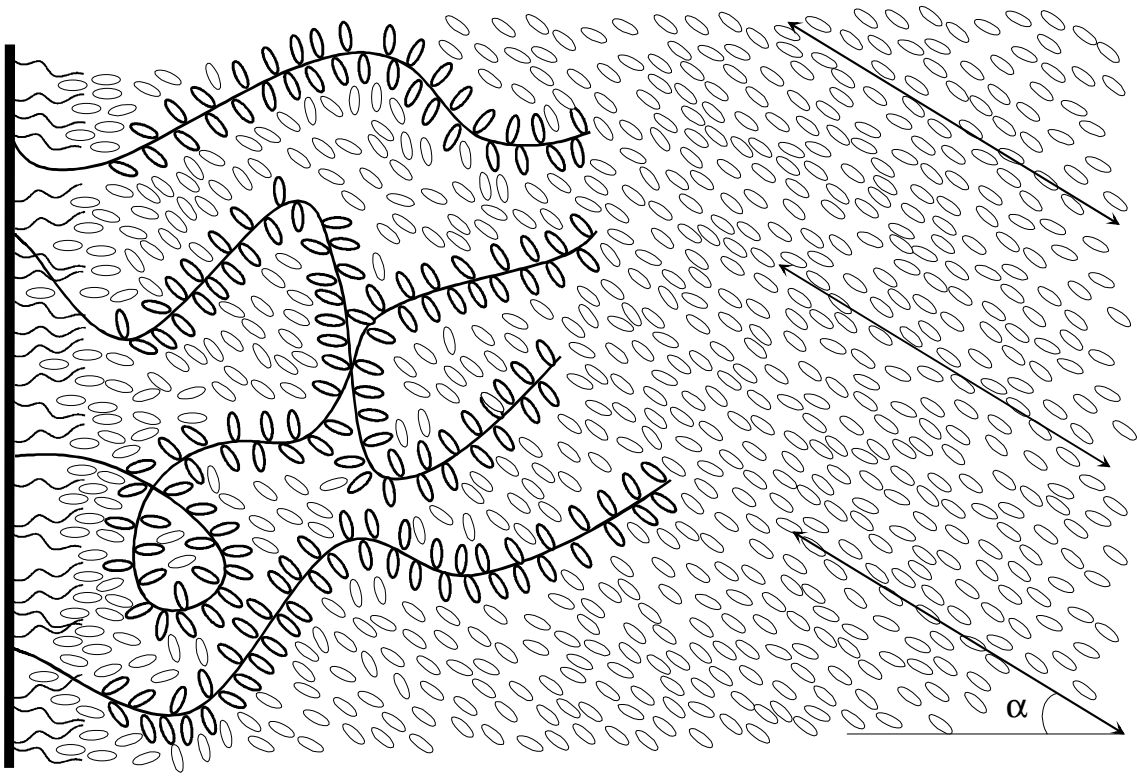

Fig. 2-1: *Schematic drawing of the side chain liquid crystalline polymer brushes (thick ovals representing the mesogenic side chains connected by thick lines as the polymer backbones) as alignment layers for low molecular weight (LMW) nematic LC molecules (thin ovals). Stretching of the polymer main chain influences the adjacent nematic molecules to an alignment parallel to the substrate, while the substrate surface, covered with amphiphilic molecules, prefers homeotropic orientation. Competition of the two orienting factors would result in a tilted alignment of the LMW nematics, the pretilt angle of which is theoretically predicted to be controllable through the grafting density of the brushes.*

The initiator

In this work, an azo initiator with the following structure (Fig. 2-2) was used for the brush preparation according to the “grafting from” technique.

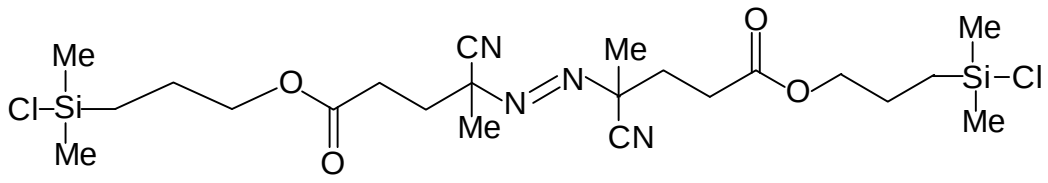

Fig. 2-2: *Chemical structure of the azo initiator for "grafting from" syntheses: **a**zo**di**chloro**s**ilane, shorted as ADCS.*

This symmetric azo initiator (abbreviated as ADCS) has been synthesized, systematically characterized and well established for the "grafting from" technique [Pruc95, Schi98]. The molecule consists of three parts:

a) the two chlorosilane end groups as the anchoring group which react with hydroxyl groups on glass substrates and thus immobilizes the initiator molecule to the surface;
b) the initiating part in the middle which has been designed according to the well-characterized initiator 2,2'-azo-bis(isobutytronitril) (AIBN);
c) an ester as the cleavable group which can be cleaved to remove the attached polymers from the surface for standard techniques of polymer characterization [Schi98].

The monomers

The selection of the monomers for the synthesis of side chain LC polymers in this work was made on the basis of the literature. The monomer depicted in Fig. 2-3 was chosen due to the fact that this type of side chain LC polymer had been very well characterized [Fink78, Fink84, Böel89, McAr89, Kann93].

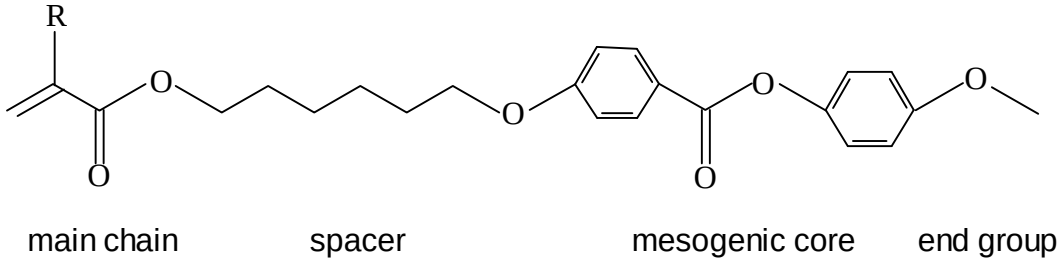

Fig. 2-3: *Chemical structure of the monomer used for the synthesis of the side chain liquid crystalline polymers. R = H or CH_3.*

The monomers belong to the type with the phenyl benzoate mesogenic core (Fig. 1-4a) and have six methylene units in the spacer and a methoxy group as the end group. They have been first synthesized by Finkelmann [Fink78] and Portgall [Port81]. The monomers undergo regular radical-chain polymerization in toluene with AIBN as the initiator. The corresponding LC polymers have molecular weights up to 400 000 g/mol. Both nematic and smectic LC phases have been observed with the LC polymers [Port82]. LC polymers with the same side chains and polysiloxane backbones have been found to have good miscibility with LMW nematics with similar structures over a wide range of concentrations [Funk82, Bent85]. Molecular order and motion of the polymers have been studied by nuclear magnetic resonance (NMR) spectroscopy [Boef89, Boef98].

Preparation of the side chain LC polymer brushes on glass substrates

The polymer monolayers were prepared according to the “grafting from” technique. A layer of the initiator ADCS is firstly immobilized on a glass substrate and an in-situ polymerization in the presence of the monomer is subsequently carried out to grow brushes on the substrate surface. In order to understand the polymerization mechanism of the LC brushes, it is essential to know the influence of the polymerization conditions on the final brush thickness.

Properties of the side chain LC polymer brushes

The final goal of this work was a thorough investigation of the liquid crystalline properties of the obtained brushes. The first central focus of this part of the study was the determination of the transition temperatures of these samples, especially on comparison to the behavior of thin spin-coated films of the same polymer. An interesting question is whether differences concerning the transition temperature between the bulk LC polymer and the LC brushes could be observed. Such differences could rise from the different polymer conformations in the two systems. Subsequently to this, it was also important to study the morphology of these films, i.e. to determine the size of the LC domains formed in these brushes. Here, the comparison of the nematic textures of the LC brushes to those from the spin-coated polymer films would also be of importance. For many practical applications, it is necessary to obtain textures with macroscopic sized domains. In the ideal case the whole sample should consist of one single domain. A very critical issue with regard to the possible use of side chain LC polymer brushes as alignment layers for LC displays is the question of the miscibility of the attached chains with a corresponding LMW nematic which would be used as the sandwiched substance in the LC cells.

Finally, should it be possible to create LC polymer brushes that form large domains (monodomains) and that are sufficiently miscible with a LMW nematic, it would be the most interesting challenge of this work to balance the alignment properties of the brushes and the underlying substrate such that the LMW nematic fluid of an LC cell is aligned at a desired tilt angle between 0° (planar alignment) and 90° (homeotropic alignment).

3 Syntheses and Characterization

3.1 General Remarks

The side chain liquid crystal polymers studied in this work consist of a phenyl benzoate mesogenic group which is attached via a flexible spacer to a methacrylate main chain. The chemical structure of the monomers is depicted in Fig. 2-3.

As a primary step, synthetic work was carried out based on techniques and methods in the literature. Firstly, the monomers were synthesized, and the corresponding polymers with various molecular weights were obtained by radical-chain polymerization. Subsequently, the LC polymer brushes were prepared according to the system developed by Rühe and co-workers (the "grafting from" technique), where an initiator layer was first immobilized onto a glass substrate and brushes were grown subsequently *in situ* from the surface [Rühe94, Pruc98].

The synthesized compounds were characterized with nuclear magnetic resonance (^{1}H- and ^{13}C-NMR). Their thermal properties were investigated with differential scanning calorimetry (DSC) and thermal gravitivity analysis (TGA). A qualitative characterization among the monomers, polymers and brushes was carried out with Fourier transformation infrared (FTIR) spectroscopy.

Surface plasmon spectroscopy (SPS) is an effective technique to measure the thickness of thin to ultrathin films on glass substrates [Knol91, Aust94]. Thickness of the brushes was measured with this technique. A series of brush samples were synthesized and the thickness was controlled by monomer and initiator concentrations.

In addition to the methacrylate monomer which is the main subject in this study, the acrylate counterpart which has the same mesogenic core and spacer in the side chain but with an acrylate backbone was also synthesized and polymerized. Brushes from this monomer were prepared and characterized in the similar way.

3.2 Synthesis of the Monomers

The chemical structure of the monomers with the phenyl benzoate mesogenic unit is given in Fig. 2-3. The IUPAC name of the methacrylate monomer is:

1-[[[6-[4-[(4-methoxyphenoxy)carbonyl]phenoxy]hexyl]oxy]carbonyl]-1-methyl-1,2-ethene.

In the following, **M6** and **A6** are used as the abbreviations for the methacrylate and acrylate monomers, respectively, where **M** stands for **m**ethacrylate, **A** for **a**crylate, and **6** is the number of the CH_2 units in the spacer. The polymers are correspondingly abbreviated as **PM6** and **PA6**, with **P** originating from **p**olymer.

Synthesis of the monomers was carried out according to a scheme developed by Ringsdorf and co-workers [Fink78, Port81, Port82]. The synthesis consists of three steps which can be briefly summarized as followed (Fig. 3-1).

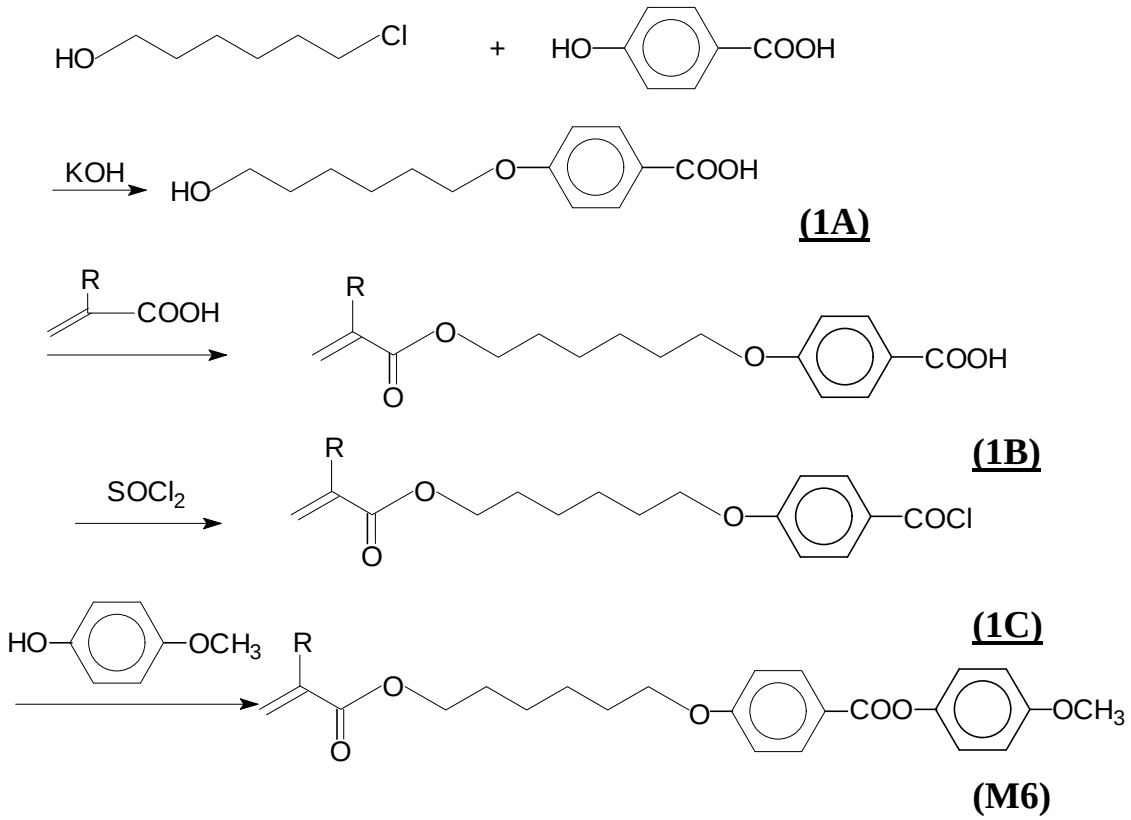

Fig. 3-1: *Schematic outline of the monomer systhesis. R = CH_3 for the monomer M6 and R = H for the monomer A6.*

Firstly, the flexible spacer was introduced through a Williamson etherification of 4-hydroxybenzoic acid and a linear 6-chlorohexanol which gave 4-(6´-hydroxy)-hexyloxybenzoic acid (**1A**). Next, the polymerizable double bond is introduced via subsequent reaction of (**1A**) with methacrylic acid for M6 (or acrylic acid for A6) in chloroform by an azeotrope esterification to get 4-(6´-(*2-methyl*)-propenoyloxy)-hexyloxybenzoic acid (**1B**). In the third step, (**1B**) was first transformed into the acid chloride (**1C**) by thionylchloride and then esterified with 4-methoxyphenol in the presence of triethylamine to give the raw product of the monomer (**M6**).

Impurities in the monomers were first removed by column chromatography. The weight ratio of the raw monomer to the silica gel was 1:80 and a solvent mixture (*n*-hexane : ethyl acetate = 5:2) was used as the eluent. The product from column chromatography was subsequently recrystallized from 2-propanol for the methacrylate monomer M6 (ethanol for the A6) several times until crystals were obtained.

It should be pointed out that the monomers themselves do not show liquid crystalline phases. Pure M6 forms regular white crystals with a melting point of 53-54.5°C (*Lit*. [Port82]: 53°C), and pure A6 forms slightly yellowish crystals which melts at 57-58°C (*Lit*. [Port81]: 63°C). After converted into polymers, however, LC phases show up.

3.3 Synthesis of the LC Polymers

Polymerization and purification

The LC polymers were synthesized by radical polymerization in solution, with 4,4’-azo-bis(isobutytronitrile) (AIBN) as initiator and dried toluene as the solvent. The reaction was carried out at 60°C under inert atmosphere, which was established by purging argon gas through the reaction tube for 10 minutes or more. In cases when the monomer concentrations were very low, freeze-thaw cycles were used to remove oxygen from the solution. The polymerization time varied from a few hours to one day.

The polymer was isolated by precipitation in *n*-hexane. After filtration, precipitation was repeated once again using a dichloromethane-methanol solvent pair. The polymer was finally dried in vacuum.

Molecular weight control of the methacrylate polymers

As will be discussed in chapter 5, LC polymers PM6 with different molecular weights were needed for the phase diagram studies. Initiator and monomer concentrations were varied to prepare polymers with different molecular weights [Elia99]. The preparation conditions of a series of PM6 polymers are summarized in Table 3-1.

Table 3-1: *Preparation conditions of the methacrylate LC polymers* [a)]

Polymer code	M6 concn. (mol/L) [b)]	AIBN (mol%)	Polymerization time (h)	Yield (%)
PM6-1	0.49	0.15	25.7	76.4
PM6-2	0.81	0.62	8.5	71.5
PM6-3	0.24	1.57	8.3	74.2
PM6-4	0.24	0.61	10.5	79.2
PM6-5	0.24	2.08	7.5	76.7
PM6-6	0.32	3.45	15.4	86.2
PM6-7	0.32	5.26	15.4	87.7
PM6-8	0.32	7.24	15.4	85.6
PM6-9	0.32	10.5	15.4	84.7
PM6-10	0.19	10.5	15.4	86.0
PM6-11	0.096	10.5	15.4	64.6
PM6-12	0.064	10.5	15.4	50.6
PM6-13	0.048	10.5	15.4	41.8

a) All polymerization were carried out at 60°C in toluene under inert atmosphere.

b) Monomer concentration: mole of M6 over volume of toluene in liter.

The number-average molecular weight, M_n, and weight-average molecular weight, M_w, of the LC polymers were determined by Gel Permeation Chromatography (GPC) with poly(methyl methacrylate) (PMMA) standards with narrow molecular weight distribution in tetrahydrofuran (THF). Table 3-2 lists the GPC results. The polymer samples were sorted according to the their GPC M_n data (from high to low).

The number-average molecular weight, M_n, of the bulk polymer samples ranges from 10 000 g/mol to 160 000 g/mol (Table 3-2), and the molecular weight distribution index,

M_w / M_n, from 1.8 to 3.8. In the literature, LC polymers with M_n between 65 000 g/mol and 380 000 g/mol have been obtained from the same monomer M6 [Port81, Port82].

Table 3-2: *Molecular weights of the methacrylate LC polymers* [a)]

Polymer code	M_n (g/mol)	M_w / M_n
PM6-1	160 400	2.83
PM6-2	156 100	3.85
PM6-3	80 300	1.79
PM6-4	79 000	3.15
PM6-5	56 500	2.27
PM6-6	33 100	3.40
PM6-7	26 900	3.31
PM6-8	22 200	3.50
PM6-9	17 900	3.36
PM6-10	14 400	2.71
PM6-11	10 900	2.16
PM6-12	9 400	1.84
PM6-13	9 200	1.68

a) Determined by GPC with PMMA standards with narrow molecular weight distribution in THF.

The molecular weight of a polymer obtained from free radical polymerization depends strongly on the initiator and the monomer concentration. When all other parameters are fixed, higher initiator concentration results in lower molecular weight polymer, whereas higher monomer concentration gives higher molecular weight polymer. When the chains are terminated by combination, the degree of polymerization (DP) is proportional to the monomer concentration [M] and to the inverse square root of the initiator concentration [I] [Bill84]:

$$DP = \frac{k_p}{\sqrt{f k_d k_t}} \frac{[M]}{\sqrt{[I]}} \qquad \textbf{(3-1)}$$

k_p, k_d and k_t are rate constants of chain propagation, initiator decomposition and chain termination, respectively, and f is the initiator coefficient.

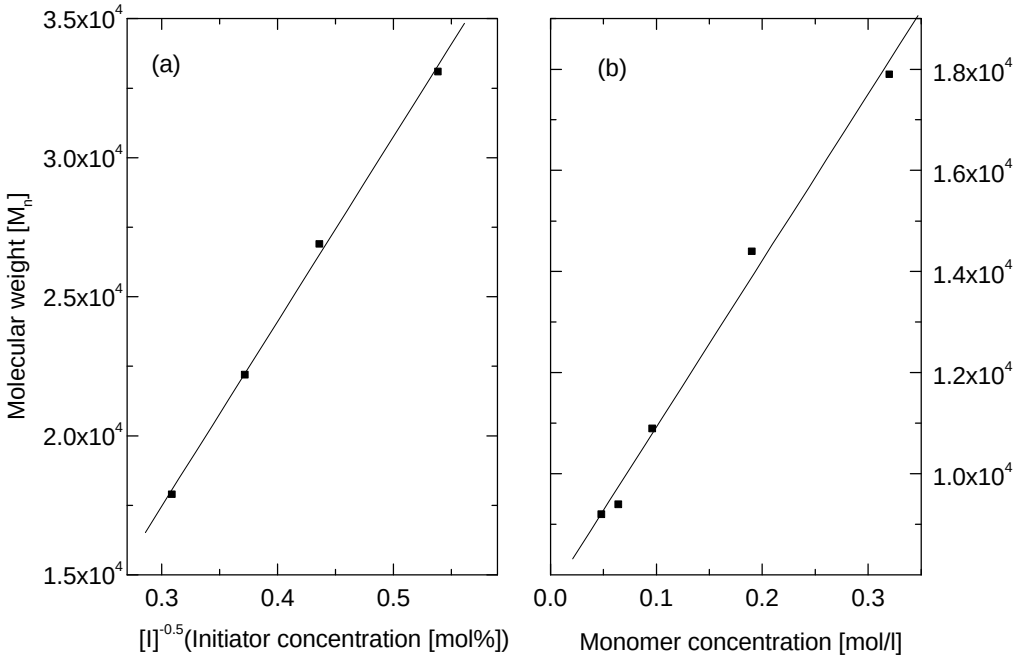

Fig. 3-2: *Influences of the initiator and monomer concentrations on the polymer molecular weight. Polymerization was carried out in toluene at 60°C for 15.4 hours with a fixed monomer concentration of 0.32 mol/l (a), or a fixed initiator concentration of 10.5 mol% (b). The straight lines are linear fittings based on the experimental points.*

Figure 3-2 shows the polymer molecular weight (M_n) as the function of the initiator concentration [I] and the monomer concentration [M]. Experimental data exhibit quite good linear relationships between the parameters M_n-$[I]^{-0.5}$ and M_n-[M], as expected according to Equation (3-1).

To check the validity of the molecular weight data obtained with GPC measurements using a PMMA calibration curve (Table 3-2), we also measured the molecular weights of two polymers by absolute methods, i.e. by static light scattering and vapor pressure osmometry. The results demonstrated that deviations from the GPC measurements are rather prominent at least for high molecular weights (Table 3-3). The GPC is a method based on the standards from other molecules and the results are therefore only relative values.

Table 3-3: *Comparison of the molecular weights determined by GPC with light scattering and vapor pressure osmometry*

Sample code	GPC [a]	Light scattering [b]	Vapor pressure osmometry [c]
PM6-3	M_w =143 500	M_w = 282 000	--
PM6-12	M_n = 9 400	--	M_n = 9 300

a) GPC data with PMMA in THF as standards.

b) Measured with light scattering in THF.

c) Measured with vapor pressure osmometry in THF at 30°C.

LC phase behaviors influenced by the polymer molecular weight

Liquid crystalline phase behavior of the synthesized methacrylate LC polymers with different molecular weights were investigated by measuring their N-I transition temperatures (T_{NI}) with an optical polarizing microscope (Fig. 3-3). A detailed description of the T_{NI} measurement follows in §4.3.

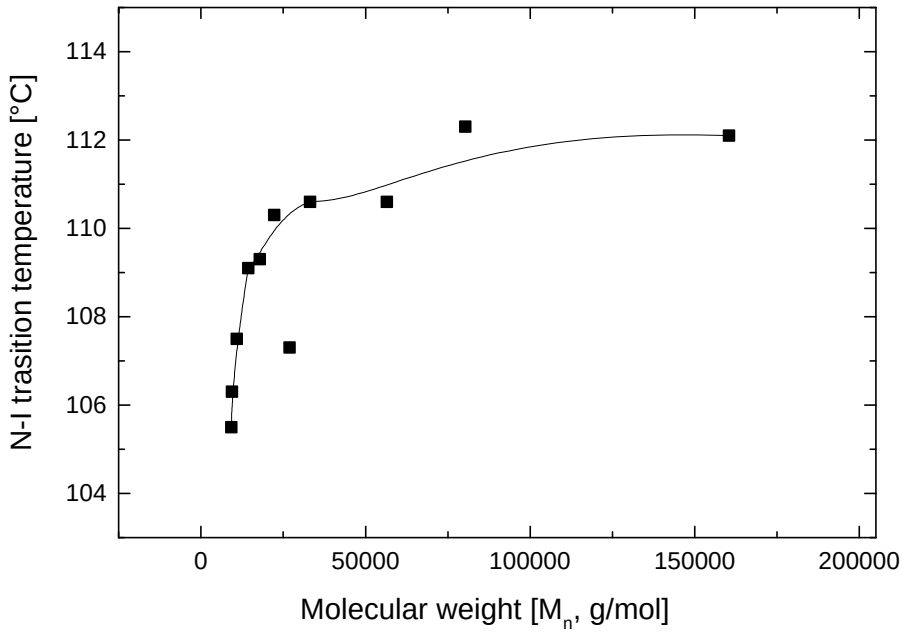

Fig. 3-3: *N-I transition temperature of the bulk LC polymers PM6 with various molecular weight. The critical M_n for the polymer is around 35 000 g/mol (resembling 85 repeating units).*

In a first consideration, it would have seemed that the N-I transition temperature should not depend on the length of the polymer main chain, i.e. on the degree of polymerization (DP), since the formation of the LC phase is predetermined by the interaction of the mesogenic groups in the side chains. However, at lower molecular weights, T_{NI} raises rapidly with increasing molecular weight, while at higher molecular weights the increase levels off and a constant value for T_{NI} is reached. For the PM6 system the critical molecular weight is about 35 000 g/mol which corresponds to a degree of polymerization of ca. 85 (Fig. 3-3).

Other side chain LC polymers show a similar behavior. A system with an acrylate main chain and a cyano-biphenyl mesogenic group in the side chain has been reported to show a similar increase of T_{NI} with increasing molecular weight. Also with this system a level-off effect of the T_{NI} is found when the degree of polymerization is above 240 [Shib84]. The authors contributed this molecular weight dependence of the T_{NI} to the intermolecular and intramolecular interactions of the mesogenic units. In the lower molar mass region, the LC phase is probably formed mainly due to intermolecular contacts of the side groups, which gives the dependence of T_{NI} on the DP. Exceeding the critical DP leads evidently to the predominance of intramolecular contacts and to a smaller number of defects, which are unavoidable when the mesophase is formed via intermolecualr contacts of mesogenic units [Shib84].

Synthesis of the acrylate polymer

An acrylate polymer from the monomer A6 was prepared the same way as with the methacrylate analog M6. The preparation conditions of the polymer PA6 and its molecular weights determined by GPC are listed in Table 3-4.

Table 3-4: *Preparation conditions and molecular weights of the acrylate LC polymer*

Polymer code	A6 concentration (mol/l)	AIBN (mol%)	Polymerization Time(h)	Yield (%)
PA6-1	0.26	1.0	20	69
GPC *	M_n = 9 700 g/mol		M_w/M_n = 2.07	

*) With PMMA in THF as standards.

3.4 Synthesis of the Initiator

The initiator was synthesized according to a route developed by Prucker [Pruc95] in three steps, which are outlined in Fig. 3-4.

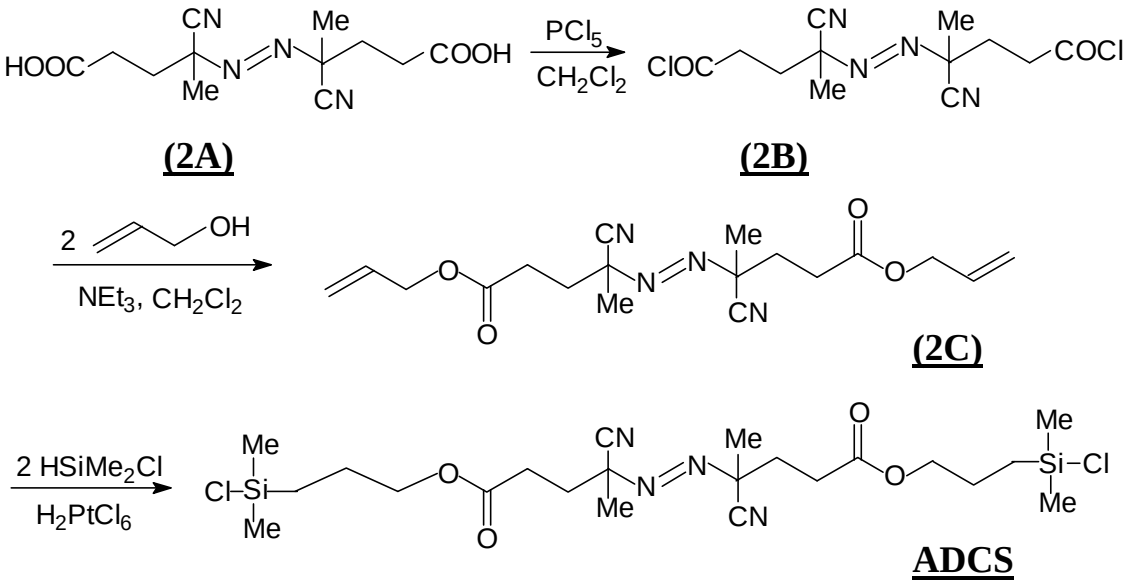

Fig. 3-4: *Outline of the initiator (ADCS) synthesis.*

4, 4´-Azobis-(4-cyanopentanic acid) **(2A)** was first converted into the corresponding acid chloride **(2B)** by phosphor pentachloride and then esterified with allyl alcohol in dichloromethane in the presence of triethylamine to get the corresponding azodiallylester **(2C)**. Finally, by hydrosilylation with dimethylchlorsilane the azodiallylester **(2C)** was transformed into the initiator **a**zo**di**chlo**s**ilane (ADCS for short) (Fig. 3-4).

3.5 Synthesis of LCP Brushes

The "grafting from" technique

LCP brushes were prepared via the "grafting from" technique [Rühe94, Pruc98]. Initiator molecules were first attached chemically to the surface of the substrate. In the subsequent step, radicals were formed upon thermal decomposition of the immobilized initiator. Chains were grown *in situ* from these radicals and have one of their ends chemically attached to the substrate surface. The polymerization was carried out at 60°C and toluene was used as a solvent. The solution was degassed by 3-5 freeze-thaw cycles

to remove oxygen traces. The “grafting from” process is schematically depicted in Figure 3-5.

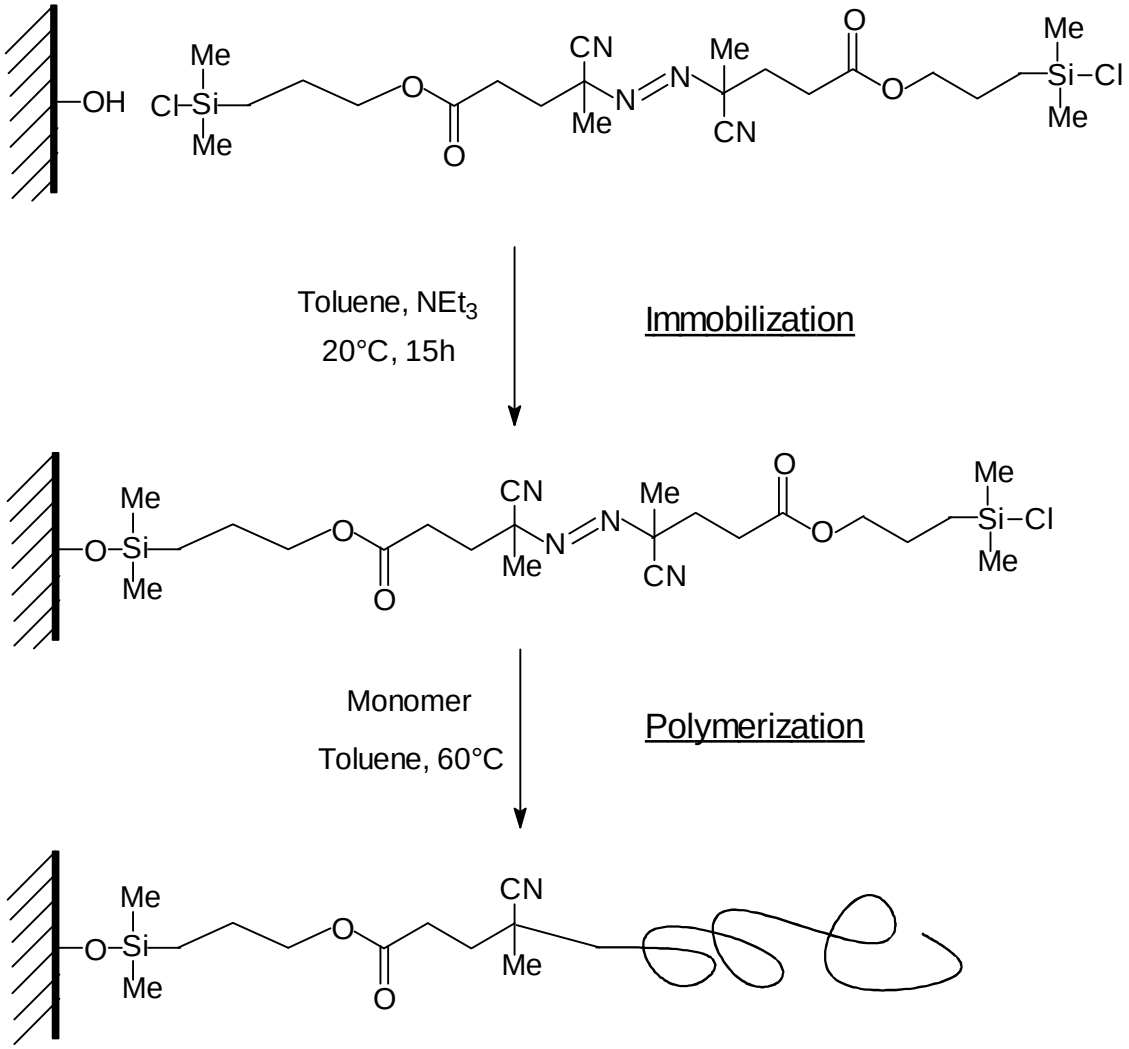

Fig. 3-5: *Schematic drawing of the “grafting from” process based on the surface immobilized initiator and in situ polymerization.*

During the polymerization step, the decomposition of an immobilized initiator molecule yields two radicals and chain propagation takes place from both of them. The one which is attached on the substrate gives a brush chain, while the other one starts a chain in solution and yields a non-attached (“free”) polymer. After polymerization, all substrates were carefully extracted with toluene in a Soxhlett setup over night to remove the free polymers and physisorbed impurities. The extracted samples were then dried in vacuum or in air.

3.6 Characterization of the Monomers, Polymers and Brushes

^{1}H-NMR and ^{13}C-NMR spectroscopy

Figure 3-6 shows the ^{1}H-NMR spectra of the monomer M6 (a) and a bulk polymer PM6-2 (b). In both cases CD_2Cl_2 was the solvent.

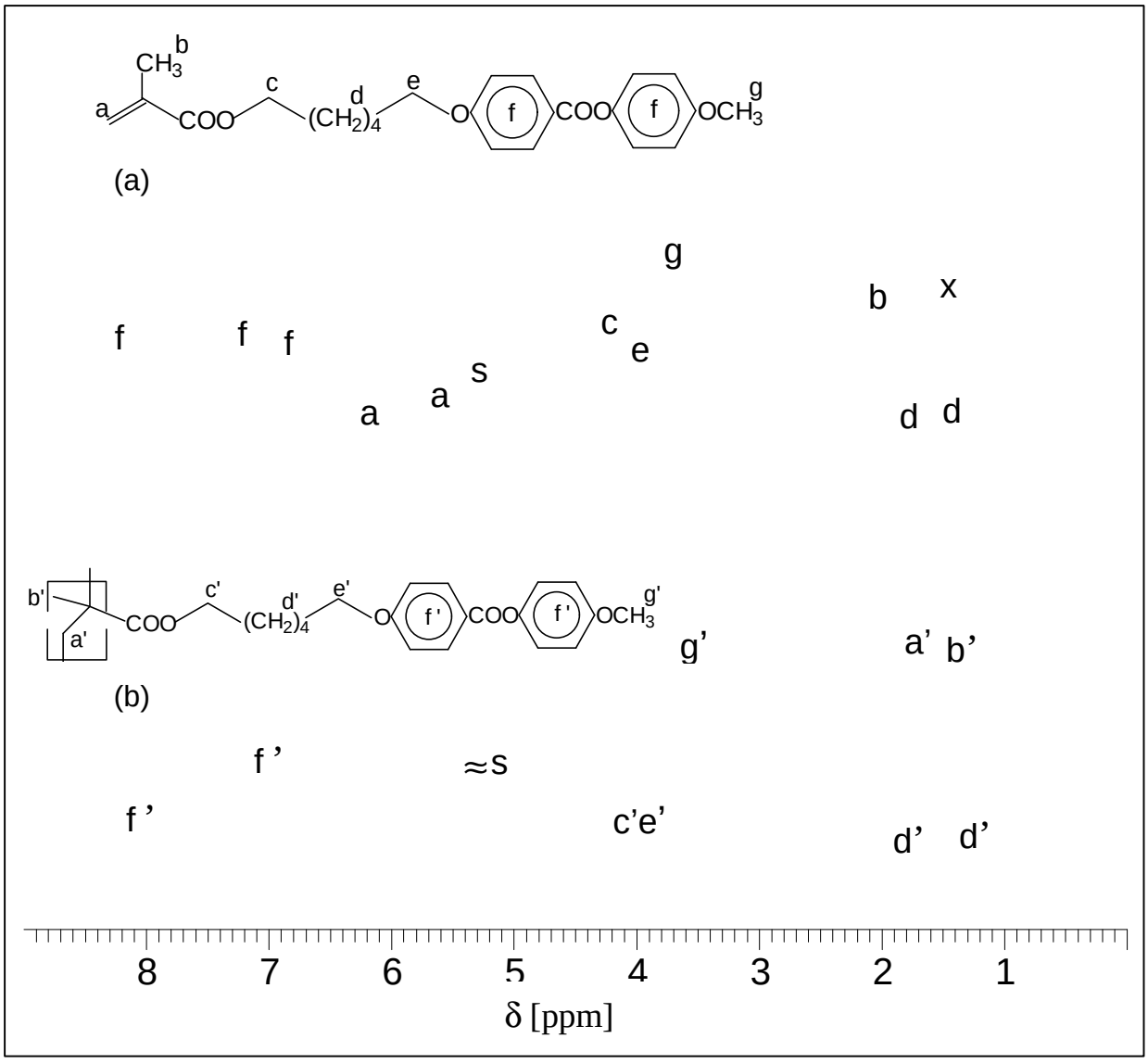

Fig. 3-6: *^{1}H-NMR spectra of the monomer M6 (a) and polymer PM6-2 (b). Signals from hydrogen atoms attached on the double bond carbon (peak **a**) shift further to lower field (peak **a'**), showing the occurrence of polymerization and the disappearance of the double bond. The peak (s) originates from the solvent CD_2Cl_2 in both spectra.*

A detailed assignment of the peaks is given in Fig. 3-6. The signals seen in these two spectra are very similar and differences can only be found for signals from the polymerizable group.

The unexpected signal in the monomer spectrum (peak **x**) comes probably from polymer that was formed by thermal polymerization as no stabilizer had been added for the NMR measurements. Except for this signal, the spectrum is in agreement with the literature [Port81].

The chemical shift values of the carbon atoms in the monomer M6 and the polymer PM6-2 ^{13}C-NMR spectra are given in Fig. 3-7. Again, similar signals are observed in both spectra, except for the carbonyl carbon atom that is directly attached to the vinyl group. Polymerization brings about an increase of about 10 ppm in the chemical shift on the carbonyl carbon (Fig. 3-7).

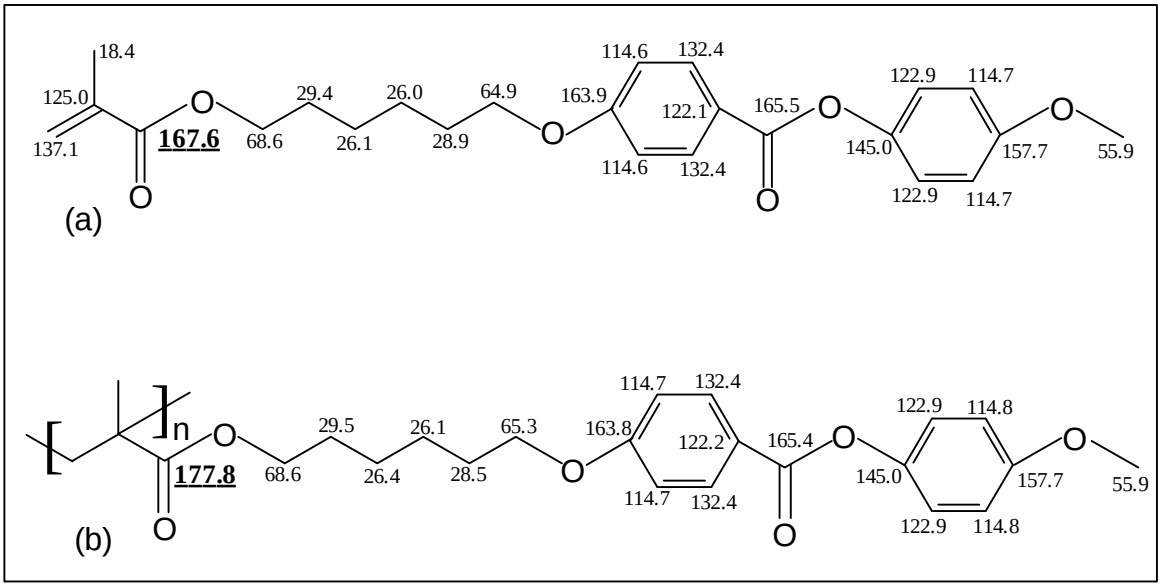

Fig. 3-7: *^{13}C-NMR results of the monomer (a) and the polymer PM6-2 (b). The numbers show the chemical shifts of the carbon atoms.*

The acrylate analogs, monomer A6 and polymer PA6 exhibit similar ^{1}H-NMR and ^{13}C-NMR spectra (see §7.2 and §7.3) as the methacrylate substances. Generally, the monomers and polymers show similar NMR peaks. Polymerization gives rise to differences in the chemical shifts only for the atoms that are directly connected with the polymerizable group.

FTIR spectroscopy

Figure 3-9 shows Fourier transformation infrared (FTIR) spectra of the monomer M6, the polymer PM6-2 and the methacrylate polymer brush monolayer attached to a silicon substrate. The monomer and polymer samples were spin-coated on silicon wafers while the brushes were grown on the substrate. Thickness of the brushes is about 65 nm.

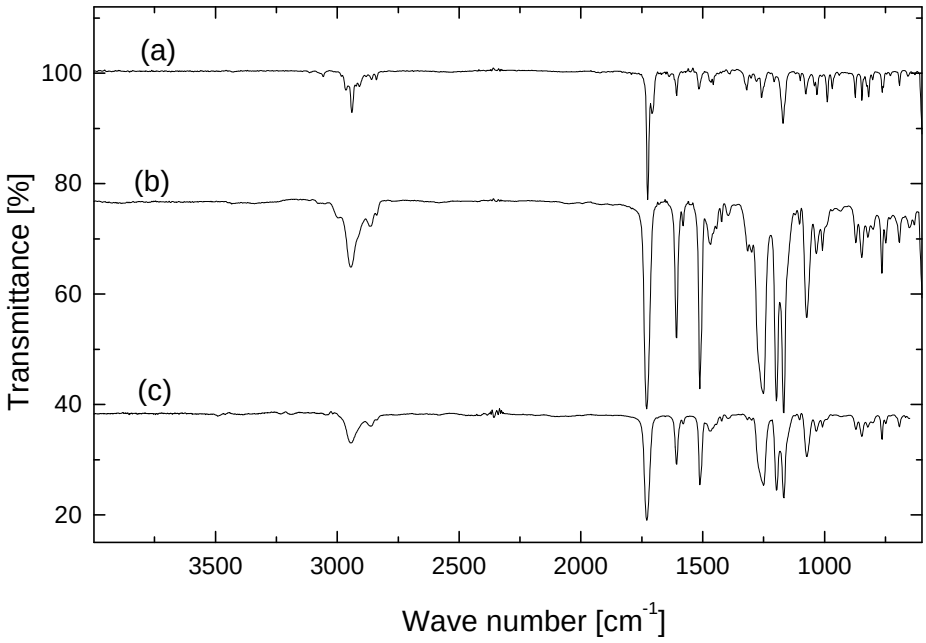

Fig. 3-8: *IR spectra of the monomer (a), the polymer PM6-2 (b), and an LC polymer brush sample (c). The curves have been vertically shifted for clarity.*

The good agreement of the spectra between the brush-coated substrate and the spin-coated polymer, concerning both characteristic absorption bands (C-H and C=O vibrations at 2944 and 1730 cm^{-1}, respectively) and absorption bands in the fingerprint region of the spectra, proves that the desired LC polymer brushes have been indeed formed during the surface polymerization reaction.

Thermal properties (DSC and TGA)

To understand the thermal behaviors, differential scanning calorimetry (DSC) and thermal gravimetric analysis (TGA) experiments on the bulk LC polymers were carried out (Figs. 3-9, 3-10 and 3-11). The DSC thermograms were obtained using a Perkin Elmer DSC system equipped with a heating system and nitrogen circulation. The TGA measurements were carried out on a Mettler Toledo STAR^e system.

Directly after preparation, spin-coated films and LCP brushes are in the isotropic state. For the methacrylate LC polymer samples, the nematic textures appear by annealing the sample at 50°C or above (§4.2). The step of the DSC thermographs (Fig. 3-9) at about 50°C is assigned to the glass transition of the bulk polymer. This interpretation is corroborated by observations on the dynamics of domain formation under the polarizing microscope in spin-coated films and brushes (§4.3).

Except for the glass transition at about 50°C, the bulk methacrylate polymer exhibit another thermal effect just at this temperature region (Fig. 3-9). In the first heating cycle (Figure 3-9, trace a), there was a pronounced endothermic signal around 50°C. This peak can be attributed to the melting of crystalline domains in the films [Peng99]. The signal was not present in the subsequent heating cycle that followed directly after cooling back to room temperature (trace b). However, when the sample had been kept at room temperature for one day, there would be enough time for the polymer chains to form crystalline domains again and the peak reappeared at 50°C (trace c).

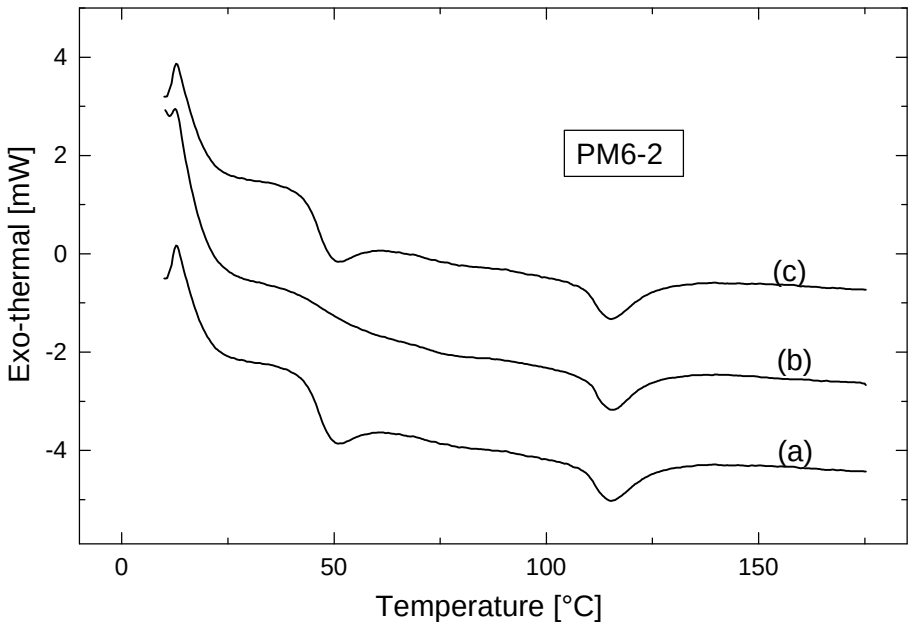

Fig. 3-9: *DSC thermographs obtained on the bulk methacrylate LC polymer PM6-2. (a) first heating cycle; (b) same sample as (a), measured direct after cooling back to room temperature; (c) same sample as (b), measured after storage at room temperature for one day. Curves b and c have been displaced for clarity. All measurements were done at a heating rate of 10°C/min.*

The peak at 113.2°C in Fig. 3-9 is attributed to the nematic to isotropic transition of the polymer film. The peak appears always at the same temperature upon repeated cooling

and heating circles, indicating that the transition is a thermodynamic first-order phase transition. Literature data for the same polymers is: g 47 n 111 i [Port82], which shows that the T_g occurs at 47°C and the nematic-isotropic transition at 111°C.

The acrylate polymer PA6 exhibits a quite different liquid crystalline behavior. Not only nematic but also smectic LC phases were observed with the polymer. In the DSC thermographs of PA6-1 (Fig. 3-10), the endothermic signal at 123°C originates from the nematic to isotropic transition, while the peak at 97.3°C is assigned as the smectic to nematic transition of the sample.

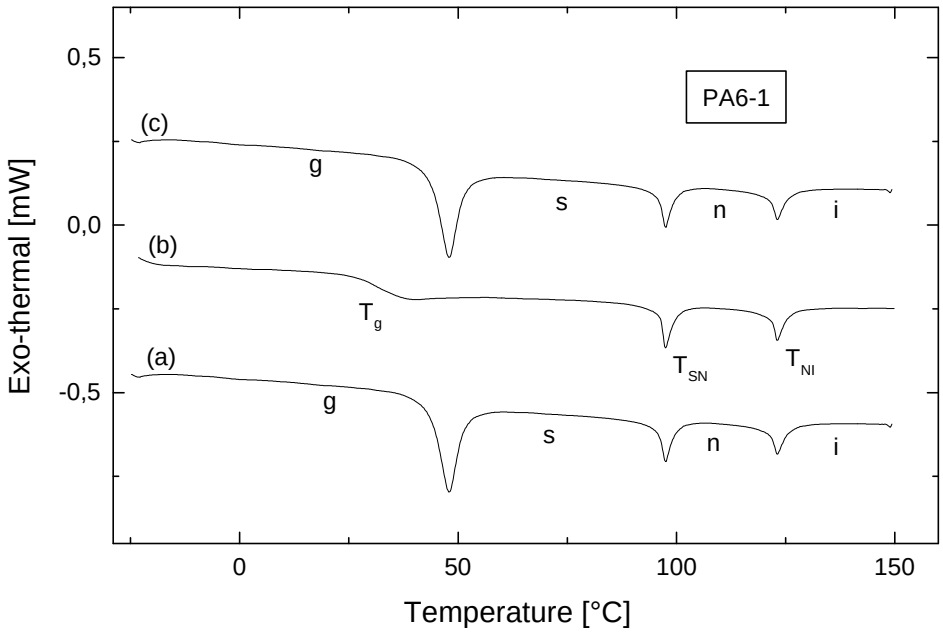

Fig. 3-10: *DSC thermographs of the polymer PA6-1: (a) the first heating cycle; (b) the second one that followed directly after cooling back. (c) the third one that measured after storage at room temperature for one day The endothermic peak at ca. 50°C in (a) is related to the melting of crystalline domains. g: glassy state, s: smectic, n: nematic, i: isotropic. T_g = 30.8 °C (2nd heating cycle), T_{SN} = 97.3°C, T_{NI} = 123.0 °C.*

The glass transition temperature of the acrylate LC polymer (T_g = 30.8°C) is lower than that of the methacrylate counterpart (T_g = 50°C). Like the methacrylate polymer (Fig. 3-9), a thermal effect related to the melting of crystalline domains in the polymer film was again noticed for PA6 just at the T_g region (Fig. 3-10a). This peak did not show up in the subsequent DSC thermograph which was carried out directly after cooling back (Fig. 3-10b). It reappeared, however, at the same place when the sample

had been kept at room temperature for one day (not shown, the curve is the same as Fig. 3-10a).

Instead of a endothermic peak, a regular step characteristic of glass transition was observed in Fig. 3-10b at 30.8°C. A similar curve has been reported in the literature [Port82] for the same acrylate LC polymer with a number-average molecular weight of 43 000 g/mol (GPC results). The endothermic effect that occurs around the T_g in the first heating like the one shown in Fig. 3-10a, however, has not been reported in the literature. The literature value of this polymer is T_g = 35°C, T_{SN} = 97 °C, and T_{NI} = 123°C [Port82].

Thermal gravimetric analysis (TGA) was carried out on the bulk LC polymers to investigate the thermal stability. The TGA curves shown in Fig. 3-11 indicate that both polymers PM6 and PA6 are stable up to 280°C. In both cases about half of the polymers is decomposed at 400°C.

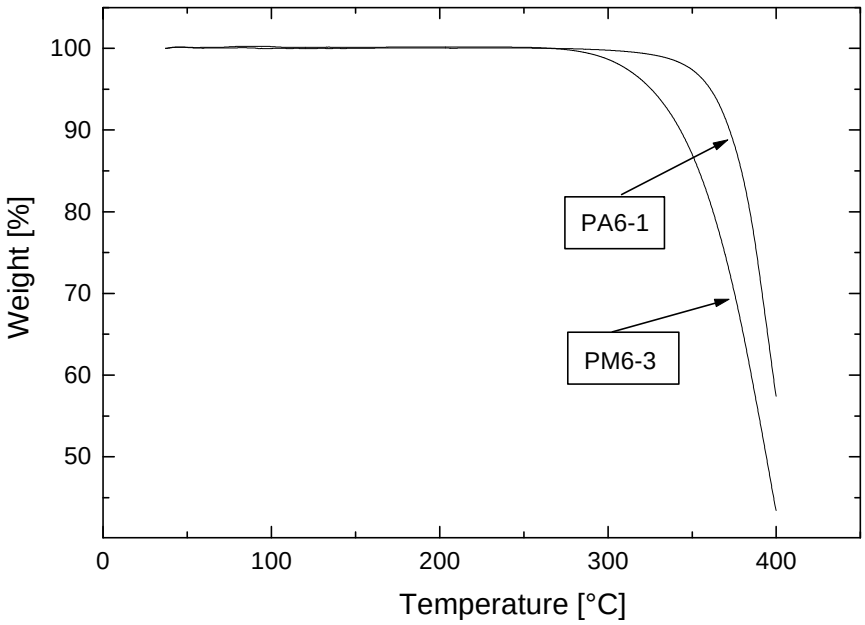

Fig. 3-11: *Thermal gravimetry analysis (TGA) data measured on bulk polymers PM6-3 and PA6-1. The polymers are thermally stable up to 280°C.*

Since all subsequent investigations were carried out at temperatures (T<160°C) much lower than 280°C at which the polymers start to decompose, it is safe to assure that no thermal degradation occurs.

3.7 Measurement of the Brush Thickness

Surface plasmon spectroscopy (SPS)

Thickness of the LCP brushes in the dry, collapsed state were determined with surface plasmon spectroscopy (SPS). Figures 3-12 and 3-13 show the principles of this technique. For a detailed description of the related theory, the reader is referred to the literature [Knol91, Aust94].

A layer of silver (around 50 nm) and a layer of SiO_x (around 30 nm) are deposited onto a glass substrate. Such a substrate is called in this work a plasmon substrate. The polymer film is subsequently produced on top of the SiO_x layer. For the SPS measurements, the substrate is placed on the bottom of a prism with the brush side toward the outside (Fig. 3-12).

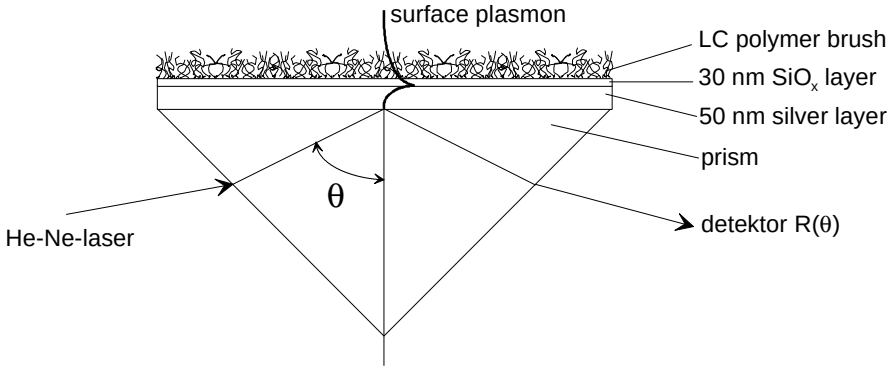

Fig. 3-12: *Schematic depiction of the surface plasmon spectroscopy (SPS) measurement. Between the polymer film and the substrate there are a layer of silver and a layer of SiO_x.*

The reflected intensity R(θ) is measured at various angles θ. Typical curves are shown in Fig. 3-13. The open squares are the reflectivity data obtained from a blank SPS substrate prior to polymerization, whilst the solid squares are data from the same substrate after the brush growth. The data were modeled using the Fresnel's equations which resulted in the solid lines in the figure.

With the blank substrate, thickness of the SiO_x layer is inferred from the position of the sharp dip (surface plasmon resonance signal) in the reflectivity curve, while thickness of the silver layer is determined by the shape of the step (edge of total reflection) located at an angle of about 38° (Fig. 3-13). A dielectric layer (for example, brushes) on the metal surface shifts the surface plasmon signal toward higher angles of incidence compared to that of the unmodified substrate. The thickness of the brush film is obtained from fitting the minimum at the new position based on the blank data.

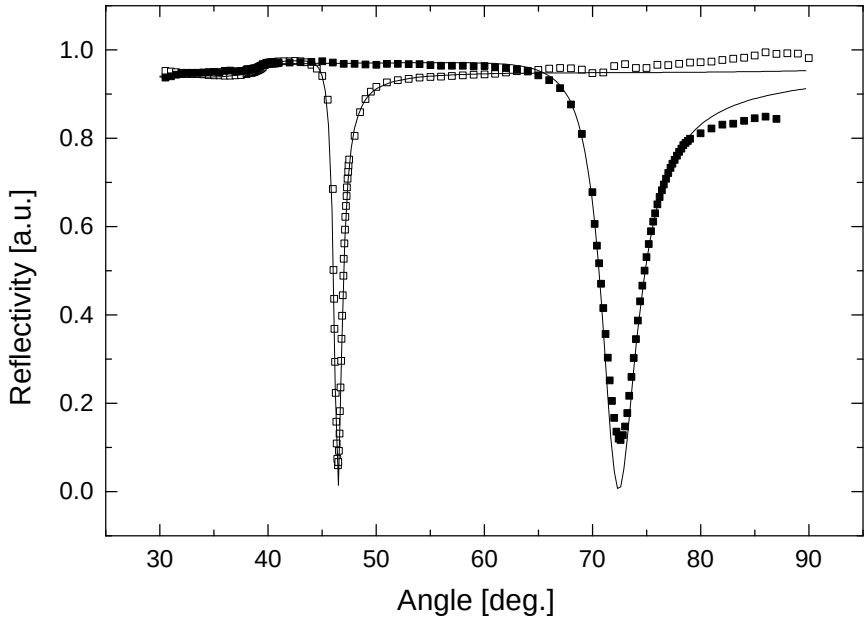

Fig. 3-13: *Surface plasmon spectroscopy (SPS): reflectivity of a blank substrate* [□] *and after growth of the brushes* [■]. *The solid lines are calculated reflectivity using the Fresnel theory. After growth of the brushes, the reflectivity minimum shifts from 46.50° to 72.45°, the latter of which infers a brush thickness of 48.9 nm.*

Table 3-5 gives some material constants (dielectric constants ε' and ε'') and the fitting results based on the data shown in Fig. 3-13. BK7 glass slides (Schott) were used as the substrates. The theoretical fitting of the reflectivity intensities measured on the blank substrate (open squares) gave the thickness of the silver and SiO_x layers as 53.1 nm and 24.3 nm, respectively.

Table 3-5: *Results of thickness and angle minimum for ultrathin layers on the SPS substrate from Fresnel fitting shown in Figure 3-13*

Layer on the substrate	ε'	ε''	Thickness (Å)	Minimum angle(°)
BK7	2.2955	0	--	--
Ag	-16.0000	0.6	531	--
SiO_x	2.1300	0	243	46.50°
PM6	2.5200	0	489	72.45°
Air	1.0000	0	--	--

The surface plasmon measured on the blank substrate occurred at 46.50°, which shifted upwards to 72.45° after the brush growth. The experimental points from the brush sample (solid squares) was modeled with the Fresnel's equation, which yielded a brush thickness of 48.9 nm for the Pm6 brushes (Table 3-5).

Determination of the refractive index

In calculating the brush thickness, a dielectric constant (ε') of the surface-attached polymer film with a value of 2.52 was used (Table 3-5). This value had been obtained from a brush sample with thicker film from the same polymer (Fig. 3-14).

With the thicker sample, two minima were obtained from the reflectivity-angle measurements, one from using p-light (Fig. 3-14a) and the other from using s-light (Fig. 3-14b). The presence of the two resonance signals allows to calculate both the thickenss and the refractive index of the layer as only one combination of the two components allows to describe the position of both resonance angles. Now two variables in Table 3-5 could be fitted, i.e. the film thickness and the dielectric constant (ε'). Different sets of thickness and ε' had been tested until the theoretical curves fitted the experimental points in the best way (Fig. 3-14), which gave a thickness of 215.5 nm and ε' = 2.52 for PM6 films. Because ε' = n^2, so the refractive index, *n*, of films from LC polymer PM6 is: *n* = 1.587. This value of the refractive index was used for modeling all the SPS data measured on the PM6 brush samples and PM6 films spin-coated on the substrates.

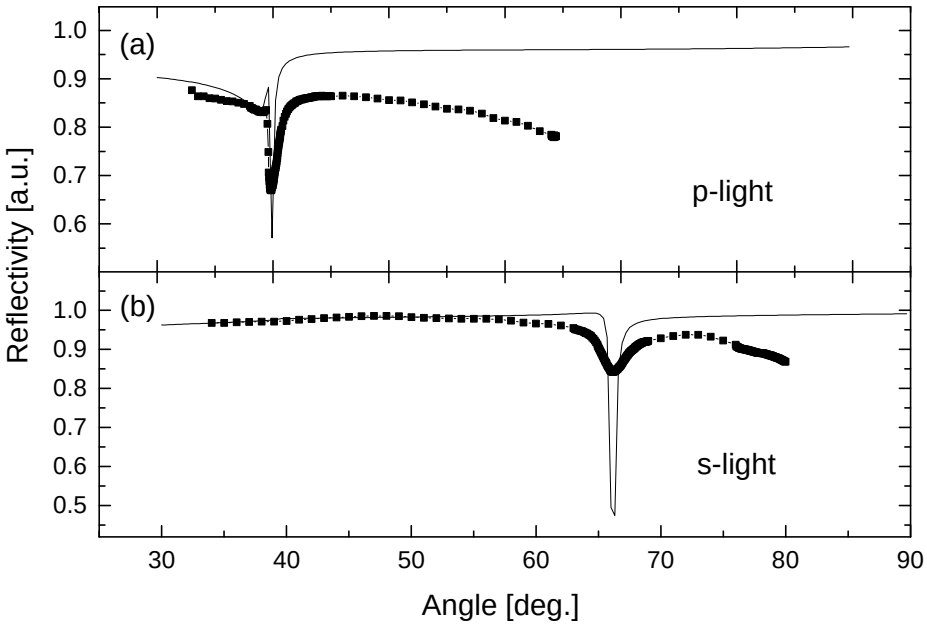

Fig. 3-14: *Determination of the refractive index for the PM6 film based on measurements on a thick brush sample using p-light (a) and s-light (b). The calculated reflectivity curves (solid lines) give a thickness of 215.5 nm and a refractive index of n = 1.587 for the film.*

Determination of film thickness of brush layers on glass substrates

The metal layer on the substrate is essential for the surface plasmon spectroscopy. However, with such a sample it is not suitable for observation of the nematic textures exhibited by the LC brushes under a polarizing microscope because that the metal layer reflects most of the light. To avoid this problem, brushes were grown directly on bare BK7 glass substrates (i.e. without the silver and the SiO_x layers) with which texture observation is much easier.

Nevertheless, determination of the brush thickness prepared on such bare substrates proves to be very difficult. In order to get the thickness, two substrates were prepared in the same reaction vessel, one being a bare glass substrate and the other a plasmon substrate with coated layers of silver and SiO_x. Brushes were grown on the two substrates under the same conditions. Thickness data were obtained from the plasmon substrates using the SPS technique, while the glass substrate were used for texture observations.

As the two substrates underwent the same reaction processes, it is assumed that the film thickness on the plasmon sample is very similar to the thickness on the glass substrate, which is difficult to determine directly. The same thickness value from SPS was therefore used for the glass samples.

3.8 Control of LC Polymer Brush Thickness

Theoretical calculation of the brush thickness

Based on the initial surface density of the azo-initiator on the substrate G_0, and the number-average molecular weight of the brushes M_n, the brush thickness d_{theo} can be theoretically calculated using the following equation [Pruc98, Schi98]:

$$d_{theo} = \frac{\Gamma_0 \left(1 - e^{-k_D t}\right) f M_n}{r} \qquad \textbf{(3-2)}$$

where k_D is the thermal decomposition constant of the initiator, f is the radical efficiency of the initiator, t is the polymerization time and ρ is the density of the polymer.

In this work, the brush thickness was controlled by the polymerization time t and the monomer concentration [M]. In the first case, the parameters like G_0, k_D, f, ρ, and M_n in the equation (3-2) are all constants so the equation can be simplified as:

$$d_{theo} = c_1 \left(1 - e^{-c_2 t}\right) \qquad \textbf{(3-3)}$$

where c_1 and c_2 are constants. It can be deduced from Equation (3-3) that increased polymerization time results in thicker brush films.

The influences of the monomer concentration [M] on the brush thickness is reflected in the parameter M_n in equation (3-2). According to the theory of radical chain polymerization [Odia92], the molecular weight is proportional to the monomer concentration, that is:

$$M_n = c_3 [M] \qquad \textbf{(3-4)}$$

where c_3 is a constant. Combining Equations (3-2) and (3-4), we get:

$$d_{theo} = \frac{c_3 f \Gamma_0 \left(1 - e^{-k_D t}\right)}{r} [M] \qquad \textbf{(3-5)}$$

or:

$$d_{theo} = c_4 [M] \qquad \textbf{(3-6)}$$

where c_4 is again a constant which is independent of the monomer concentration. A linear relationship between the monomer concentration and the brush thickness is theoretically expected from Equation (3-6).

Reflectivity curves from the brush samples

The minimum (surface plasmon resonance signal) of the reflectivity curve of the blank substrate occurs generally at the angle of 46.5° (Fig. 3-13). Figure 3-15a gives the reflectivity curves of a series of selected samples with different brush thickness. The solid curves are the results of calculations based on the Fresnel equation, with thickness indicated in the figure. The tendency that growing of the polymer brushes on top of the SiO_x layer shifts the minimum to higher angles can been clearly observed.

Figure 3-15a shows explicitly the relationship that the surface plasmon of thicker films occurs at higher angles. This holds until the film thickness reaches ca. 70 nm, with which the minimum peak disappears. However, thicker samples could then be investigated with optical waveguide spectroscopy, where instead of p-polarized light which is used in the surface plasmon spectroscopy, s-polarized light is used. The first mode for s-polarized light is visible for thickness of ca. 78 nm. Again, this mode shifts to higher angles for thicker brushes (Fig. 3-15b).

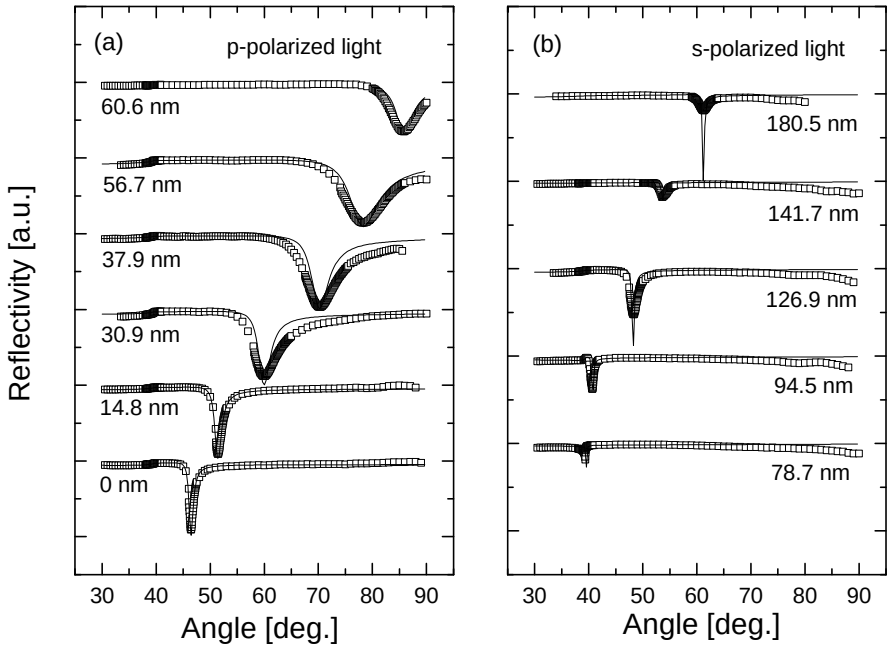

Fig. 3-15: *Surface plasmon and optical waveguide reflectivity curves of selected brushes with various thickness measured with p-polarized light (a) and s-polarized light (b). The thickness below each curve was obtained from theoretical modeling which gave the solid lines.*

Dependence of the brush thickness on monomer concentration and polymerization time

The brush thickness as functions of the monomer concentration and the polymerization time has been theoretically discussed at the beginning if this section. Figures 3-16a and 3-16b show the experimental results and a comparison with the theoretical equations. The data points are averages from measurements from at least three different spots on the samples. The error bars indicate the variation of thickness across the sample surface. A general agreement could be observed between the theoretical curves and the experimental points in Fig. 3-16.

Theoretically, it is expected that the thickness increases with the polymerization time at the beginning of the reaction, and the curve tends to level off at very long times (Equation 3-3). The tendencies can be observed in Fig. 3-16a. Chemically, the increase in the brush thickness generated through longer polymerization time is largely caused by an increase in the number of decomposed initiator molecules and accordingly the number of formed polymer chains on the substrate surface, i.e. an increase in the grafting density.

Equation (3-6) anticipates that the brush thickness increases linearly with the monomer concentration. The experimental data are in good agreement with the theoretical predictions (Fig. 3-16b). In the chemical point of view, the increase of the brush thickness achieved by using higher monomer concentration originates from an increase in molecular weight of the surface-attached polymer chains. Deviations from a direct proportionality between the thickness and the monomer concentration have been observed, which are attributed to chain transfer to the solvent [Schi95].

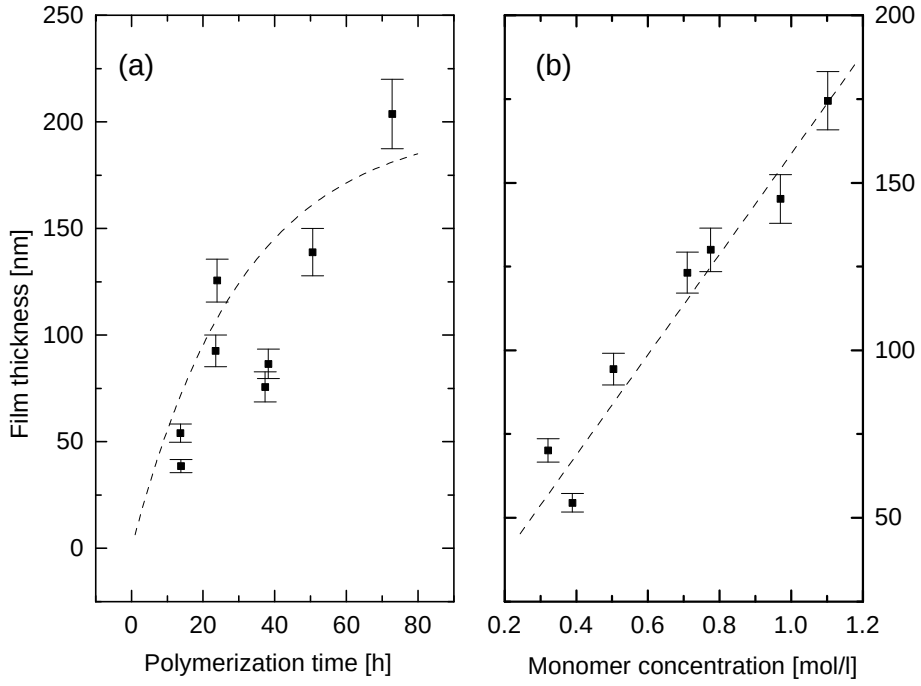

Fig. 3-16: *Thickness of the methacrylate LC polymer brushes as a function of the polymerization time (a) and the monomer concentration (b). Polymerization was carried out in toluene at 60°C. The polymerization time was kept at 24h for (a) and the monomer concentration at 0.8 mol/L for (b). The dashed lines are calculations based on the theoretical equations (3-3) and (3-6).*

In this work, methacrylate LC polymer (PM6) brushes with a thickness ranging from a few nanometers to 230 nanometers were prepared under conditions of various polymerization time and monomer concentrations. Other parameters and methods like reaction temperature, additives, solvent types, and solution viscosity could also be used to control the brush thickness [Schi95]. The mechanism and detailed discussions on the control of the brush thickness have been reported [Pruc98, Schi98].

The slight scattering of the experimental data were observed. The reasons might lay in the presence of impurities in the polymerization solutions, come from uncertainties in the monomer concentration, or in the errors form experimental operation. Another reason that scattered the experimental data come from inhibition and retardation during the polymerization, which have been observed for radical-chain polymerization [Bill84]. Although each reaction solution was carefully degassed with repeated freeze-thaw cycles, unexpected inhibitors and retarders such as oxygen might still exist in the solution which slow or postpone the polymerization. Brushes that are unusual thin even if after very long polymerization time might be caused by this kind of problems.

In the “grafting from” technique, there are generally two types of initiator [Pruc93]: the symmetric ADCS with two chlorosilane groups at the two ends of the molecule and the asymmetric AMCS (azomonochlorsilane) which has only one chlorosilane group. The theoretical work for brush thickness calculations has been done on the basis of AMCS. For the thickness of brushes generated with ADCS, experiments have showed that the brushes are about one third thinner than those prepared with AMCS [Schi98], which gives also an explanation of the data scattering observed in this work, where bifunctional ADCS was used as the initiator.

Free polymers formed during brush growth

Free polymers were formed during the brush growth (§1.4 and §3.5). According to the theory of radical-chain polymerization, the molecular weight of the polymers is linearly related to the monomer concentration (Equation 3-4). When the monomer concentration is kept constant, the polymerization time does not have much influences on the molecular weight of the polymer [Bill84, Odia92].

Figure 3-17 shows the molecular weight of free LC polymers generated during the brush growth with different polymerization time. The molecular weight M_w are almost independent of the polymerization time, as predicted by the theory. All the polymerization were carried out in M6-toluene solution at 60°C under inert atmosphere with a constant monomer concentration of 0.8 mol/L. The free polymers were collected from the reaction vessel after the polymerization by precipitating the solution into *n*-hexane, filtrated and repeated the precipitation with dichlormethane-methanol solvent pair. The weight-average molecular weight of the polymer samples were measured by GPC with PMMA in THF as the standards. Similar horizontally linear behaviors between the molecular weight and the polymerization time have been reported in the literature [Schi98].

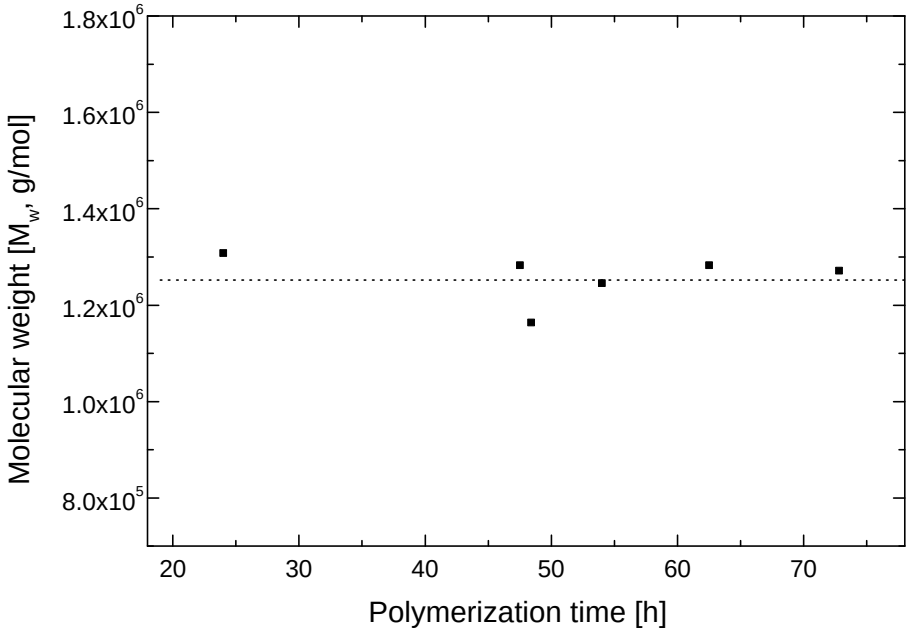

Fig. 3-17: *GPC molecular weight (M_w) of the free polymers formed during brush growth with various polymerization time. The monomer concentration was kept at 0.8 mol/L in all cases. The dotted line is the average of all the M_w's drawn here to guide the eyes.*

Thickness of the acrylate LC polymer brushes

Polymer brushes from the acrylate monomer A6 were also prepared. Again, thickness of the PA6 brushes can be controlled by the monomer concentration and the polymerization time. Figure 3-18 shows several selected surface plasmon reflectivity curves, indicating that the brush thickness was increased with increasing of the monomer A6 concentration of the solution for the brush growth.

It has been reported that under similar preparation conditions, the molecular weights of the methacrylate polymers PM6 are obviously higher than those of the acrylate polymers PA6 [Port81]. Similar phenomena have been observed in this work both in the syntheses of the bulk polymers PM6 and PA6 (cf. Tables 3-2 and 3-3), and in the preparation of their corresponding brushes (cf. Figs. 3-15 and 3-18). It seems much more difficult to get PA6 brushes with high thickness (Fig. 3-18). Brushes were grown with high monomer A6 concentrations (0.82 mol/L) for up to two days, nevertheless, a maximum thickness of only about 12 nanometers was obtained.

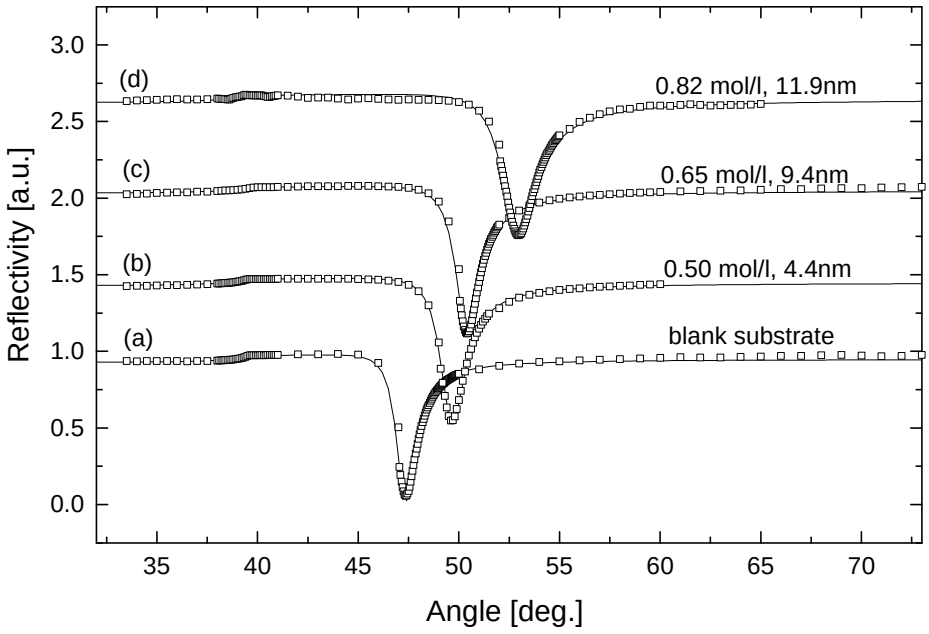

Fig. 3-18: *Selected surface plasmon reflectivity curves measured on PA6 brush samples prepared with various monomer concentration. Polymerization was carried out at 60°C in A6-toluene solution for 45 hours. The solid lines are Fresnel fittings, giving the brush thickness.*

Spin-coated polymer films

Spin-coating is one of the most widely used technique for the preparation of thin polymer films [Pett00]. A substrate is placed on a spinner and several drops of solution dissolved with the desired polymer is deposited on the substrate surface. After starting the spinner, most of the solution is spun off the substrate, but some of the polymer remains physisorbed on the surface. The thickness of the polymer film can be adjusted in a range from a few dozen nanometers to a few micrometers by varying the concentration of the solution and the spin speed.

Spin-coated LC polymer films and the LC polymer brushes investigated in this work are chemically the same. Both of them are based on the same monomer. The spin-coated films are physisorbed on the substrate surfaces, while the brushes are chemisorbed. It could be, therefore, of great interest to compare the properties between the two types of polymer thin films. For these reasons, a series of spin-coated samples with different thickness were prepared (Table 3-6).

Table 3-6: *Preparation conditions of spin-coated films from the LC polymer PM6*

Sample code	Polymer code	Concentration (mol/L)	Rotation rate (rpm)*	Thickness (nm)
SC057	PM6-5	0.020	2 000	56.7
SC064	PM6-5	0.020	1 500	63.7
SC086	PM6-5	0.020	1 000	85.7
SC101	PM6-2	0.027	1 000	101.4
SC104	PM6-5	0.020	600	104.2
SC110	PM6-3	0.027	700	110.4

*) rpm: rotation per minute.

For the preparations of the spin-coated polymer film, THF was used as the solvent for the polymer solution and the spinning time was usually 60 seconds. Thickness of the films was measured with the surface plasmon spectroscopy (SPS) technique.

4 Textures of LC Polymer Brushes in the Dry State

4.1 General Remarks

The term “texture” designates a specific optical pattern of a thin layer (generally 10-100 µm) of liquid crystal as observed with a polarizing microscope. The features of various textures are caused by the existence of defined arrangements of the molecules and different kinds of defects in the arrangements. LMW nematics show so-called Schlieren textures which arise from a continuous change in the molecular orientation. In the Schlieren textures there are distinct points where discontinuities occur. The textures of LMW liquid crystals have been both theoretically and experimentally thoroughly investigated [deGe93, Demu98].

Generally, the microscopic observation of the textures of LC polymer samples is more complicated than that of LMW liquid crystals, owing to the former’s multiphase nature (existence of polycrystalline and amorphous material), the polydispersity and the high viscosity of the liquid crystalline melts. Nevertheless, thread and Schlieren textures of spin-coated LC polymers in the nematic state have been observed, indicating their LC characters [Noël89].

The nematic textures of spin-coated films both from main chain and from side chain LC polymers have been reported extensively [Noël89, Shiw90, Demu98]. Usually, irregular nematic textures with small domain sizes in the micrometer range have been observed under the polarizing microscope. Thermal studies on the textures have shown that the domains grow with time when the LC polymer samples are annealed at elevated temperatures.

As quite thick monolayers of the side chain LC brushes with the polymethacrylate backbone could be prepared following the “grafting from” approach, a direct observation of the nematic textures of the brush samples was possible. This was the first time to use optical microscope to investigate the textures of side chain LC polymers that are chemically attached on the substrates.

Unfortunately, due to the low molecular weight of the polymers with the acrylate backbone, the brushes were too thin for the observation with the polarizing microscope. Accordingly, nematic textures of only the LC polymer brushes from the methacylate monomer M6 were studied.

4.2 First Heating of an LC Polymer Film and Simultaneous Formation of Nematic Textures

Polarization microscope

The characteristic textures exhibited by liquid crystalline materials are investigated by the polarizing microscope. A polarizing microscope consists essentially of a pair of polarizers which are 90° crossed to each other (Fig. 4-1).

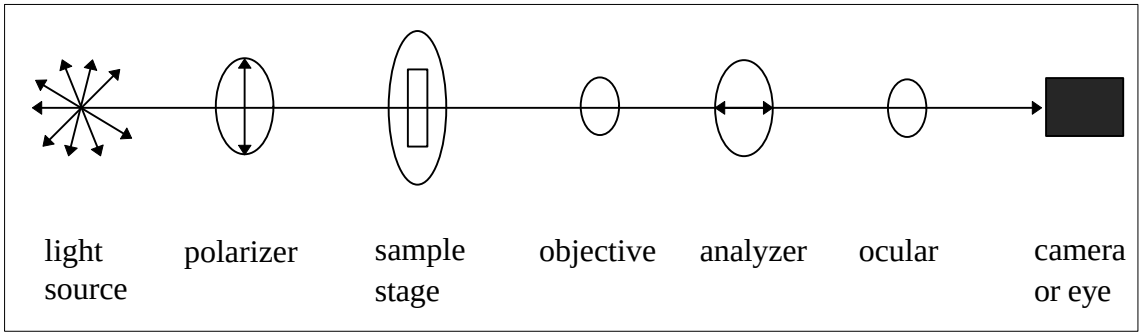

Fig. 4-1: *Schematic sketch of the light path in a polarizing microscope. The polarizer and analyzer are 90° crossed to each other.*

Light from the source is polarized by the polarizer and extinguished by the analyzer when the direction of the polarized light is not changed by the sample. When the sample is birefringent such as a crystal or a liquid crystal, the direction of the polarized light passing through the sample will be changed so that textures can be seen or be detected by a camera, which give information about the structures of the sample (textures).

We used a Zeiss-Axiophot polarization microscope equipped with a Linkam TH600 hot stage to adjust the temperature of the sample holder on which the sample was placed. The temperature can be controlled to an accuracy of 0.1°C. The optical microscope was implemented with a camera with which pictures of the textures were taken.

The first heating cycle of an LC polymer film

Immediately after synthesis (i.e. dried from the solution or after evaporation of the solvent), an LC polymer film (either spin-coated or LCP brushes) appears dark under the polarizing microscope. Apparently, the polymer chains have been quenched into an isotropic glassy state. When heated to temperatures above the glass transition point of the polymer (T_g = 50°C for PM6, cf. the DSC thermographs in Fig. 3-9), segments of the polymer chains are able to reorient and a liquid crystalline texture begins to appear. Texture formation is usually very slow when the temperature is just a few degrees above the T_g. The rate of the texture formation increases with increasing temperature. At temperatures above 100°C, textures can be formed in less than one minute.

In contrast to low molecular weight liquid crystals, which usually crystallize on cooling, LC polymers being cooled down undergo a glass transition. The mesogens in the side chain which have been arranged into a liquid crystalline state at higher temperatures will not return to their former random state even if the temperature is lowered below the glass transition point. An LC structure characteristic of the mesophase is then preserved in the glassy state. The LC state is thus "frozen" in the glassy state and we actually deal with polymers that show intrinsic anisotropic behavior of optical, mechanical, electrical and other properties. This phenomenon has been observed for most side chain LC polymers [Shib84].

In the first heating cycle, an LC polymer film undergoes phase changes as illustrated in Fig. 4-2.

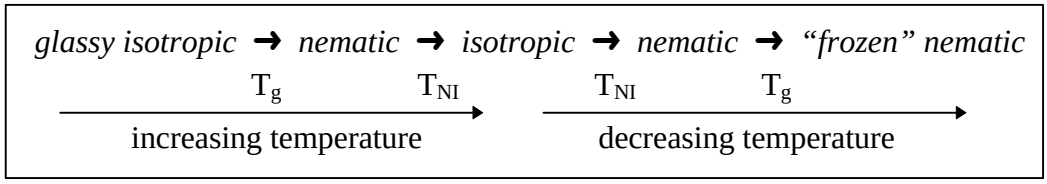

Fig. 4-2: *Phase change of an LC polymer film during the first heating cycle. A nematic texture is formed by heating the sample. This texture will not return to their starting isotropic state when the temperature returns. The texture is frozen in a glassy state.*

In the first heating cycle of the LC polymer film, the arrangement of the mesogenic units into the nematic state is completed in the heating procedure and remains so when the temperature returns back. This heating cycle is, therefore, irreversible and has great importance. The characteristic liquid crystalline texture of the LC polymer film is formed in this heating procedure. The texture will not be erased unless the sample is

heated over the N-I transition point or washed with solvent to erase the arrangement of the mesogens.

Standard heating procedure

Heating an LC polymer film at rates between 2°C/min and 20°C/min produces the same textures. No significant influence of the heating rate on the texture patterns has been noticed. In order to eliminate possible errors, nevertheless, the heating process is standardized so that textures of all the samples are formed under the same thermal conditions and the samples have the same thermal history.

All samples from the methacrylate LC polymers, either spin-coated films or polymer brushes, before undergoing any thermal history, were heated in the standard process described as the following: a sample is heated at 15°C/min from the room temperature to 125 °C, which is well above the transition point of the methacrylate polymer brushes (T_{NI} = 113 - 114°C). The sample is then kept at 125°C for three minutes to ensure total isotropization and erase any possible thermal effects before being cooled down to room temperature at the same rate (15°C/min).

4.3 Nematic Textures of LC Polymer Brushes

Nematic texture of an LCP brush sample

Figure 4-3 shows a picture of the nematic texture of a methacrylate LC polymer brush sample B228 (thickness 228.2 nm) observed under the polarizing microscope. In this work, the LC brush samples are coded like B228, where B means **b**rush(es) and the number after B is a rounded thickness value in nanometer as measured by surface plasmon spectroscopy. The magnification of the microscope was 1000 (ocular = 10, objective = 100). The original picture was digitized with a scanner Hewlett-Packard ScanJet4C.

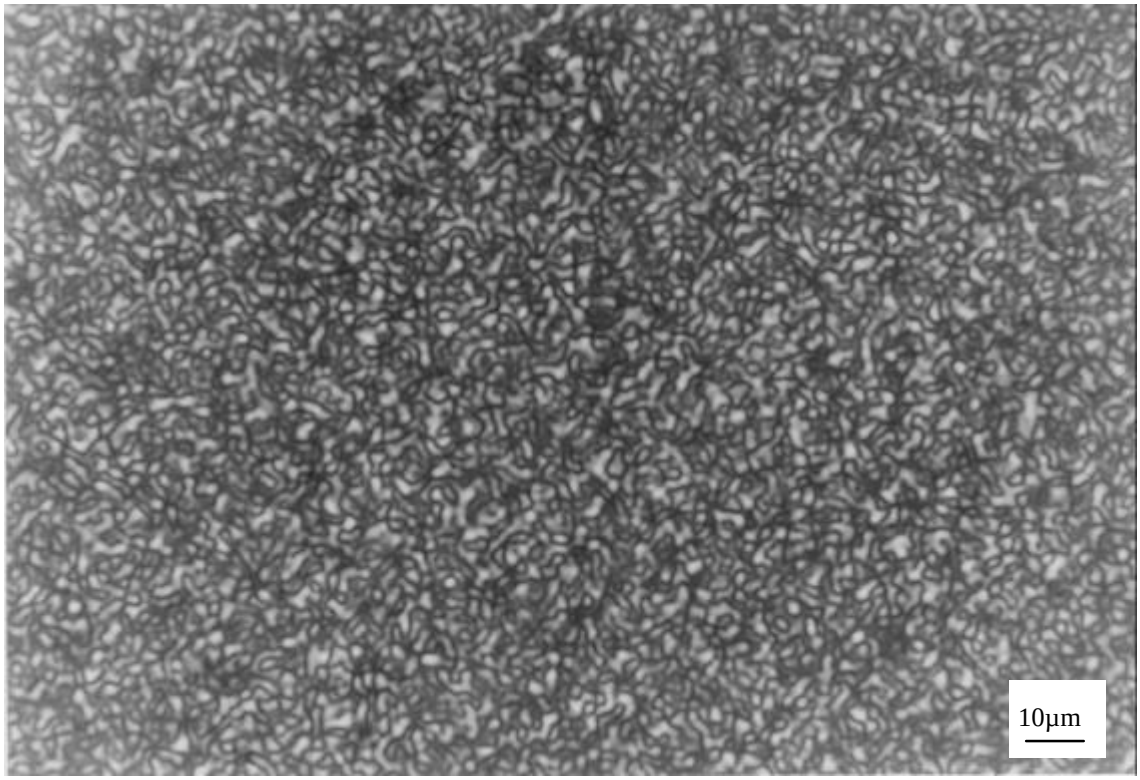

Fig. 4-3: *Nematic texture of the LCP brush sample B228 (thickness = 228.2 nm) under the polarizing microscope with a magnification of 1000. The whole picture corresponds to a 92 µm ∗* 136 *µm area on the original sample which has a size of 1.9 cm ∗ 2.6 cm.*

For the side chain LC polymer brushes based on the methacrylate monomer M6, we have successfully synthesized samples, following the “grafting from” approach, which are thick enough for direct observation of their textures with the polarizing microscope. That LC brushes with sufficient thickness can be prepared opens an area where the liquid crystalline properties of these brushes can be conveniently investigated by the optical method.

It is somewhat surprising that the brush domains are big enough to be observed directly with the optical microscopy. A brush film is a monolayer in the direct sense of the definition, that is, it consists of a single layer of polymer chains. While the film thickness is in the nanometer range, the domains have a size of micrometers. Apparently, the film thickness is not the natural scale of the lateral pattern of nematic orientation.

White and gray areas in the image of the nematic LC texture of the sample B228 indicate the presence of domains with varying optical properties (Fig. 4-3). The shape of the domains, or texture pattern, is irregular. Different domains are separated by thick dark lines, one observes neither a line ending anywhere nor a junction of an odd number of lines. This behavior is typical of topological defect lines [deGe93]. Determination of the molecular organization associated with this microstructure presents a challenge because the domain size approaches the resolution limit of the optical microscope. Transmission electron microscopy studies [Wood85, Shiw90] have shown that this microstructure can be considered as an assembly of "effective domains" due to a particular arrangement of disclinations. The fine domains are believed to correspond to regions of uniform orientation correlation within nematic structures bounded by disclinations.

Similar texture patterns have been observed with spin-coated films, whose thickness is in the micrometer range, from both side chain and main chain LC polymers [Thom85, Noël98]. Different from the well known Schlieren or thread textures usually observed for LMW nematics, these textures are ill-defined with fine speckle patterns of small size. The texture such as the one depicted in Fig. 4-3 is called according to different authors a "grainy", a "tight", a "dense", a "multi-domain" or a "polydomain" texture [Noël98].

Rotation of a texture pattern under polarizing microscope

Under the polarizing microscope, domain shapes of the nematic textures change continuously when the sample is rotated with respect to the polarizers. Figure 4-4 shows pictures of a spin-coated LC polymer film taken at the rotation angels of 0° (a), 45° (b), and 90° (c) (counter-clockwise rotation).

The domain shapes change significantly when the sample is turned a few degrees away from the original position (cf. Figs. 4-4a and 4-4b). Actually, no domain with similar shapes can be found within the two pictures (Fig. 4-4a and 4-4b). Interestingly, when the sample is rotated 90°, the same pattern reappears, but with a inversion in the brightness (Figs. 4-4a and 4-4c). That is to say, a domain with a **gray** brightness in Fig. 4-4a will be found with exactly the same shape at exactly the same place in Fig. 4-4c, but with a **light** brightness, and vice versa.

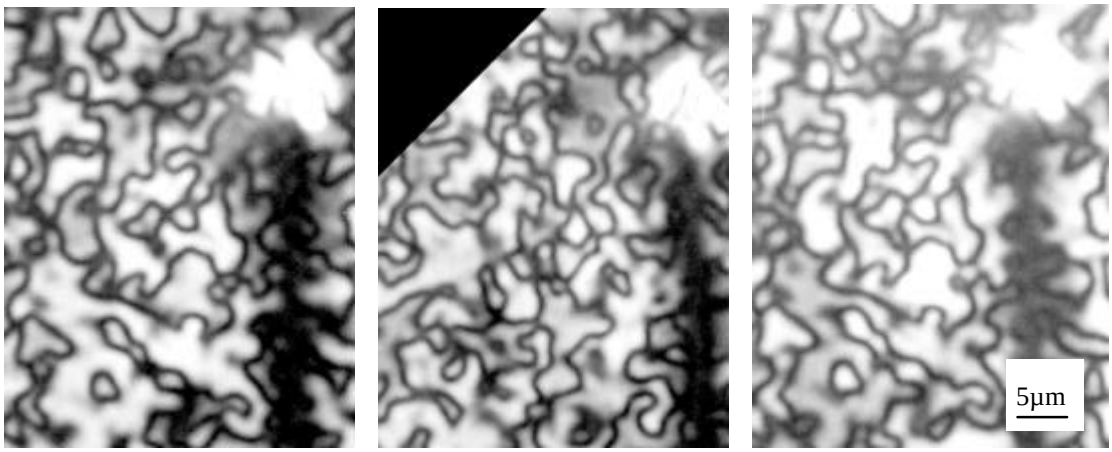

a) b) c)

Fig. 4-4: *Nematic texture of the spin-coated LC polymer film SC110 (thickness 110.4 nm) under the polarizing microscope. The sample was counter-clockwise rotated to the angles of (a) 0°, (b) 45°, and (c) 90°.*

This kind of pattern inversion has been observed by Nehring and Saupe [Nehr72]. They sandwiched LMW nematic molecules between two glass substrates with a layer thickness of 10 µm. Typical Schlieren textures appeared under the polarizing microscope. By rotating the sample, they have found that the same pattern, with an inversion of the texture pattern, showed up again after a rotation of 22.5° or 45°, depending on the types of the textures formed by the LMW nematic molecules. They explained the phenomena with a model of specific arrangements of the LMW nematic molecules and gave detailed theoretical treatments.

The sample for Figure 4-4 was a spin-coated film which, as will be discussed in §4.6, can be annealed to get much larger domains for better observations. Before taking the pictures, the film had been annealed at 109°C for 1h to obtain the large domains. The thick dark line at the right side of the pictures of Fig. 4-4 is a scratch purposely produced on the sample surface for finding the exact same location back more easily and for better comparison of the textures.

With LC brush samples (not shown), similar behaviors were observed upon rotation. The domain size is nevertheless much smaller (see, for example, Fig. 4-3) and does not vary with time even after the sample is annealed at high temperatures for a long time (see §4.6).

Homogeneity of LCP brush samples

The pictures of the nematic textures shown in Fig. 4-3 is only a small part of the whole brush sample B228. The picture covers an area of about 92 µm ∗ 136 µm, which is only about 0.01% of the whole surface area of the original sample. Several images on different spots on the sample surface were taken, all of which showed the same characteristic behavior, indicating that the homogeneity over the sample is good. Due to the general homogeneity throughout the sample, selection on this specific spot on the substrate to take the picture was somewhat random for the following investigations.

4.4 Nematic Texture of Various Thickness

Textures of LC polymer brushes with various thickness

Observed under the polarizing microscope, nematic textures from LC brush samples with various thickness exhibit similar patterns (Fig. 4-5). All the textures consist of many domains which have irregular shapes just like the one shown in Fig. 4-3. No obvious dependence of the texture patterns as well as the domain size on the brush thickness could be noticed, although the thickness increases 10 times (from 29.2 nm in Fig. 4-5a to 228.2 nm in Fig. 4-3).

The sharpness of the pictures in Fig. 4-5, or the clearness of the domain borders, does depend greatly on the brush thickness. When the brushes are thin, the pictures are not sharp and the domain borders are indistinct (Figs. 4-5a, 4-5b). For samples with a brush thickness around 100 nm or thicker, clearly defined pattern with sharp textures could be observed (Figs. 4-5d, 4-5e and 4-5f). More texture pictures from LC brush samples with other thickness are shown in the Figures 4-3 (228.2 nm), 4-8 (125.6 nm), and 4-14 (85.6 nm).

Thickness limitation for texture observation

The LC polymer brushes studied in this work are ultrathin films. The sight field of a brush sample under the polarizing microscope was therefore usually very dark. Objectives with large magnifications (50x or 100x) had to be used for the polarizing microscope in order to resolve the textures of the brush samples, which approaches the limits of the optical microscopy.

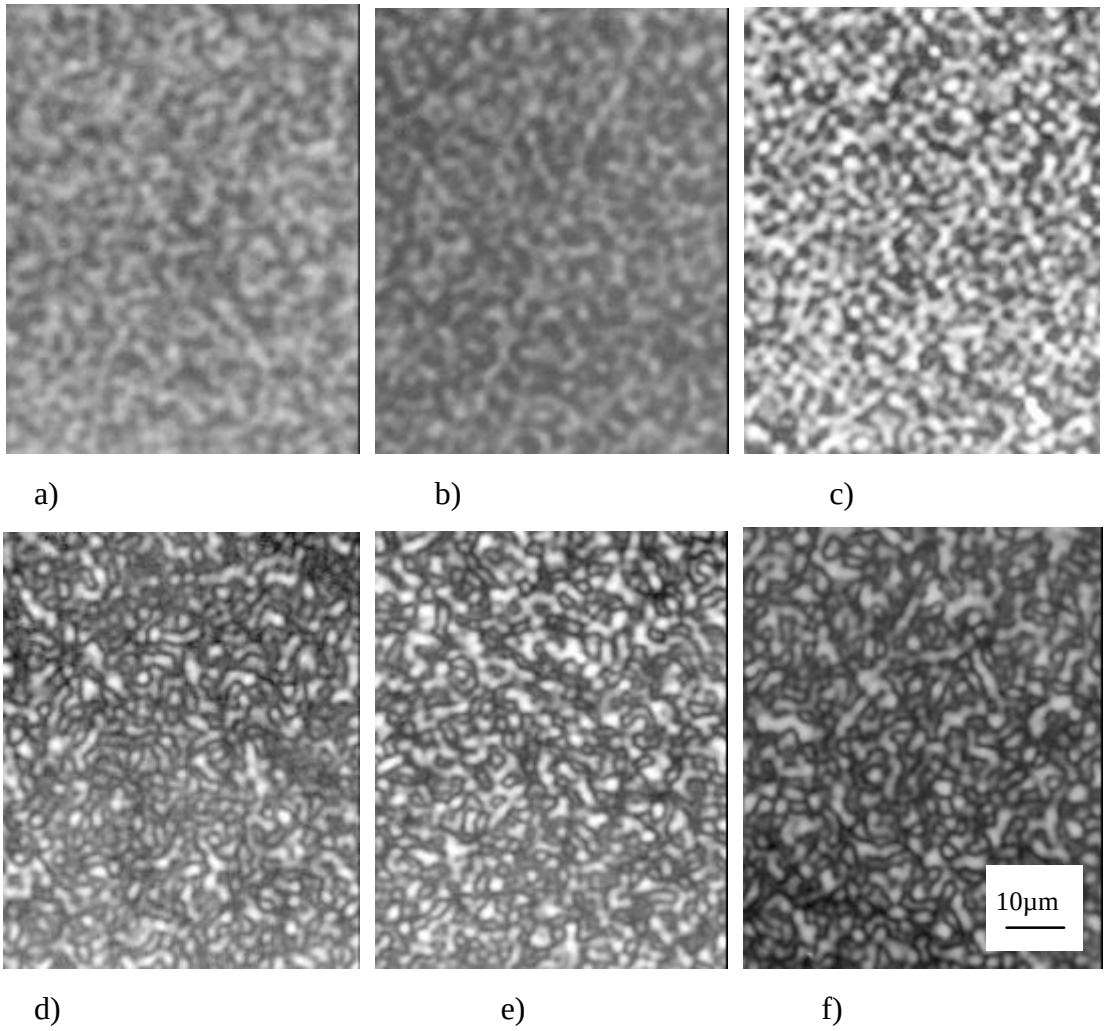

Fig. 4-5: *Nematic texture from LCP brushes with various thickness (sample code in the brackets) of: a) 29.2 nm (B029), b) 38.9 nm (B039), c) 61.8 nm (B062), d) 97.0 nm (B097), e) 164.2 nm (B164), and f) 203.7 nm (B204). Although the brush thickness varies an order of magnitude, similar texture patterns with quite similar domain sizes are observed (Fig. 4-9).*

The sharpness of the nematic pictures decreases with decreasing of the brush thickness (Fig. 4-5). Experiences on the observation of the textures of LC brushes with various thickness showed that it was easy to handle brush samples thicker than 100 nm to get clear pictures with sharp patterns. For samples with thickness between 50 to 100 nm, contrasts of the textures decreased and the domain borders became blurred. For brushes with a thickness down to the range of 30 to 50nm, the sight field was so dark and the contrast between the dark and the gray domains was so small that only under the best conditions of the microscopy it was possible to see the textures.

For even thinner samples, there existed a thickness limit for the observation of texture with the optical microscopy. The limit for the PM6 brushes grown on bare, untreated

glass substrates is around 25 nm. Below this thickness it was not possible to see any textures, even if the textures might have existed.

Domain size of LC polymer brushes with various thickness

The domain size of a brush texture, such as the one for the sample B228 shown in Fig. 4-3 and the ones in Fig. 4-5, can be quantitatively measured by counting the number of domains on a certain area (2 cm ∗ 2 cm) on the pictures taken with the implemented camera. Usually the domain numbers from five different spots on a picture were counted and averaged as the domain size of the sample. The number of domains on such a 4 cm^2 area is between 24 to 32 for the samples with different thickness. The values resemble a real domain size between 8.75 and 6.56 μm^2, respectively. Figure 4-6 depicts the domain size of a series of LC polymer brushes. The average domain size from all measured samples is 7.84 μm^2 (the dotted horizontal line in Fig. 4-6).

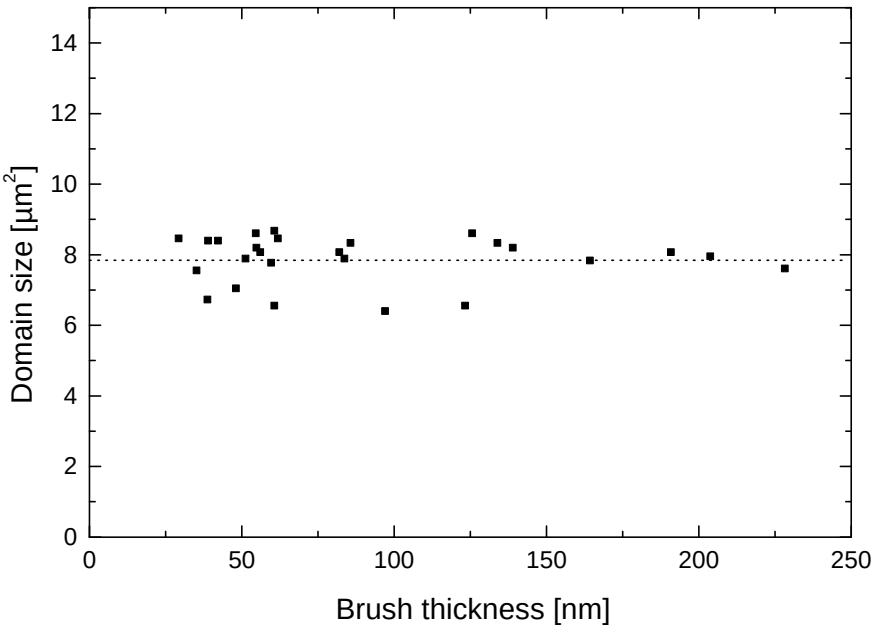

Fig. 4-6: *Domain size of nematic texture from LCP brushes with various thickness. The dotted horizontal line is the average value from all samples.*

A gentle fluctuation is noticed for the domain size values which vary slightly around the average line (Fig. 4-6). Although the samples were prepared under very different conditions and the thickness of the samples differ by an order of magnitude, the data points do not deviate much from each other. As has been discussed in §3.8, the thickness of brush samples is related to the molar mass of the polymer chains (regulated

by the monomer concentration) and to the grafting density of the chains on the substrate (regulated by the polymerization time). It can be seen from the data in Fig. 4-6 that the domain size of the brushes neither depends on the length nor on the grafting density of the polymer chains.

The light transmission of LC polymer brushes with various thickness

The brightness of a brush sample under the polarizing microscope, or the integrated transmitted light intensity, can be determined by exposure time of the implemented camera in the microscope. Exposure time is the time needed for the camera to accumulate transmitted light to a certain intensity. The reciprocal value of the exposure time is then the integrated light transmission.

Although the domain size from different thickness is quite similar, the overall brightness of the sample, or the integrated light transmission, observed under the polarizing microscope did change with the thickness. A linear relationship is observed in the transmission-thickness curve (Fig. 4-7).

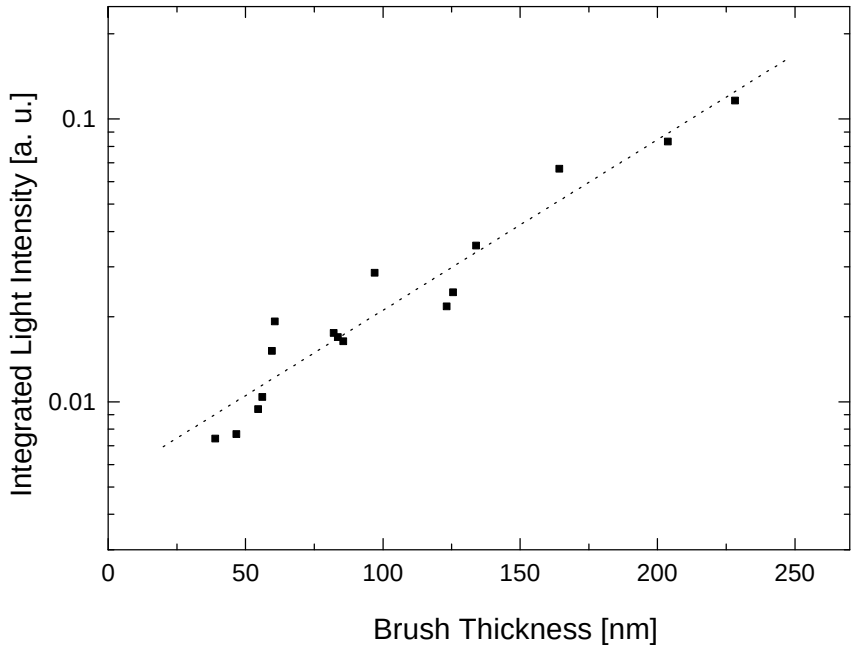

Fig. 4-7: *Integrated light transmission of LCP brushes with various thickness. The dotted line is a linear fit from the experimental points.*

4.5 Nematic Texture at Various Temperature

Textures of LC polymer brushes at different temperatures

The nematic textures of LC brushes at different temperatures were investigated by the polarizing microscope. Figure 4-8 shows a sequence of textures obtained on the brush sample B126 (thickness 125.6 nm) at temperatures of 22°C (a), 100°C (b), 113°C (c), and 113.7°C (d). The N–I transition or the film occurs at 113.7 ± 0.1 °C. The pictures were taken after the sample had been kept at the given temperatures for at least three minutes to ensure the thermal equilibrium.

For the first two pictures (Figs. 4-8a and 4-8b), neither changes in the texture patterns nor great fluctuation in the light transmission (cf. Fig. 4-10) were observed, although the temperature difference spanned a region of 78°C (from 22° to 100°C). The experimental data show that even at temperatures a few degrees below the N-I transition, brushes are very stable in their nematic state.

Figure 4-8d depicts a coexistence between the nematic and the isotropic phases of the brushes at the point of the N-I transition (113.7 °C). Slight changes in the temperature would disturb the coexistence. It is clear that a definite temperature point at which the nematic and the isotropic phases are at equilibrium could be observed. The presence of this sharp point makes it possible to use the polarizing microscope in measuring the transition temperature (see later). A description on Figs. 4-8b and 4-8c will be given in the next subsection.

Anchoring transition of LC polymer brushes

Although the pattern of the nematic textures do not change upon heating the sample until the N-I transition, changes in the brightness of the textures were noticed when the temperature approached the T_{NI} (Figs. 4-8, 4-10). The dark line that encircles a domain shown in Fig. 4-8b disappeared and the domain turned into a dark patch with the same shape (Fig. 4-8c). This happened at 113°C which was just before the N-I transition occurred at 113.7 ± 0.1 °C.

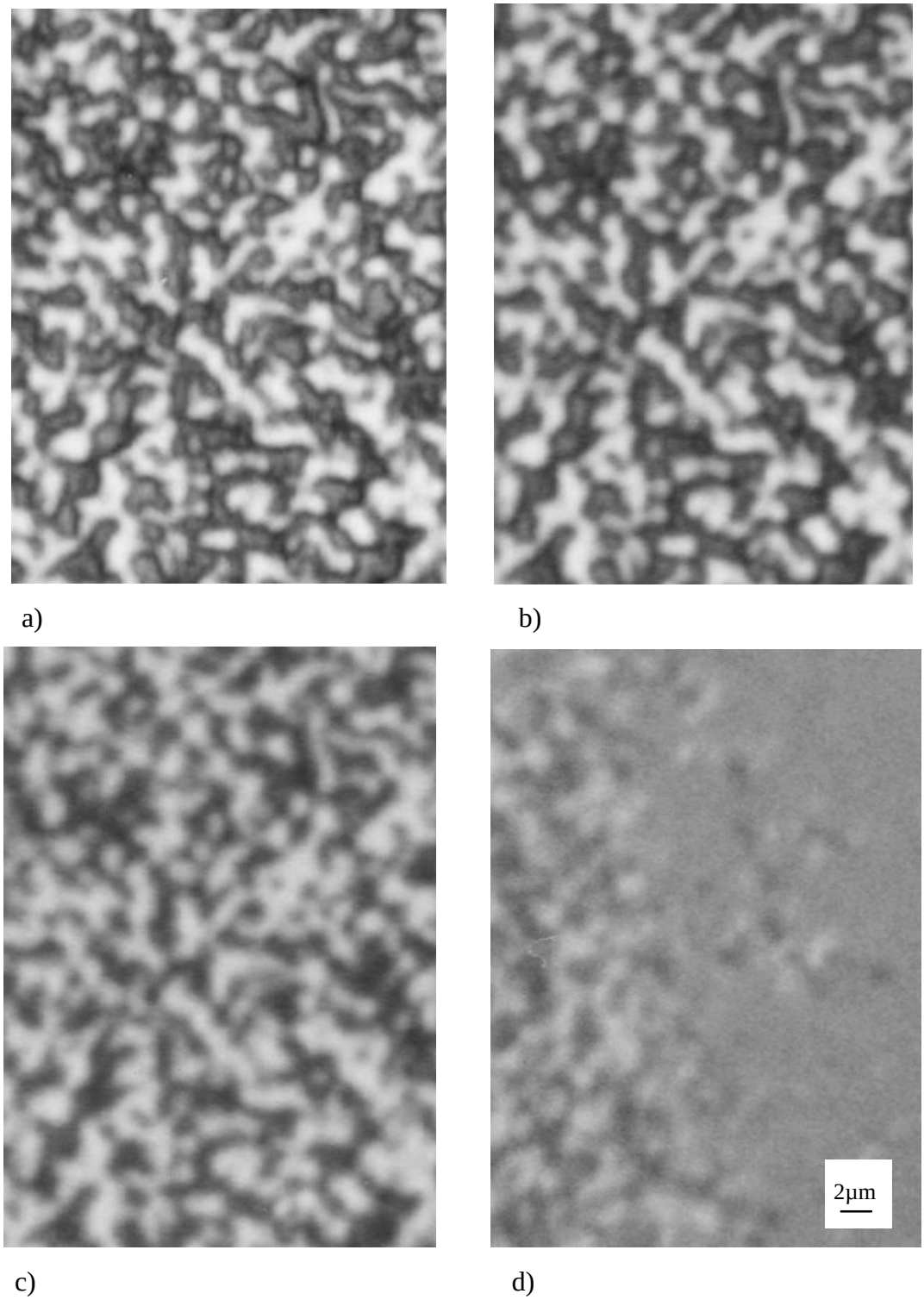

Fig. 4-8: *Liquid crystalline textures obtained from the brush sample B126 at temperatures of 22 °C (a), 100 °C (b), 113.6 °C (c), and 113.7 °C (d). T_{NI} = 113.7± 0.1°C. The dark lines (disclination walls) disappear just before the T_{NI}, which might be caused by an anchoring transition. A coexistence was observed at the nematic-isotropic transition point (d), indicating the presence of a sharp N-I transition temperature.*

To look further into the disappearance of the dark lines at temperatures before the N-I transition, spin-coated films from the LC polymer were prepared which have much larger domains and made the observation more conveniently. Figure 4-9 shows two pictures taken before and after the disappearance of the bordering dark lines. Gray domains surrounded by enclosed dark lines are observed in Fig. 4-9a showing a nematic texture of the spin-coated film SC104 which had been annealed at 110-113°C for collectively 5 hours to get the domain size of about 10 micrometers. The texture patterns remained unchanged until the temperature approached the N-I transition point which is 110.7°C. At 110.4°C, the dark lines vanished and the domains turned into, without changing the shapes, dark patch-like patterns (Fig. 4-9b).

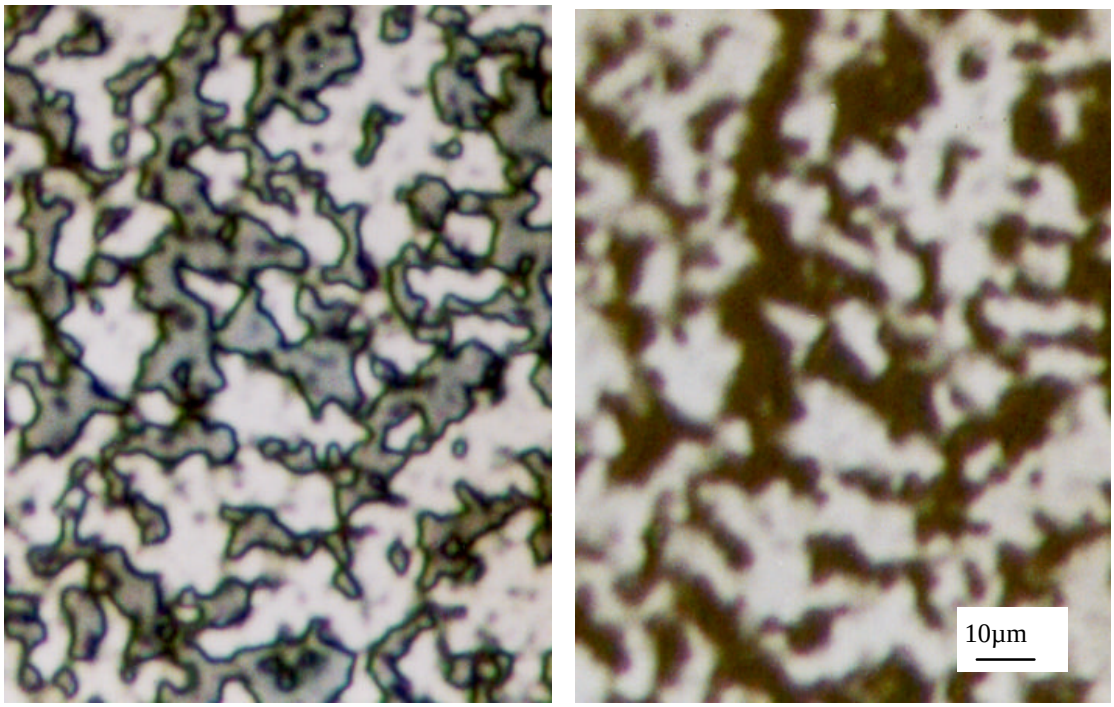

a) b)

Fig. 4-9: *Pictures of nematic textures from the spin-coated LC polymer film (SC104) taken at temperatures of 25 °C (a) and 110.4 °C (b). The dark lines that surround the domains (a) disappeared just before the T_{NI} (= 110.7°C) (b) and the domains turned into dark patches.*

Although we do not know the exact nature of the dark lines, we believe them to be related to disclination walls originating from conflicting boundary conditions at the top and the bottom interfaces of the brushes [Nehr72, Peng99]. Presumably, the film–air interface imposes homeotropic alignment, while the substrate favors parallel alignment. This kind of conflicting anchoring is quite common for thin films and has been used to study the phase behavior of low molecular weight liquid crystals under strong orientational stress [Witt96]. Under this assumption the nematic director in the brush

undergoes a splay-bend distortion in order to accommodate both boundary conditions. The sense of rotation in this distortion may take two different signs. Domains with a different sense of rotation can not be continuously connected to each other. The boundary is topological defect. Close to these disclination walls the nematic order is reduced, which makes them appear as dark lines. Disappearance of the lines close to the nematic-isotropic transition is possibly the consequence of an underlying homeotropic-to-homogeneous anchoring transition at the film–air interface. Such an anchoring transition driven by a change in order parameter has been observed before [Rysc76, Teix93].

Light Transmission with temperature

To investigate the influence of the texture brightness of the brush samples by temperature, the light transmission of the brush sample B61 (thickness 60.6 nm) was measured at various temperatures (Fig. 4-10). Before each measurement, the sample had been kept at a constant temperature for at least three minutes to ensure thermal equilibrium. The nematic-isotropic phase transition of the brushes is most conveniently demonstrated by the transmission-temperature graph, where a noticeable drop of the transmitted light is observed (Fig. 4-10). At the N-I transition temperature the nematic

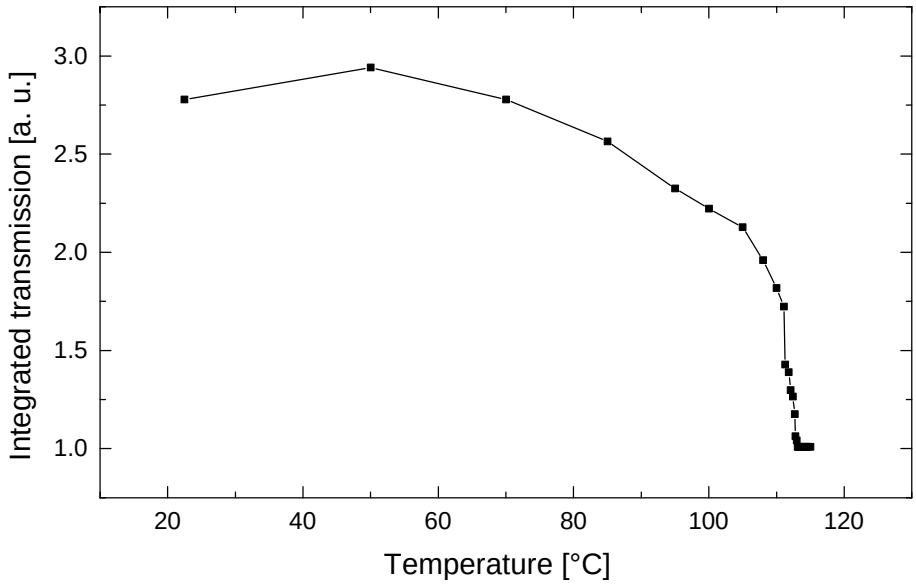

Fig. 4-10: *Integrated light transmission as a function of temperature for the brush sample B61 (thickness 60.6 nm). The sharp drop of the transmitted light at about 113°C is caused by the N-I transition of the sample.*

state is destroyed and an isotropic state shows up. As the polarizing microscope has a crossed polarizer geometry (Fig. 4-1), no light is transmitted when the sample is in the isotropic state (see, e.g. Fig. 4-12b). The abrupt disappearance of textures which occurs within a very narrow temperature region makes it possible to measure the N-I transition temperature with a microscope (see below).

In a broad temperature range between room temperature and just a few degrees below the N-I transition point, a slow decrease in the light transmission can be seen. The only exception in the decrease is a slight kink at around 50°C, which is reproducible in different samples. This thermal stability of the LC brush textures is in agreement with the microscopic observation (Fig. 4-8).

Figure 4-11 gives an enlarged view of Figure 4-10 at temperatures close to the N-I transition. The sharp drop in the transmitted light that occurs within about 2 degrees (111-113°C) clearly shows the nematic-isotropic transition of the brushes. After the transition, the brushes turned into the isotropic phase which shows a dark field. Further increase of the temperature had no effect on the isotropic state so the transmission stayed constant. The intersection between the dropping line and the horizontal line is then the transition temperature of the sample.

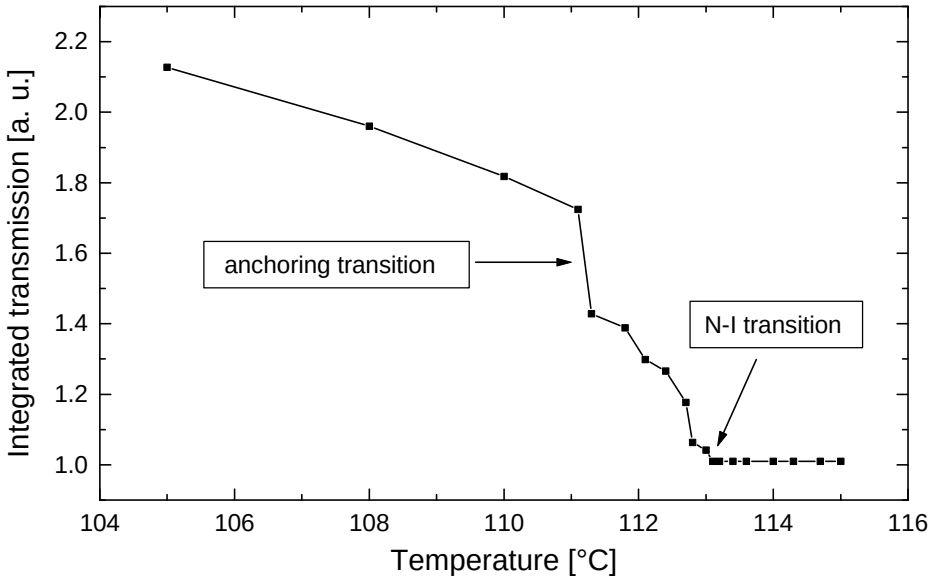

Fig. 4-11: *An enlarged view of Fig. 4-10 close to the transitions. Transmitted light intensity drops steeply at the N-I transition, at which the nematic textures disappear completely within a very narrow temperature range. The slight kink just before the T_{NI} is reproducible and could be due to an anchoring transition at the brush-air interface.*

The experimental principle for measuring N-I transition temperatures with a microscope is, therefore, that a T_{NI} is determined as the temperature at which a nematic texture disappears completely. The reproducibility of the measurements is within ± 0.1°C.

Transition Temperature of LC Polymers Thin Films

The nematic-isotropic transition temperature T_{NI} is one of the most important physical properties of the LC polymer films. T_{NI} from spin-coated polymer films, polymer brushes and a polymer bulk sample were measured with the polarizing microscope and the results are plotted as a function of the film thickness in Fig. 4-12. The conditions under which the spin-coated samples were prepared are listed in Table 3-6.

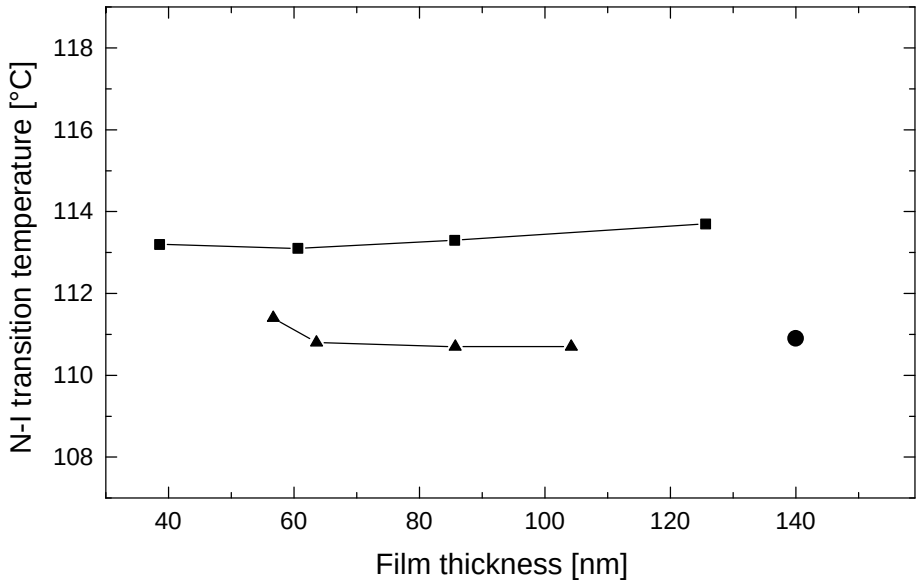

Fig. 4-12: *Transition temperature of LC polymer samples: bulk PM6-2* (●), *spin-coated films* (▲) *and brushes* (■).

The N-I transition temperature of the brushes does not significantly depend on the film thickness (Fig. 4-12). This is somewhat surprising, because one might have expected that the strong orientational stress exerted by the asymmetric interfaces would destabilize the nematic phase and therefore decrease T_{NI} [Witt96].

Interestingly, T_{NI} seems to be 2-3 °C higher in the brushes than in the corresponding spin-coated films (Fig. 4-12). The transition temperature in the spin-coated LCP films also depends only weakly on the thickness. It can be excluded that this difference in the T_{NI} originates from differences between the molecular weight of the brush and the spin-

coated polymer from the finding that T_{NI} depends only weakly on the molecular weight of the polymer when the polymer chain exceeds a certain critical length (see Fig. 3-3). It could be possible that chain stretching of the polymer backbone of the brushes stabilizes the nematic phase [DeGe75, Schä89].

Changes in the N-I transition temperature of LC polymers have been observed when the sample is under external mechanical forces. A continual shift of the T_{NI} of a side chain LC polymer to higher temperatures has been reported when an external stress with increasing strength is exerted on the sample [Schä89]. An increase of 2°C has been observed when the external stress reached 600 $N*mm^{-2}$.

4.6 Memory Effect of LCP Brushes

Annealing behavior of spin-coated LC polymer films

Texture growth of spin-coated films upon annealing has been reported both with main chain and with side chain LC polymer samples [Noël98]. The growing-rate depends on the annealing temperature and the molecular weight of the LC polymers. Experiments have shown that the domain size increased faster at higher annealing temperature or LC polymers with lower molecular weight was used.

The relations between the texture domain size and the annealing time of spin-coated LC polymer films have been quantitatively investigated based on experimental data, which can be expressed by the following equations [Shiw90]:

$$x_d(t) \propto r(t)^{-1/2} \propto t^{0.35} \qquad \textbf{(4-1)}$$

where $\xi_d(t)$ is the average domain size, $\rho(t)$ is the number density of disclinations, i.e., the defects in the textures seen under the polarizing microscope, and *t* is the annealing time at a given temperature.

Based on small-angle X-ray scattering (SAXS) results on main chain LC polymers, the dark lines bordering domains in the textures are found to originate from a spatial distribution of the disclinations. Annihilation of the neighboring disclinations, caused by reorientation of the mesogenic units, results in disappearance of the dark lines and hence a decrease in the domain number. The domain size is therefore increased. Equation

(4-1), semi-empirically from experimental data, reveals the relationships between the domain size ξ_d and the number density of the disclinations ρ, and the annealing time *t*. The expression shows that the longer the annealing time, the lower the disclination density and the larger the domain size.

Figure 4-13 shows two pictures from the spin-coated films prepared from the polymer PM6-3. The pictures were taken before and after the annealing. A notable increase in the domain size can be observed after the polymer film had been annealed at 109°C for an hour (Fig. 4-13).

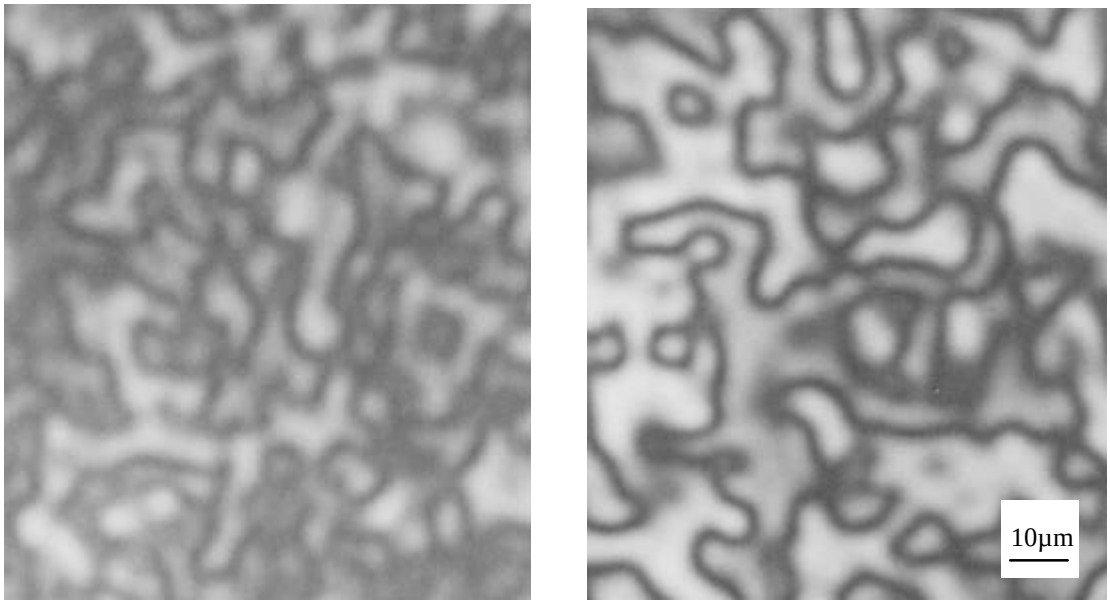

a) b)

Fig. 4-13: *Nematic textures for spin-coated film sample SC110 upon annealing. (a) The sample was cooled down from the isotropic state very quickly to room temperature. (b) The same as (a) after being annealed at 109 °C for one hour, the domain grew significantly.* T_{NI} *= 110.7°C for the film.*

Surface memory effect upon thermal treatment

Under the polarizing microscope, brushes of side chain LC polymers exhibit similar nematic texture patterns as the spin-coated films generated from the same LC polymer. It would be interesting to investigate the time dependence of the textures from the LC brush samples, that can be done by comparing the textures after the samples have been annealed at elevated temperatures or even heated to the isotropic state, in order to observe how the domain size and the textures would change.

Figure 4-14 shows three pictures of textures from an LC brush sample B086 (thickness 85.6 nm) being under various thermal treatment. Figure 4-14a was the texture obtained at room temperature after the sample had been heated in the standard way. At 120°C which was well above the T_{NI} of the brushes (= 113.7 °C), an isotropic state without any optical structure was observed (Fig. 4-14b). As expected, a nematic texture similar to those before the isotropization reappeared when the temperature decreased to a value below the T_{NI} (Fig. 4-14c). Upon close inspection of the two pictures before and after the isotropization (Figs. 4-14a, and 4-14c), it can be seen that not only similar but virtually identical textures were observed, although between them there had been an isotropic state at which the arrangements of the mesogens had been completely destroyed (Fig. 4-14b).

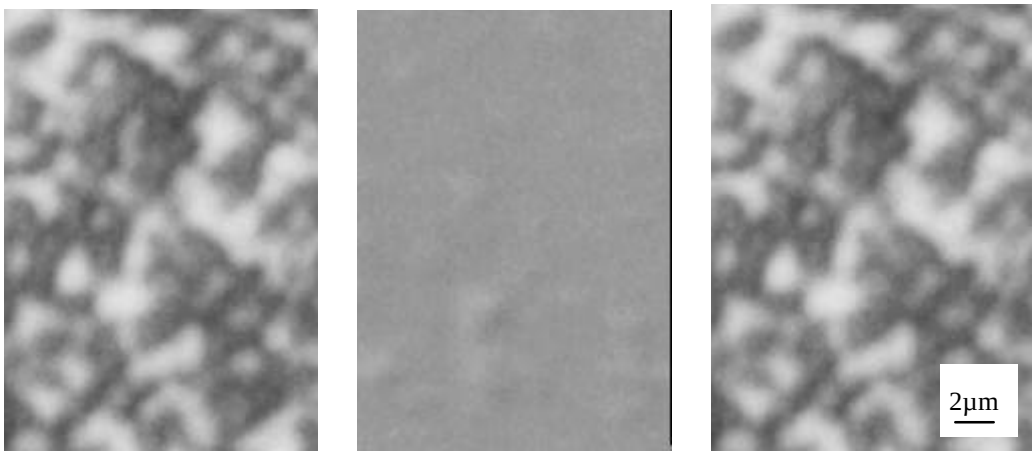

a) b) c)

Fig. 4-14: *Surface memory effect of LCP brushes (sample B086) upon thermal treatment. a) LC texture at room temperature. b) At 120°C, the LC phase was destroyed (T_{NI} = 113.7°C). c) The identical texture patterns as those of a) reappeared upon cooling back the sample.*

This "**surface memory effect**" [Peng99] is very well reproducible. For a series of brush samples with various thickness and after isotropization times from a few seconds to more than half an hour, this effect was always present.

To further investigate the surface memory effect, the brush sample B228 (thickness 228.2 nm) was annealed at 110°C (T_{NI} = 113.7°C) for 24 hours and subsequently isotropized at 120°C for 26.5 hours, then 130°C for 3.5 hours and 140°C for 3.5 hours. At certain times during the test, the sample was briefly cooled back to about 90°C (at which the brushes are nematic) to take a picture of the nematic textures of the sample. Comparison of the pictures (not shown) taken at different test points gave the evidence that the domain structures had survived thermal treatments below and above the N-I

transition point for very long annealing time and remained unchanged, indicating the thermal durability of the surface memory effect of the LC brushes.

Subsequent overnight isotropization at 150°C of the sample caused darkening and blurring on the texture, possibly due to oxidation of the brushes from the continued heating at high temperatures in air. With these pictures, textures could still be seen but damages on their patterns made it difficult to test the memory effect.

Memory effect upon solvent treatment

The textures observed in the nematic state of the LC polymers can be easily quenched and super-cooled to room temperature. The nematic texture is destroyed only when the sample is heated to temperatures higher than the T_{NI}. Another way to delete the nematic state is to wash the brush sample in a good solvent of the LC polymer, where the polymer chains are freed and the arrangement of the mesogenic units is erased. The solvent treatment is specially suited for brush samples because the chemical attachment of the polymer chains ensures that the thin film would not be damaged by solvents. A solvent exposure just relaxes the polymer molecules and the sample turns into an isotropic state just as the one from the synthesis.

Figure 4-15 shows texture pictures taken before (Fig. 4-15a) and after (Fig. 4-15c) the LC brush sample B86 had been immersed in dichloromethane for two hours. Dichloromethane is a good solvent for the LC polymer and strongly swells the brushes, rendering the surface-attached film completely isotropic (Fig. 4-15b). Clearly, the textures before and after the solvent treatment are identical and the brushes have memorized their texture patterns on the substrate surface against the solvent treatment of the sample.

Discussions on the memory effect

We have shown that LC brushes prepared on glass substrates can memorize their nematic textures upon thermal isotropization or solvent treatment. Both thermal isotropization and solvent treatment have the same effect in deleting the ordered mesogenic units into random arrangements, rendering the sample into an isotropic state. Neither of these two methods has an effect in changing the texture of the brush sample, though. The mesogenic units always get their former arrangements back when the sample returns to its nematic state again (e.g. by heating).

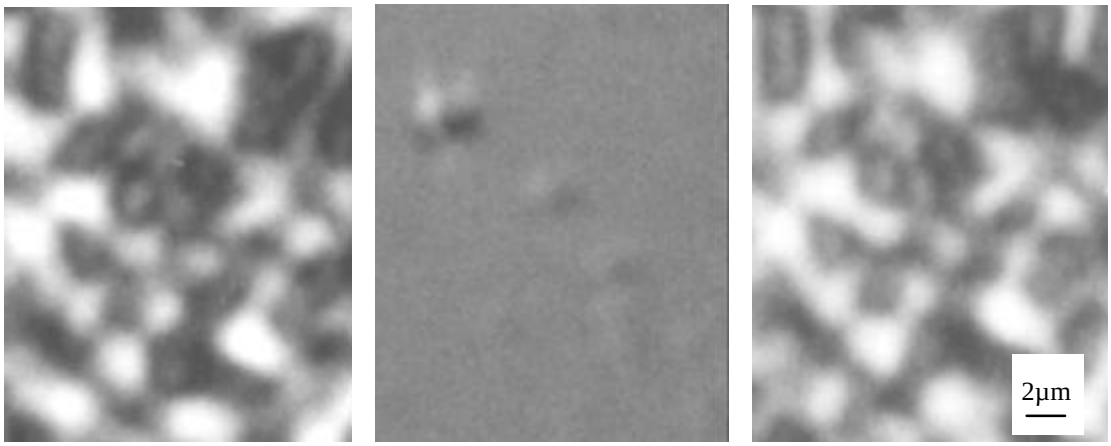

a) b) c)

Fig. 4-15: *Surface memory effect of LCP brushes (sample B086) upon solvent treatment. a) LC texture at room temperature; b)after immersing in dichloromethane for two hours, the LC state was destroyed; c) the identical texture patterns as those of a) reappeared by heating the sample. All the pictures were taken at room temperature.*

It is clear that spin-coated polymer films do not retain their texture patterns upon thermal treatment so they do not show memory effect at all. Experiments revealed that isotropization of a spin-coated film for even a few seconds changed the texture patterns completely. Contrary to spin-coated LC polymer films, LC brushes change neither the domain size, nor even the domain shapes upon thermal or solvent treatments (the surface memory effect). For a brush sample, the LC textures seem to be permanently inscribed on the substrate surface like a stamp. Neither heating nor solvent could erase or destroy such a stamp-like pattern which makes the same texture appear again and again as long as the sample goes in the nematic temperature region.

If brushes and spin-coated samples are compared, similarities and differences have to be taken into consideration. Parameters which are easily comparable in the two systems include:

a) Chemical structure of the polymers was the same in both cases. Molecular weight and molecular weight distribution were comparable.

b) Substrate treatment. The same glass substrate (BK7, Schott) was used which was cleaned and pre-treated in the same way.

c) Thermal history of the samples. The films were heated in the same standardized way (§4.2) and treated such that they had the same thermal history.

Moreover, for a detailed discussion of the two systems, also some differences have to be recognized. They include:

a) Chain conformation and 3-D structures. Although the polymers have chemically the same repeat units, the brushes exhibit a different chain conformation and 3-D structures as the spin-coated films [Alex77, deGe76, deGe80].
b) Anchoring behavior. Although the substrate treatment was the same, the anchoring behavior for the mesogenic units might no be the same due to the differences in the film preparation procedures.
c) Chain movement and free energy relaxation which are in connection with the annihilation of the disclinations when a sample is annealed.

4.7 Texture of Spin-Coated Acrylate LC Polymer Films

Nematic textures of the acrylate LC polymer PA6 were investigated with the polarizing microscope in a similar way. A small amount of PA6-1 sample (see Table 3-4) was placed on a clean glass slide, another slide was then covered on the top. The sample was heated to 130°C (at which the polymer was isotropic) for several minutes to erase thermal stress and history. The polymer between the two slides then formed a thin film. Pictures of the sample's nematic textures were taken and shown in Fig. 4-16.

Quenched from the isotropic melt at 130°C rapidly to room temperature, very small domains in the micrometer range were formed with the PA6 film, which is quite similar to the PM6 spin-coated films treated the same way (Fig. 4-16a, cf. Fig. 4-13a for the PM6 film). As expected, the domains grow upon annealing the sample at elevated temperatures. The domain growth rate is, however, much faster for the acrylate polymer sample than for the methacrylate analogs. After being annealed at 100°C which is 23°C lower than the T_{NI} of PA6 for only ten minutes, for example, the PA6 domains grew almost 50 times bigger (Fig. 4-16b). The domains could be annealed to really large size (Fig. 4-16c). Given a little longer time and at higher temperatures, even a monodomain could be produced in which all the disclinations were annihilated and a homogeneous domain with the size of the substrate was obtained (Fig. 4-16d).

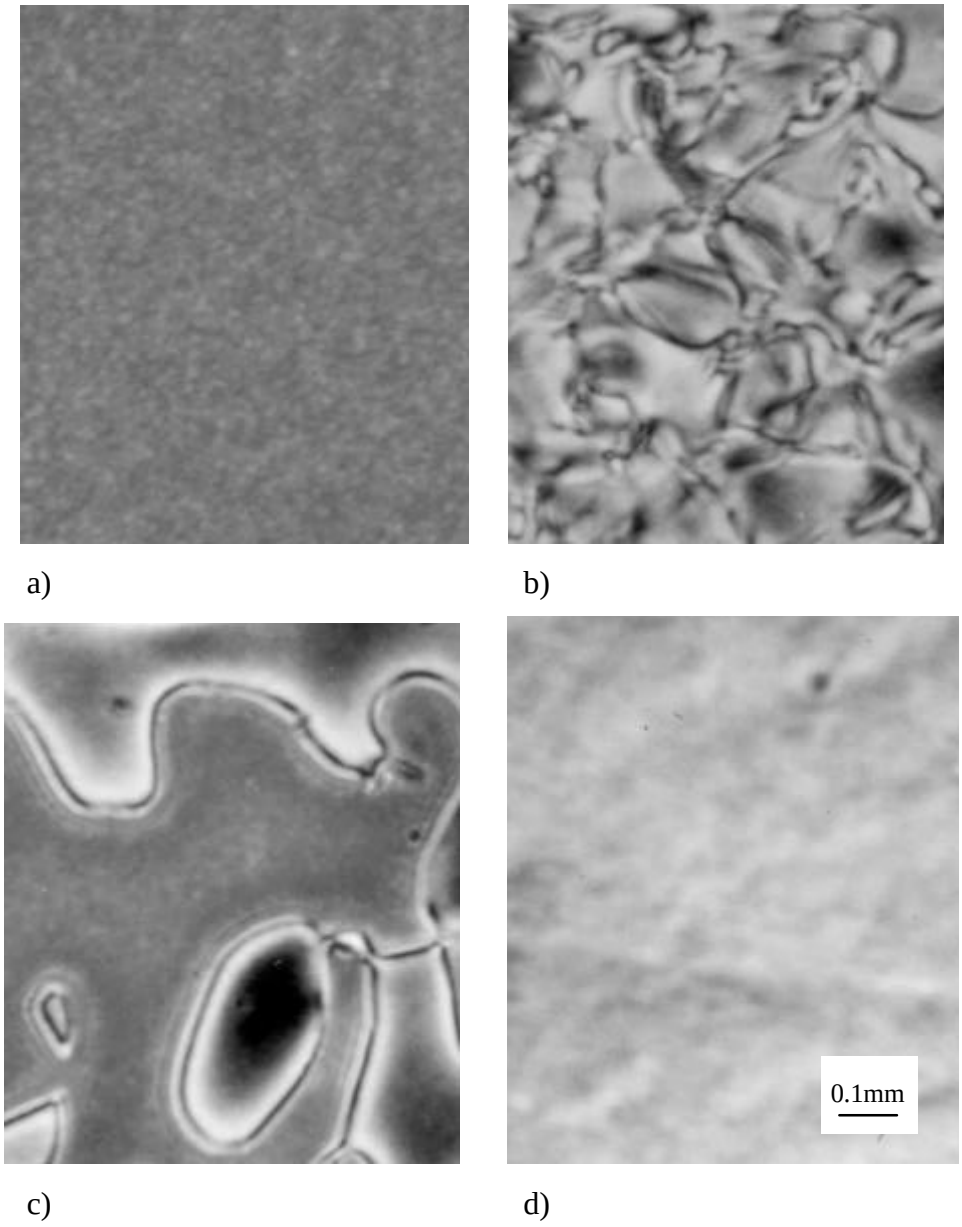

Fig. 4-16: *Liquid crystalline textures of the polymer PA6-1 under the annealing procedure: (a) after the sample had been cooled down from the isotropic state very quickly to room temperature; (b) the same as (a), after being annealed at 100°C for 10 minutes; (c) and then at 106.5°C for 3 minutes; (d) subsequently at 122°C for 30 minutes.* T_{SN} *= 97.3°C and* T_{NI} *= 123.0°C for the bulk PA6-1 polymer.*

The thermal behavior of the methacrylate counterpart differs from that of PA6 mainly in the growth rate (cf. Fig. 4-13). Attempts have been made, both with main chain and side chain LC polymers, to obtain large domains. They have been achieved only after days or even weeks of careful annealing [Neöl98]. Due to the simplicity in the synthesis and the possibility to form large domains and monodomains in a short time, the acrylate side

chain LC polymer PA6 could be suggested to be a good candidate for the investigation of the thermal behavior of LC polymers.

The reason for the rapid growth of the PA6 domains might lay in the enhanced mobility of the acrylate polymer backbones which are less hindered due to the absence of the methyl group on the side of the main chain, in comparison to the methacrylate polymer. This argument has been used for the explanation of the great difference in the glass transition temperature of acrylate and methacrylate polymers [Mark86]. The glass transition temperatures of poly(methyl methacrylate) (PMMA) is 105°C, whereas that of poly(methyl acrylate) is 6°C. The difference in T_g between PM6 and PA6 is smaller (T_g for PM6 = 50°C, and for PA6 = 30.8°C), but there does exist a big disparity in the annealing behavior between the two side chain LC polymers.

5 Phase Diagram

5.1 General Remarks

A prerequisite for the LCP brushes to be used as alignment layers is a sufficient miscibility of the brushes with the ambient low molecular weight (LMW) nematic medium. Otherwise, swelling and concomitant chain stretching into the nematic bulk as predicted by the theories will not occur.

In order to obtain information about the miscibility between the LCP brushes and the LMW nematics. Phase diagrams of the bulk LC polymer mixed with the LMW nematic were investigated. The crystal-nematic and the nematic-isotropic transition temperatures of the LC polymer - LMW nematic mixtures with varying compositions were measured and plotted against the composition to get the phase diagram curves. The transition temperatures can be obtained from differential scanning calorimetry (DSC) thermographs as well as from observation of the nematic textures with the polarizing microscope.

According to the rule of Arnold and Sackmann [Arno60], liquid crystalline polymers containing a mesogenic unit identical to a low molecular mass LC might be miscible with that low molar mass LC over a wide range of compositions. In order to get a good miscibility, a LMW nematic was selected which was based on the same mesogenic core as in the side chain of the LC polymers, i.e., the nematic is a derivative of the phenyl benzoate compounds.

Results of the phase diagram studies carried out on the free LC polymers can be applied to the brush systems generated from the same polymer. Because the polymer chains in the brush systems are chemically attached on the surface, wetting the brushes with the LMW nematic can only swell the polymer chains. The swelling process at the brush/nematic interface can also be investigated with the polarizing microscope, where information about the swelling behavior as well as the swollen textures could be observed.

5.2 LC Polymers and Low Molar Mass Nematics

Selection of the low molecular weight nematic

The LMW nematic for the polymer-nematic phase behavior studies has been selected according to the rule of Arnold and Sackmann [Arno60]. From a structural point of view close to the LC polymer, the nematic should possess a phenyl benzoate group as the mesogenic unit. A general formula of the nematics having the phenyl benzoate group is depicted in Fig. 5-1.

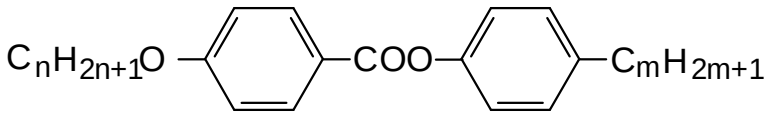

Fig. 5-1: *General structure of low molar mass nematics used for the miscibility studies.*

A series of the phenyl benzoate derivatives depicted in Fig. 5-1 (n = 1-10, m = 0-19) have been prepared to study their LC phase behavior [Mete73, Neub80]. Depending on n and m, these compounds have N-I transition temperatures between 50° and 100°C. For the phase diagram with PM6, a mixture consisted of two of these phenyl benzoate derivatives was selected in order to lower the crystal-nematic transition temperature to values below room temperature. The mixture is commercially available from Merck and has the name of ZLI-1052. The following subsection gives a detailed description of this nematic.

The low molar mass nematic ZLI-1052

The LMW nematic used in this work, ZLI-1052, is a binary eutectic mixture of aromatic esters which have the same phenyl benzoate core but different end groups (cf. Fig. 5-1). The two components of ZLI-1052, named ZLI-1004 and ZLI-245, are themselves nematics which show their LC phases at temperatures higher than room temperature. Mixing the two compounds at a weight ratio of two to one lowers the crystal-nematic transition (the melting point) to 15°C so that the mixture is nematic at room temperature, which is necessary for its application in LC displays. Figure 5-2 shows the chemical structures of ZLI-1004 and ZLI-245. Some physical constants of ZLI-1052 and its two components are listed in Table 5-1.

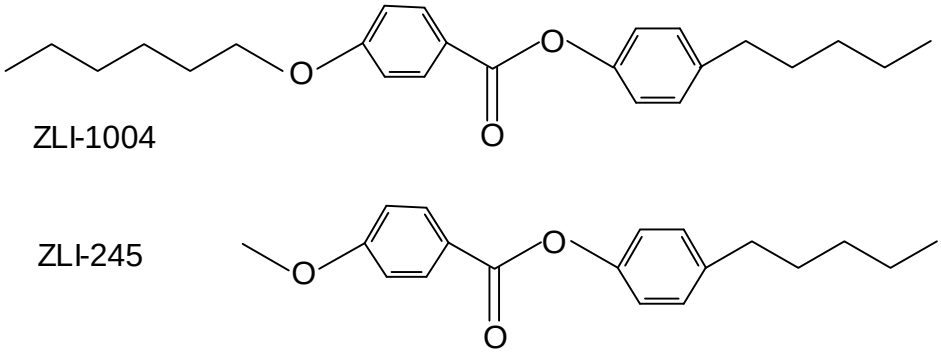

Fig. 5-2: *Structures of the components of ZLI-1052, binary eutectic mixture of the aromatic esters ZLI-1004 and ZLI-245 with a weight ratio of 2:1.*

Table 5-1: *Physical properties of ZLI-1052 and its components*

Commercial name	Melting point (°C)	T_{NI} (°C)	n_o (20°C, 589nm)	Δn
ZLI-1052	15	48	1.5063	+0.1449
ZLI-1004	50	62	--	--
ZLI-245	32	42	--	--

ZLI-1004 and ZLI-245 are solids at room temperature. The preparation of ZLI-1052 was carried out simply by mixing the two components (without any solvent) at a weight ratio of (ZLI-1004 : ZLI-245 = 2:1), which liquefied the mixture to an opaque solution at room temperature. The mixture was stirred at 50°C (i.e. above the T_{NI}) overnight to ensure complete mixing.

5.3 N-I Transition of the LC Polymer-Nematic Mixtures

Sample preparation

Various mixtures of the LC polymer PM6 and the nematic ZLI-1052 were prepared by dissolving the desired amounts of the two components in THF and stirring the solution overnight. To get homogeneous samples for DSC measurements, the solvent was slowly evaporated in vacuum when the solution was cooled with dry ice/ethanol. The temperature of the solution was kept around -40°C. As a consequence, the evaporation proceeded very slowly under these conditions. Complete solvent removal was achieved after one night.

For the optical measurements, a drop of the THF solution was deposited on a clean glass plate. After evaporation of the solvent, another glass plate was placed on top of the dried droplet. Before the measurements, the sample was heated to 120°C which is well above the N-I transition of the mixtures, to eliminate possible thermal stress.

N-I transition temperatures as measured by DSC and polarizing microscopy

The heating rate for all the DSC measurements was set to 10°C/min. Figure 5-3 shows a typical data set taken on different mixtures from PM6-1 and ZLI-1052. The nematic-isotropic transition is seen as an endothermic peak on the DSC thermographs whose minimum gives the T_{NI} value.

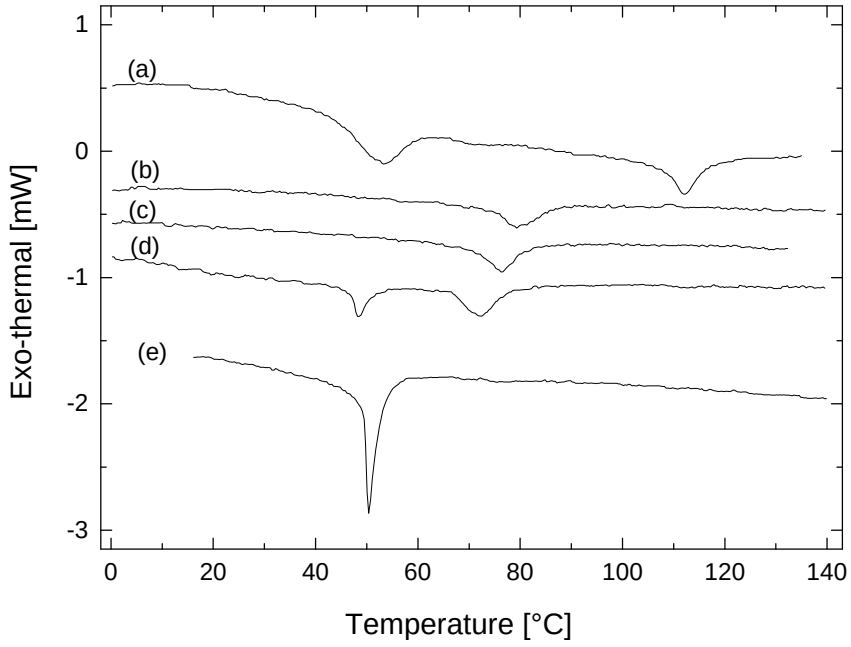

Fig. 5-3: *DSC thermographs obtained from the bulk polymer PM6-1 (a) and three mixtures with ZLI-1052 with 60% (b), 50% (c), and 30% (d) polymer weight fraction, and the pure nematic ZLI-1052 (e). The two peaks in curve (d) indicate the occurrence of phase separation. The curves have been vertically shifted for clarity.*

The N-I transition temperatures of the LMW compound ZLI-1052 (T_{NI} = 48.8°C, Fig. 5-3e) and the polymer PM6-1 (T_{NI} = 113°C, Fig. 5-3a) are quite different due to the presence of the polymer backbone. Note that the asymmetric peak at 50°C in the trace of the pure polymer (Fig. 5-3a) is connected to the glass transition (cf. the DSC curves and the discussion in §3.6).

Coexistence of two phases is observed for samples with polymer content below 50%. The two distinct peaks obtained from the sample with 30% polymer (Fig. 5-3d) are clear evidence for phase separation. Clearly, the two peaks represent two different nematic-isotropic transitions.

For samples with a polymer fraction of 50% or higher, a single nematic-isotropic transition endothermic peak occurs. The transition temperature decreases when the polymer weight fraction decreases (cf. Figs. 5-3b, 5-3c). The occurrence of a single peak suggests that the compounds are miscible over the entire temperature range. Observations with optical microscopy revealed, however, that this not the case. There are two transitions but they are so close together that they cannot be resolved by the DSC. This highlighted the necessity for optical observations.

The principle of the N-I transition temperature measurement for the LC polymer-nematic mixtures is the same as for the LC polymer brush samples, that is, the complete disappearance of the nematic textures defines the transition temperature. The microscopic observation revealed, furthermore, details of optical nematic textures of the mixtures, where two phases could be clearly seen when the phase separation happened at lower polymer fractions (Fig. 5-4).

The pictures in Fig. 5-4 show examples of a single phase (Fig. 5-4a), a phase separation where two nematic phases (nematic I /nematic II) coexisted (Fig. 5-4b), and a phase separation where a nematic phase (nematic I) and an isotropic phase coexisted (Fig. 5-4c). The nematic phase is recognized by its characteristic Schlieren texture, while the isotropic phase appears featureless dark.

Phase diagram

Phase diagrams can be obtained by plotting the nematic-isotropic transition temperatures of the polymer-nematic mixtures against the polymer content (Fig. 5-5). A general agreement can be observed in Fig. 5-5 between the experimental data generated from DSC thermographs (open triangles) and from observation of texture disappearance under the polarizing microscope (solid squares).

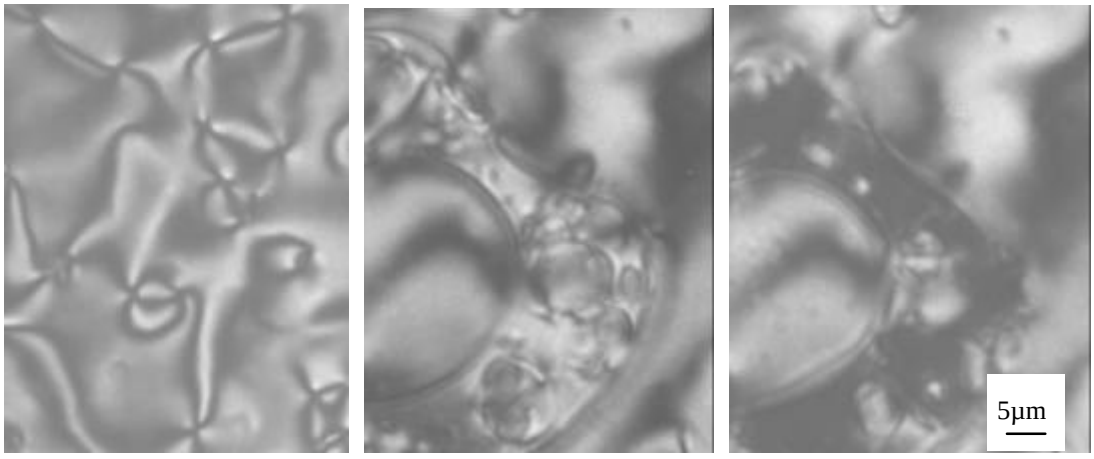

a) b) c)

Fig. 5-4: *Optical textures of PM6-1 / ZLI-1052 mixtures as observed under the polarizing microscope. (a) Single nematic phase (60% polymer weight fraction at 28 °C); (b) nematic I / nematic II coexistence (30% polymer weight fraction at 47 °C); (c) nematic I / isotropic coexistence (the same composition as **(b)** at 49 °C).*

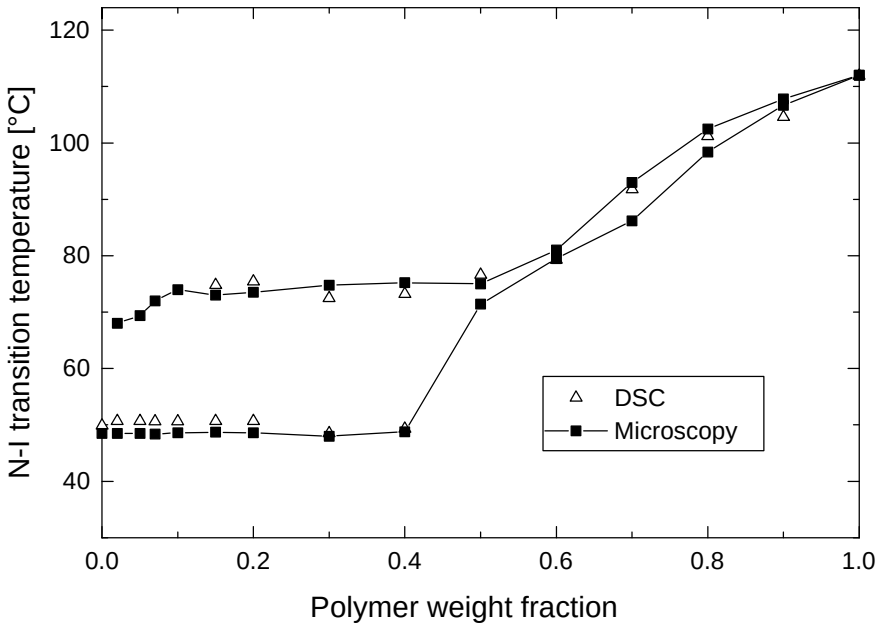

Fig. 5-5: *Phase diagram for the mixtures of polymer PM6-1 / ZLI-1052. The transition temperatures from DSC measurements (open triangle) generally agree with the microscopy data (solid square).*

It should be pointed out, however, that for samples with polymer fractions higher than 50%, only one endothermic peak appears in the DSC thermographs (see Figs. 5-3b and 5-3c), while microscopy measurements reveal narrow transition regions (1—5°C). A DSC peak usually spans a temperature range of 5—10 °C (cf. DSC peaks in Fig. 5-3), such narrow transitions can not be resolved by the DSC. The resolution of the optical microscope is typically ±0.1°C. Therefore, this technique for the detection of the transition temperature for the phase diagrams was pre-dominantly needed for all subsequent investigations.

5.4 Phase Diagram

Phase diagrams of PM6 and ZLI-1052

The phase diagrams of the LC polymer / nematic system from polymers with a high (PM6-3, M_n = 80 300 g/mol) and a low (PM6-11, M_n = 10 900 g/mol, both are GPC data) molecular weight are shown in Fig. 5-6. The symbols represent nematic-isotropic transition temperatures measured with the polarizing microscope.

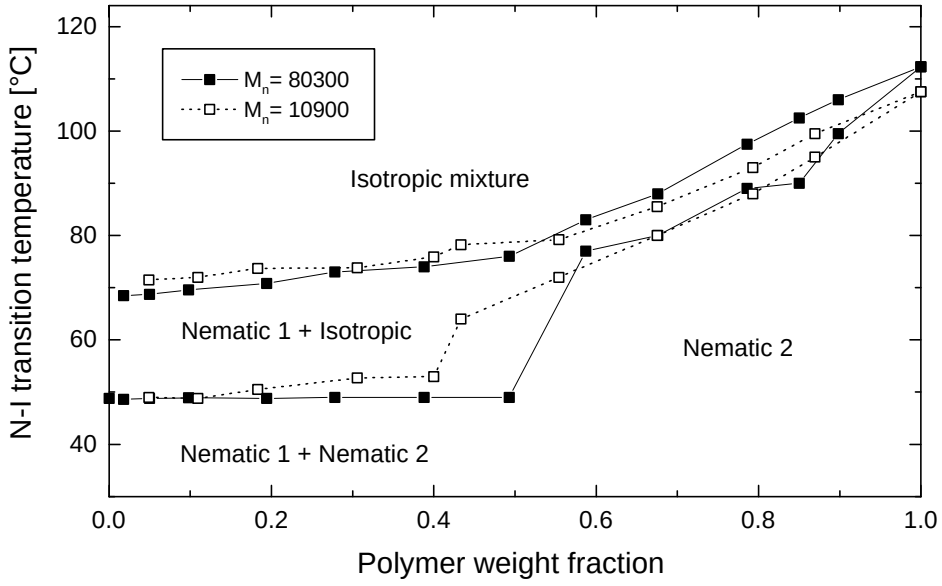

Fig. 5-6: *Experimental phase diagrams of PM6-3 / ZLI-1052 and PM6-11 / ZLI-1052. The molecular weights M_n (GPC) of the polymers PM6-3* (■) *and PM6-11* (□) *are 80 300 g/mol and 10 900 g/mol, respectively. The transition temperatures were measured with the optical microscope. The two substances have good miscibility at high polymer contents. A miscibility gap appears, however, when the polymer fraction is lower than 50%.*

Both LC polymers with different molecular weights are miscible well with the LMW nematics at high polymer contents. The phase diagrams show, nevertheless, the existence of a miscibility gap as the polymer fraction goes below 50%, in spite of the fact that the nematic components and the mesogens in the polymer side chains have similar chemical structures. An extension of the LC temperature range have been noticed in an LC polymer - LMW nematic system where the LC polymers consist of polysiloxane backbones and side chains the same as PM6 and the LMW nematics are also phenyl benzoate derivatives [Fink82]. Similar miscibility gaps have been found in such a system, too [Bent85]. It is obvious that the rule of Arnold and Sackmann [Arno60], which applies very well in multi-component LMW LC systems, could not be simply employed for the LC polymer - LMW nematic systems due to the presence and the influence of the polymer backbones.

The nematic-isotropic transition of the pure polymer PM6 occurs at 113°C. The N-I transition temperature decreases when ZLI-1052 is added to the polymer. At high polymer fractions, PM6 and ZLI-1052 are miscible. Immiscibility shows up for polymer content around 50%, at which two phases coexist. Further addition of ZLI-1052 to the system does not change this coexistence, which continues throughout the whole concentration range down to very low polymer concentration (Fig. 5-6). We could not detect miscibility of small amount of PM6 in the nematic solvent, although this is expected theoretically.

For LC polymer / ZLI-1052 mixtures with a polymer content below 50%, where the phase separation occurs, we find two clearly separated N-I transition temperatures. The lower transition temperature $T_{NI,1}$ is found at 48°C for all compositions in this range. This temperature is also the transition temperature for pure ZLI-1052. The upper transition temperature $T_{NI,2}$ is found around 72 - 73°C. Again, no significant dependence on the polymer content is noticed for $T_{NI,2}$.

Judging from these temperatures and micrographs, we found the following phases as a function of temperature for all composition with the polymer fraction less than 50%. Below 48°C, two phases coexist. The first nematic phase “nematic 1” is “solvent-rich”, i.e. it is the pure nematic ZLI-1052 with only a tiny amount of the polymer, if any. The second nematic phase (denoted “nematic 2”) is polymer-rich in that it has just the 50% composition to which these two components are miscible (note the constant $T_{NI,2}$). As the mixture is heated to a $T_{NI,1} < T < T_{NI,2}$, the solvent-rich phase clarifies and a nematic polymer / ZLI-1052 phase coexists with the isotropic solvent-rich phase. Finally, above $T_{NI,2}$ the mixture becomes one isotropic phase.

Phase diagrams from polymers with various molecular weight

In order to increase the miscibility of the LC polymers with their LMW nematic analogs, attempts were made to use polymers with shorter chains. A series of the LC polymers with various molecular weights were therefore prepared and the transition temperatures of their mixtures with ZLI-1052 were measured with the polarizing microscope. Figure 5-7 shows the results.

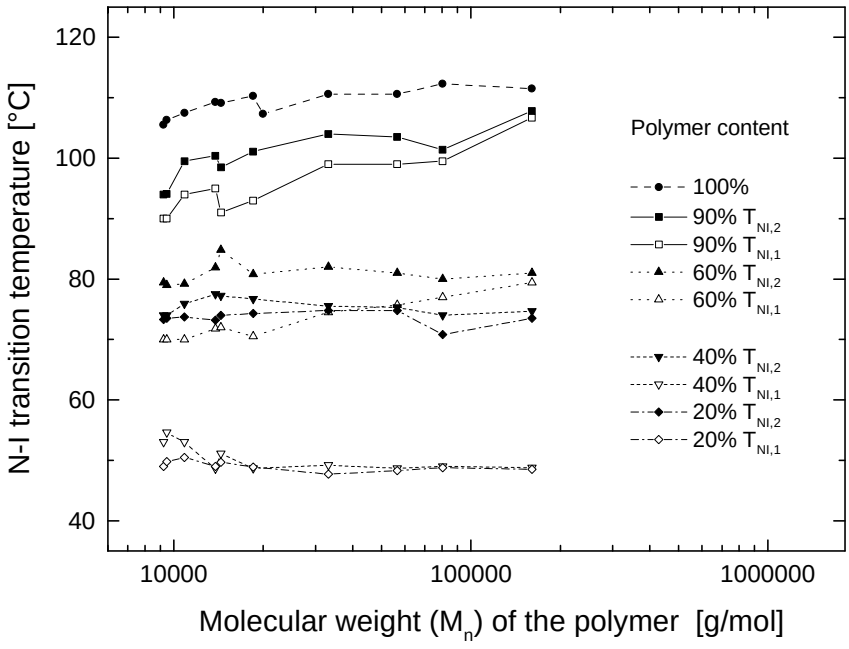

Fig. 5-7: *N-I transition temperatures of PM6/ZLI-1052 mixtures with the polymer molecular weight M_n (GPC) ranging from 160 400 to 9 200 g/mol. The solid and open symbols represent the upper($T_{NI,2}$) and lower ($T_{NI,1}$)boundary of the nematic/isotropic coexistence, respectively.*

Table 3-2 lists the molecular weights (GPC) of the LC polymers. The lowest of them is M_n = 9 200 g/mol which corresponds to 22 repeat units. Phase diagrams of all the polymers have very similar shapes with a miscibility gap when the polymer fraction is lower than 50%. The dependence of the miscible gap on the molecular weight is rather small (Fig. 5-7). Therefore, increasing the miscibility by the use of short polymer chains is not an option for the system investigated here.

In conclusion, the mixtures of the LC polymers PM6 and their LMW counterparts ZLI-1052 are miscible at high polymer contents, but exhibit a miscibility gap when the polymer fraction is less than 50%. Apparently, influences of the polymer backbone on

the LC phase behavior of the mesogenic units in the side chains are considerable, not only in increasing the N-I transition temperature of the related polymers, but also in preventing the polymer from mixing with the otherwise similar LMW nematic liquid crystals.

The phase behaviors of the polymer PM6 / nematic ZLI-1052 binary system has also been theoretically calculated using a mean field model by combining the Flory-Huggins model for isotropic mixing and the Maier-Saupe theory for nematic ordering. By adjusting several parameters, the model gives phase diagram curves that fit the experimental data quite well. The reader is referred to the literature for a detailed description [Benm99].

Phase boundary at the brush/nematic interface

The findings from the phase diagrams have consequences for the expected segment density profile of LC polymer brushes swollen with the LMW nematic. One expects a phase boundary between a polymer-rich and a solvent-rich phase at the outer edge of the brushes. At room temperature, a brush can only be swollen to about twice its dry thickness (50% content of the nematic). Beyond that point, a phase boundary is expected, where the polymer concentration drops rapidly from about 50% to close to zero (Fig. 5-8).

5.5 Swelling of the LCP Brushes with the Low Molecular Weight Nematic

Nematic textures of swollen LC brushes at room temperature

The nematic textures of the LC polymer brushes swollen with the LMW nematic was investigated with the polarizing microscope. A drop of ZLI-1052 was put on the surface of a brush sample B139 (thickness 138.9 nm). The amount of the LMW nematic substance was in great excess compared to that of the brushes on the surface of the substrate due to the thinness and hence the tiny amount of the brushes. After swelling for a given time, pictures were taken on a spot of the brush surface where most of the excess nematic liquid had been temporarily removed in order to get clearer textures. Figure 5-9 shows pictures of nematic textures for the brush sample B139 swollen with excess ZLI-1052 at room temperature in a sequence of several days.

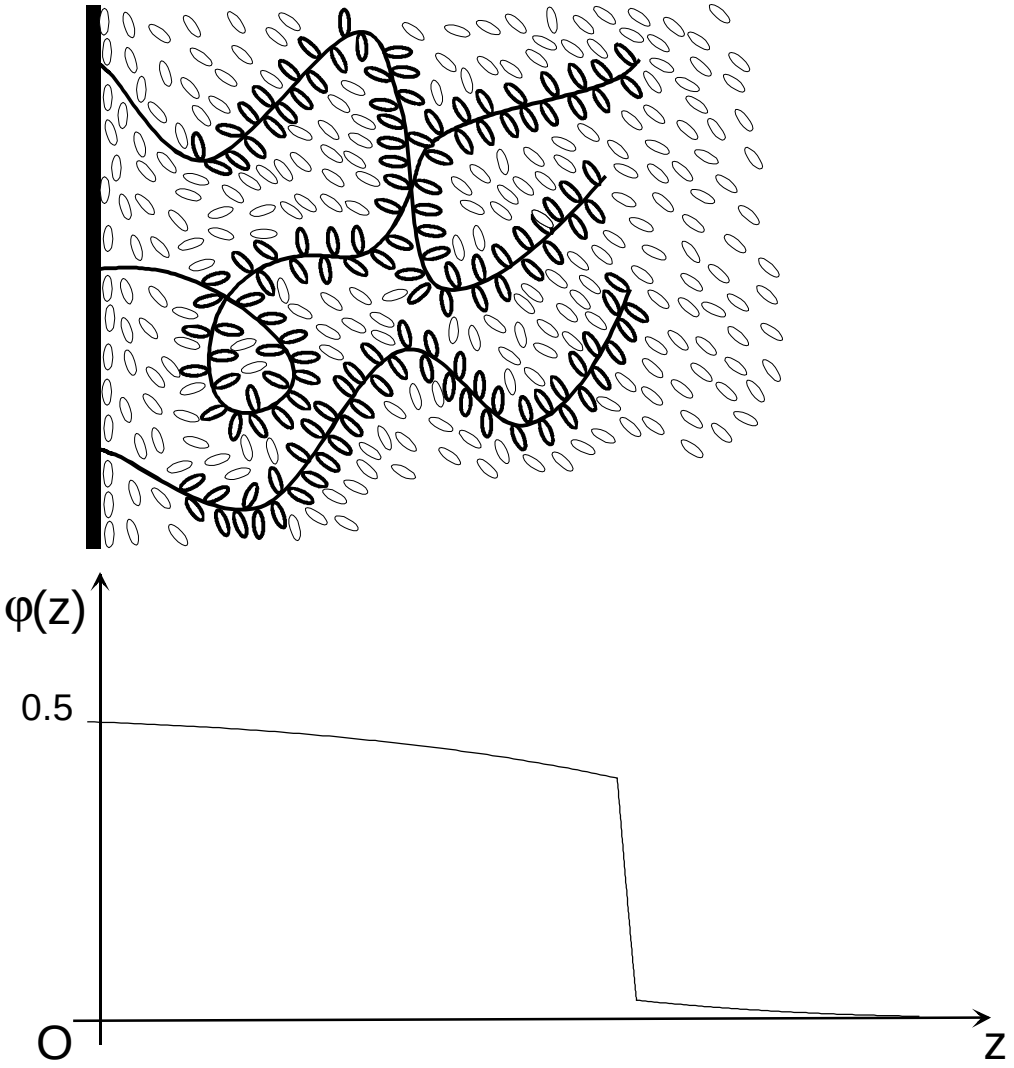

Fig. 5-8: *Schematic drawing of a phase boundary at the brush/LMW nematic interface based on the findings of the phase diagrams. The brushes are swollen by the nematic molecules twice the original thickness. At the outer edge of swollen brushes the concentration of the polymer chains drops abruptly from ca. 50% to close to zero.*

Observations showed that domain size of the brushes, swollen with excess ZLI-1052, increased with the swelling time. The nematic texture of B139 in the pure, dry state is shown in Fig. 5-9a. After swelling for 15 hours, the domain size increased 5 to 10 times (Fig. 5-9b) compared to that in the dry state. The domains were about 20 to 30 times bigger than their starting size after swelling for one week (Fig. 5-9c). Accelerated tests to swell the brushes at higher temperatures for a time much longer than one week gave similar domain size as the one shown in Fig 5-9c.

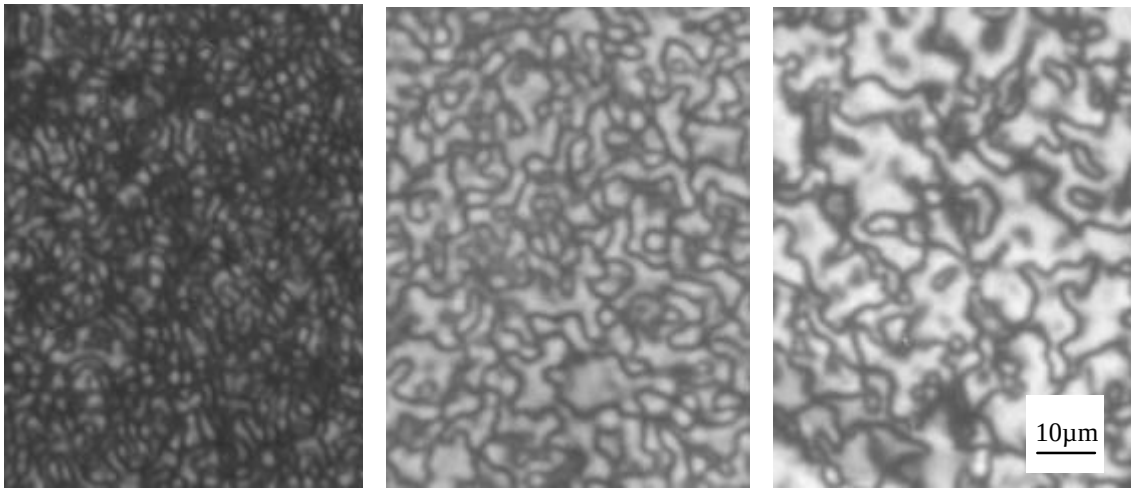

a) b) c)

Fig. 5-9: *LC textures of the brush sample B139 in the pure dry state (a); after swollen with excess ZLI-1052 for 15 hours (b); and for seven days (c). Both the ZLI-1052 and the underlying swollen brushes have attributed to the nematic textures shown in (b) and (c). All experiments were carried out at room temperature.*

Nematic textures of swollen brushes at elevated temperatures

The N-I transition temperature of the brushes drops dramatically after being mixed with sufficient ZLI-1052 (from 113°C to about 72°C, cf. the phase diagram of Fig. 5-6). Nevertheless, it is still higher than T_{NI} of the pure LMW nematic which occurs at 48°C. Therefore, there exists a temperature region (from 48°C to 72°C), at which the nematic solvent is isotropic, while the swollen brushes are nematic. This interesting property of the brush / nematic system not only allows the textures of the underlying swollen brushes to be directly observed with the polarizing microscope, it is also a necessary condition for the investigation of the system with dynamic light scattering [Benm00]. Figure 5-10 shows pictures of the nematic textures of the swollen brushes observed under the polarizing microscope at different temperatures.

The pictures of Fig. 5-10 were taken on a spot of the sample B139 after the brushes had been sufficiently swollen with ZLI-1052. There was a thin lay of excess ZLI-1052 on the top of the swollen brushes. Therefore, the field of view (Fig. 5-10a) was much brighter than that of pure brushes (see, e.g. Fig. 5-9a). At 55°C (Fig. 5-10b), the excess ZLI-1052 has become isotropic. The picture reveals the textures of the underlying swollen brushes alone. Identical patterns are observed in the two pictures (cf. Figs. 5-10a, 5-10b). The brightness of the latter (Fig. 5-10b), though, is much lower, because the LMW nematic is isotropic and only the much thinner swollen brushes are responsible for the polarized light. The identity of the texture patterns between the swollen brushes and the excess nematic on the top indicates that the brush could transfer its orientation to the adjacent

nematic bulk, which is the prerequisite if the LC polymer brushes are to be used as alignment layers for nematic liquid crystals.

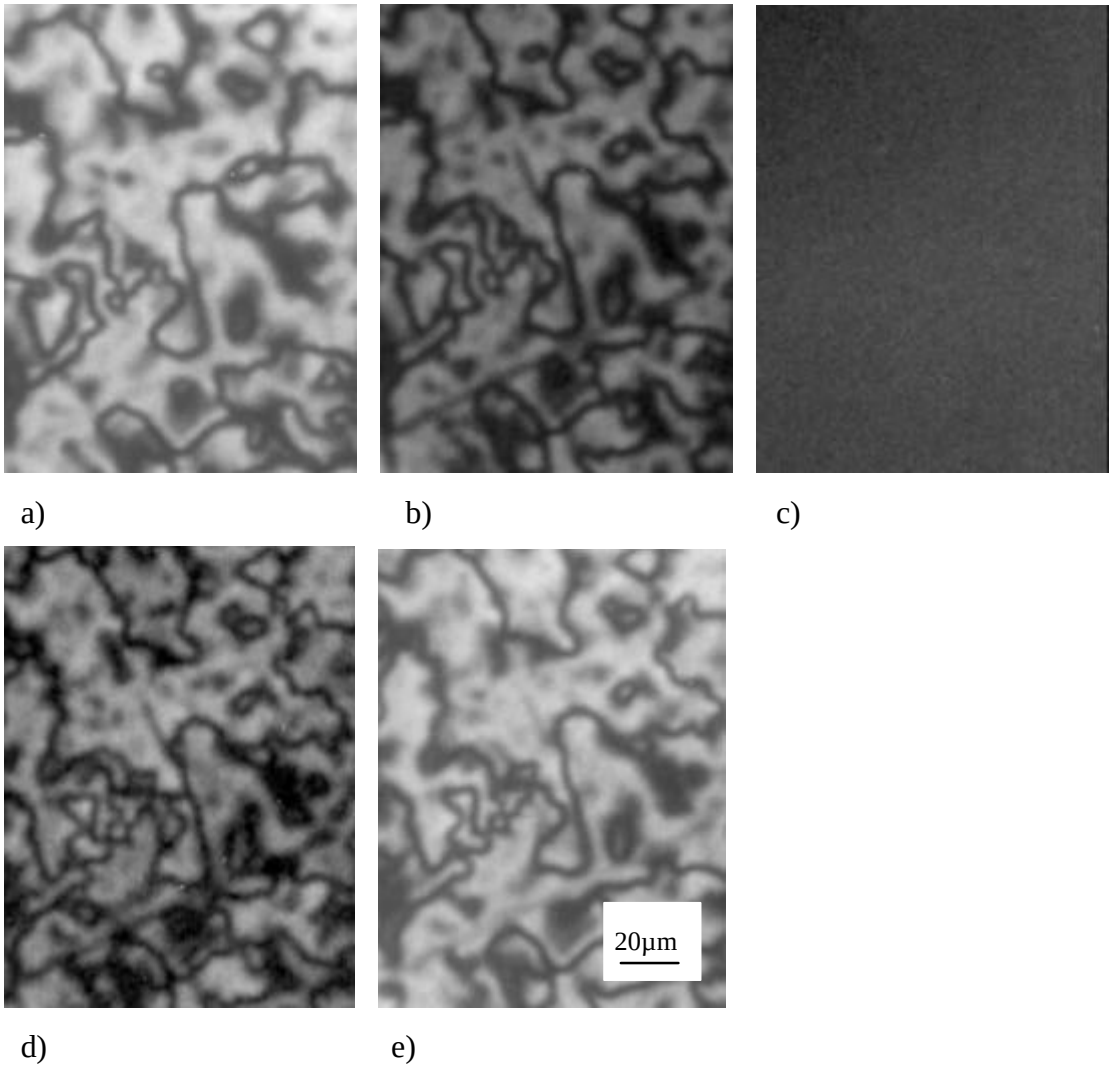

Fig. 5-10: *LC textures of PM6 brushes (sample B139) after swelling with ZLI-1052 and heated to temperatures of: (a) room temperature; (b) 55°C; (c) 80°C; (d) 65°C; and (e) room temperature. The N-I transition temperatures of the pure LMW nematic and the swollen brushes are 48°C and 72°C, respectively.*

At 80°C, which is well above the T_{NI} of the swollen brushes, the whole system changed into isotropic and the field of view turned completely dark (Fig. 5-10c). Cooling back to a temperature where the bulk LMW nematic was still isotropic, but where the brushes were in the nematic state (e.g. 65°C), a texture reappeared (Fig. 5-10d). Careful comparison of the two pictures before and after the isotropization (i.e. Figs 5-10b, 5-10d) shows that identical textures are obtained, in spite of the fact that the sample went through an isotropic state at which all the arrangement orders had been wiped out.

The surface memory effect operates on the swollen LC polymer brushes, as well. It can be seen that side chain LC polymer brushes, whether in the un-swollen dry state or swollen with a LMW nematic, can memorize their characteristic textures on the substrate surface.

Further cooling of the sample back to room temperature brought back the presence of the nematic state of the free ZLI-1052 (Fig. 5-10e). As expected, Fig. 5-10e has the same textures as that of Figs. 5-10d, 5-10b and 5-10a. The phenomenon that the swollen brushes can transfer their orientation to the adjoining nematic bulk was observed once again in the cooling process (cf. Figs. 5-10d and 5-10e).

6 Homogeneously Aligned LC Polymer Brushes

6.1 General Remarks

Observed under the polarizing microscope, LC polymer brushes grown on clean, untreated glass substrates exhibit irregular polydomain textures whose domain size is in the micrometer range (§4.2). Mixing with a LMW nematic solvent like ZLI-1052 swells the brushes and the domain size increases, but still remains in the micrometer range (§5.6). In order for the brushes to be used as alignment layers, homogeneous domains of at least the millimeter size are required, i.e. the mesogenic units are homogeneously oriented throughout the whole domain. The methods to align LMW liquid crystals include application of external forces or the introduction of an anisotropy on the surfaces (§1.2.2). Generally, those methods can also be adopted for the preparation of homogeneously aligned LC polymer brushes.

The LMW liquid crystals in the LC states exhibit liquid-like behaviors, that is, the molecules diffuse freely much like those in liquid. The arrangement of the LC molecules can be therefore easily carried out by external forces like magnetic and electric fields, or forces generated by a flow in a certain direction etc. In choosing an external force, the magnetic field is a more practical way to orient the LC molecules than the electric field is because the presence of an electric current can cause electrochemical reactions and therefore damage the substance, especially when impurities exist in the system.

The energy needed to align LMW LC molecules is quite small. An isotropy on the surface, for example, can arrange the LC molecules to a certain orientation. The situation with the alignment of LC units in polymers is, however, much more complicated where the orientations of the mesogenic units depend not only on the movement of the mesogenic groups themselves but also on the movement and conformation of the polymer backbones. Although the influence of the backbone conformation is reduced by the spacer inserted between the mesogenic unit and the backbone, it is still difficult to orient the LC units due to the high viscosity of the polymer melts. Hence, very strong magnetic field are needed for this purpose [Hess85]. To avoid the difficulties connected with the high viscosity, a practical alternative could

be, therefore, to align the mesogenic groups before or during the polymerization, where only the monomer molecules are involved.

6.2 Growth of LC Brushes under an Orientated Nematic Medium

Nematic media for brush growth

The first idea to prepare LC brush samples with large domains was to carry out the polymerization in a nematic environment in the presence of strong magnetic field. Under these conditions, the nematic molecules are orientated by the magnetic field and the brushes were grown in an environment where a certain alignment of the nematic molecules existed. It was hoped that the brushes thus prepared would have their mesogenic units in the side chains also aligned according to orientation of the LMW nematic surrounding.

The nematic medium can of course be a pure monomer itself which shows the nematic phase at the polymerization temperature (usually at 55 - 70 °C, in this work at 60 °C). Figure 6-1 shows two monomers that possess such a property.

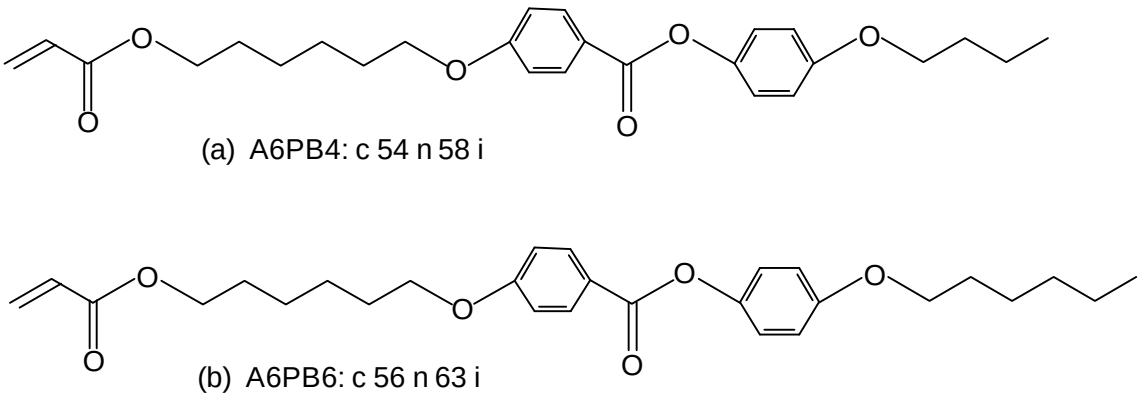

Fig. 6-1: *Monomers that exhibit nematic phase at the polymerization temperatures (55° — 60°C): a) A6PB4: c 54 n 58 i; b) A6PB6: c 56 n 63 i; where c stands for crystal, n for nematic and i for isotropic phases.*

All of the monomers depicted in Fig. 6-1 have similar chemical structure as that of the monomer A6. The differences among them lay in the length of the repeating CH_2 units in the alkyloxyl end groups: A6 has one, while A6PB4 has four and A6PB6 has six CH_2

units in the end groups that are attached to the phenyl benzoate mesogenic core (hence the short names A6PB4 and A6PB6).

Another possibility to create a nematic environment is to use mixtures of two compounds. One component of the mixtures should be the monomer M6 which has been well characterized in this work. Since M6 shows no LC phases, the other component must be a nematic itself and should have a chemical structure similar to M6 such that no immisibility problems would occur. Figure 6-2 shows a nematic which meets the demands.

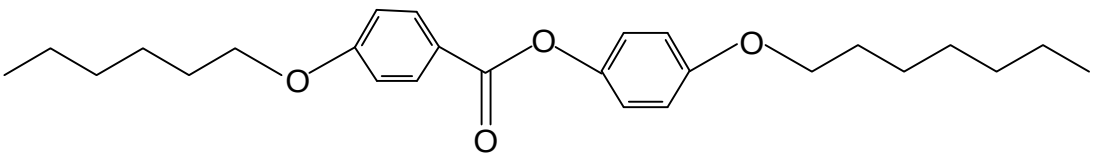

6PB7: c 55 n 86 i

Fig. 6-2: *Nematic 6PB7 that is mixed with the monomer M6 to get a nematic phase at the polymerization temperature.*

The nematic 6PB7 has, like M6, a phenyl benzoate group as the mesogenic unit to which two end chains with 6 and 7 methylene units are attached (hence the abbreviation 6PB7). Pure 6PB7 shows the nematic phase at temperatures (55° - 86° C) higher than the polymerization temperature. After mixing with M6, the LC phase regions decrease (Table 6-1).

The mixtures show complicate phase behaviors under the polarizing microscope as well as in DSC thermographs. Nevertheless, with increasing 6PB7 fraction, the C - N as well as the N - I transition temperatures increase. At the polymerization temperatures of 55°-60°C the mixture should be in the nematic phase. Mixtures with a 6PB7 content between 40% and 100% reach this requirement (Table 6-1).

Brushes grown in a nematic medium

LC brushes were grown under a strong magnetic field in an oriented nematic medium of M6-6PB7 mixture. A B-H15 (Brucker) electromagnet served as the source for the magnetic field. An M6 - 6PB7 mixture with 40% 6PB7 was placed on a glass substrate that had been immobilized with the initiator ADCS. Degassing was carried out under vacuum for one hour at 45°C at which the mixture was liquid. The system was then put between the poles of the magnet with the magnetic field perpendicular to the surface of

the substrate. Polymerization was done under vacuum at 55°C for 39.5 hours with a magnetic field intensity of 16 000 Gauss.

Table 6-1: *Phase transition temperatures of M6-6PB7 mixtures*

Weight percent of 6PB7 (%)	Microscopy (°C)		DSC (°C)	
	C → N	N → I	C → N	N → I
20	25-40	48.8-54.3	27-38	47.3-54.3
42	27-42	60-70	23.3	60.8
60	37-45	60-67.7	41.8	68.4
75	25-59.8	66.3-81	43.3	71.3
86	--	75-86.4	48.2	79.4
90	35-48	77.8-82	--	--
100	55	86	55	86

After completion of the reaction, formation of free LC polymer in the reaction vessels was qualitatively detected, indicating the occurrence of the polymerization. After extraction of the substrates with toluene, drying and subsequently heating, nematic textures of the brush sample was observed under the polarizing microscope and shown in Fig. 6-3.

It can be seen that polydomain structures are obtained for the LC polymer brushes which were grown in the oriented nematic medium generated by the strong magnetic field. The textures of the brushes are similar to those grown without the magnetic field (Fig. 6-3a). Swelling the LC brushes shown in Fig. 6-3a with ZLI-1052 increased the domain size (Fig. 6-3b), but the resulted domains are not larger than expected.

Further experiments with systematic variation of the reaction parameters such as the composition of the mixtures (40% - 60% 6PB7), the degassing time (1 - 4 hours), the polymerization temperature (55° - 60°C), the polymerization time (24 - 72 hours), and the magnetic field intensity (16 000 - 18 000 Gauss) gave similar results, that is, LCP brush with polydomain nematic textures.

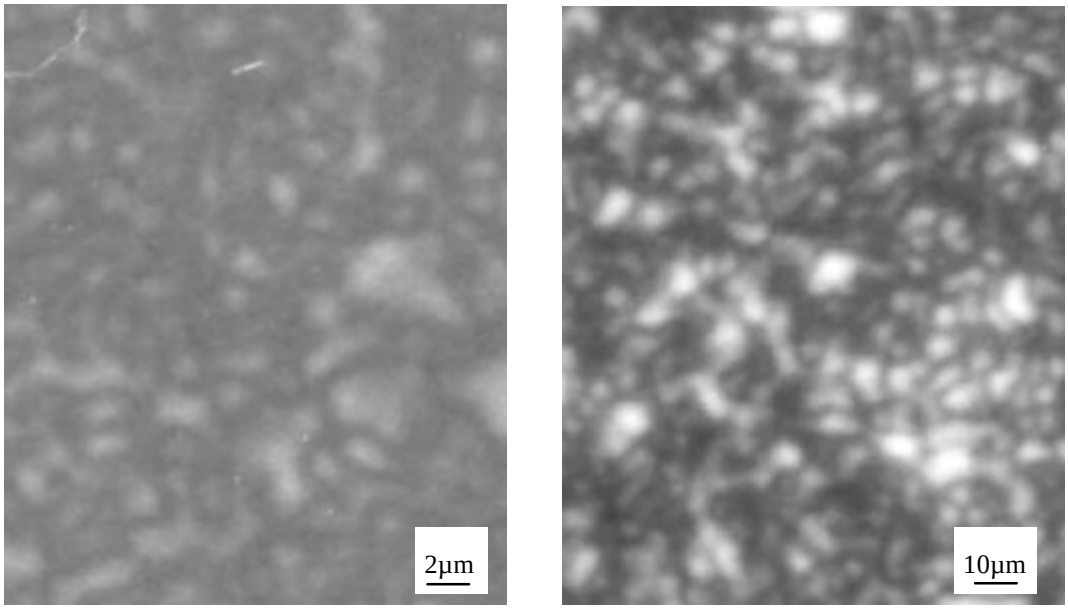

a) b)

Fig. 6-3: *Nematic textures of LC brushes grown in the magnetic field with an intensity of 16 000 Gauss: in the pure, dry state (a); and after being swollen with the nematic ZLI-1052 (b).*

The idea to grow brushes in a nematic medium under strong magnetic field has been proved unsuccessful for the systems studied here. Another idea to introduce the desired orientation was aimed at the substrate surface. The surfaces of the glass substrates are isotropic. This in-plane isotropy can be broken by mechanical treatments such as surface rubbing. Subsequently, an anisotropy appears. In the following it was studied whether the mesogenic units of the LCP brushes could align themselves on the substrate surface according to this anisotropy.

6.3 Preparation and Properties of Homogeneously Aligned LC Polymer Brushes

Substrate rubbing and preparation of homogeneously aligned brushes

As has been discussed in §1.2.2, rubbing a substrate is a wide-spread technique to destroy the in-plane isotropy of a surface for purposes of LC alignment [Berr73]. Material such as cloth, paper, Teflon, and other textiles have been used to rub the substrate. As the rubbing material, a special kind of velvet cloth (Yoshikawa YA-20-R) was used for the rubbing process in this work.

Glass substrates were cleaned by sonification in 2% Hellmanex solution and subsequent rinsing with milli-Q water and ethanol. To rub a surface, a dried substrate was put face down on a piece of the velvet cloth. A gentle vertical pressure was exerted on the substrate by hand while the substrate was drawn over the velvet. This was usually repeated three times so that the whole rubbing length reached ca. 65 cm. Fibers that are loosely absorbed on the surface were blown away with a stream of air.

Rubbed substrates were subjected to immobilization and polymerization in the same way as described in §3.5 to generate the LC polymer brushes. A series of brush samples were prepared under similar conditions with a monomer concentration of [M6] = 0.78 - 0.80 mol/L and a polymerization time between 11 and 14 hours. All reactions were carried out at 60°C. After the brush growth, the substrates were carefully extracted with toluene overnight to remove the physisorbed polymers from the surface. Thickness of one brush sample in the dry state was measured with an Alpha-step 200 (Tencor Instruments) setup as 65.3 nm. Because all brushes were grown under similar conditions, a thickness around the value 65.3 nm is expected also for other brush samples.

The heating of the samples was carried out as described in §4.2. Subsequent microscopic observation revealed that the brushes grown on the rubbed substrates show homogeneously aligned nematic textures called monodomain textures. It can been noticed that this simple one-step treatment, rubbing, brings about effective alignments of the mesogenic units in the side chains into uniform arrangements. The following subsections give a detailed description of a systematic studies on the properties of these samples monodomain textures.

Optical texture of LCP brushes grown on rubbed substrates

Under the polarizing microscope, the PM6 brushes grown on substrates that had been rubbed previous to the immobilization and the film growth displayed quite different nematic textures compared to the samples with the same brushes grown on untreated substrates. Two prominent differences were noted upon inspection of the textures of these two types of samples:

a) The texture of the brushes grown on untreated substrates consists of a great number of tiny, irregular domains (see Fig. 4-3), while the whole surface of a brush sample on the rubbed substrates contains virtually only one domain with occasional defects (Fig. 6-4d).

b) The average brightness of a polydomain sample under the polarizing microscope remains the same with the rotation of the sample with respect to the crossed

polarizers, while for a monodomain sample the rotation gives rise to periodical changes in the brightness (Fig. 6-4, see also Fig. 6-5).

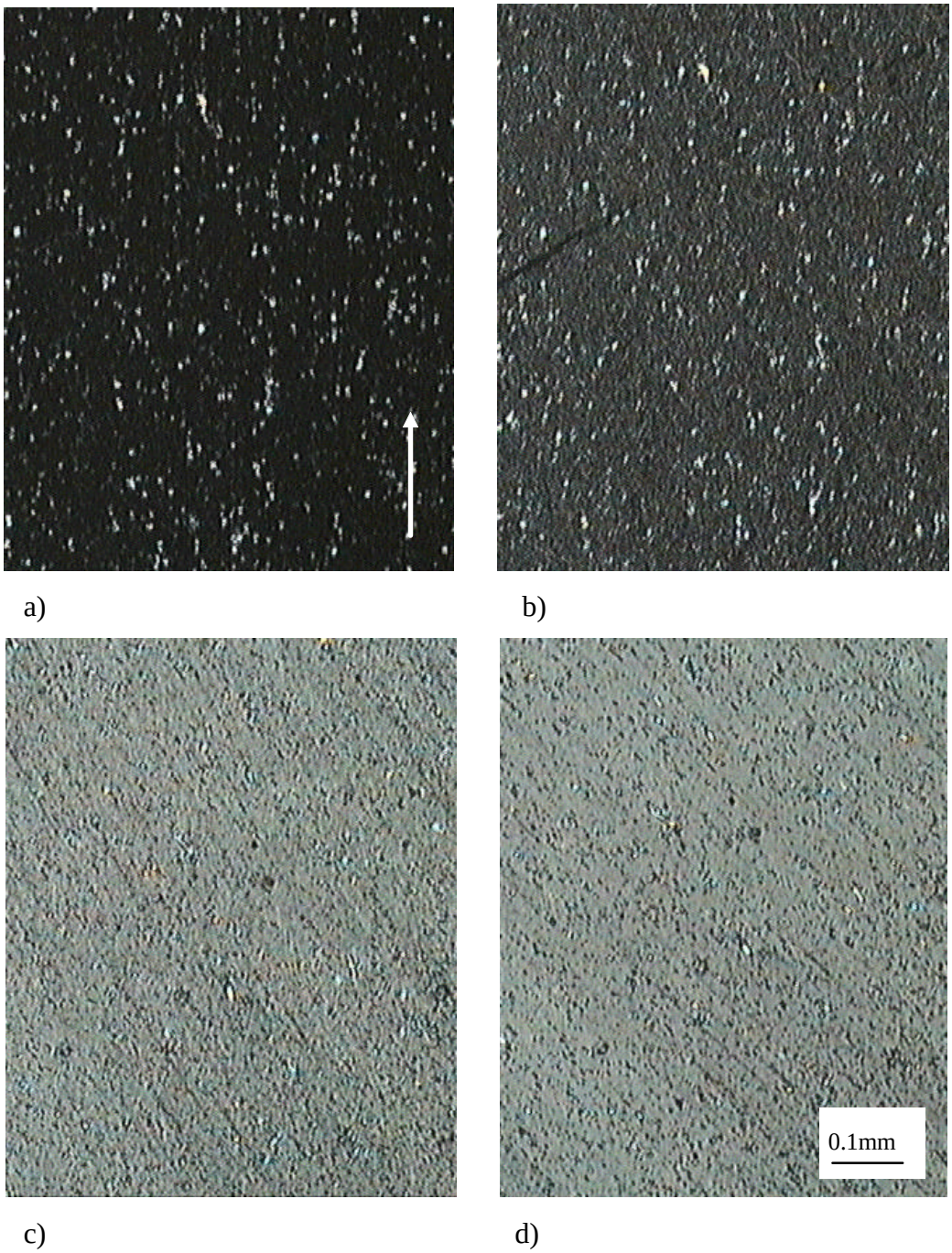

Fig. 6-4: *Nematic texture under the polarizing microscope of a homogeneously aligned LCP brush sample at the rotation angles of a)0°, b)15°, c)30°, and d)45°. The brightness changes regularly with a period of 90°C (see also Fig. 6-5). The arrow shows the rubbing direction.*

The irregular domains are the disclinations resulted from specific arrangements of the mesogenic units in the brushes. The arrangements and the related disclinations are quite common both with LMW nematics and spin-coated LC polymer films [deGe93, Noël89]. These typical polydomain textures are not observed on LC brushes grown on rubbed substrates, which show monodomain textures (Fig. 6-4). Admittedly, there are numerous small spots that scatter irregularly on the sample surface. They come from defects that were introduced during the rubbing process (details see §6.5), not from the mesogenic units.

If the LC molecules are planar aligned to a macroscopic size, rotating the sample will give rise to periodical change in the transmitted light intensity due to the birefringent character of LC molecules [Coll98]. This is just the case for the monodomain brush samples, where the mesogenic units are planar oriented (see later). For the polydomain LC brush samples, although the mesogenic units within a single domain range are aligned, the alignment directions are different in different domains. The effects from all the domains are diminished with each other, therefore, no periodical change of the brightness by rotation is observed with these samples.

Transmission light intensity of LCP brush monodomains

The average brightness of an anisotropic sample under the polarizing microscope can be quantified as the integrated transmitted light intensity, which is measured with the implemented camera in the microscope (§4.3). The light transmission-rotation angle curves from a PM6 brush monodomain and an LC cell are shown in Fig. 6-5.

The transmission-rotation behavior of the monodomain brush sample can be more clearly illustrated by observing together Fig. 6-4 (showing the optical texture) and Fig. 6-5 (the open squares showing the transmission intensity). The rubbing direction is parallel to the 0° direction (indicated by the arrow), at which the transmission of the sample was at the lowest position (Fig. 6-4a). The sample became more and more bright when it was anti-clockwise rotated (Figs. 6-4b and 6-4c) until it reached its brightest position at 45° (Fig. 6-4d). This rotation process induces the corresponding continual increase of the transmission from 0° to 45° in Fig. 6-5. The rubbing direction and the preferred orientation of the nematic textures can be observed more clearly when the sample is at the 45° orientation (Fig. 6-4d).

Figure 6-5 shows a second transmission-rotation curve (solid squares) of an LC cell filled with ZLI-1052 (the preparation see later). The nematic ZLI-1052 molecules in the cell are homogeneously aligned parallel to the substrate surface, which was accomplished by rubbing the glass substrates with the velvet cloth, a well-established

method to produce uniform parallel alignment [Cogn82]. Clearly, the LC cell showed a regular transmission-rotation behavior with a period of 90° (Fig. 6-5).

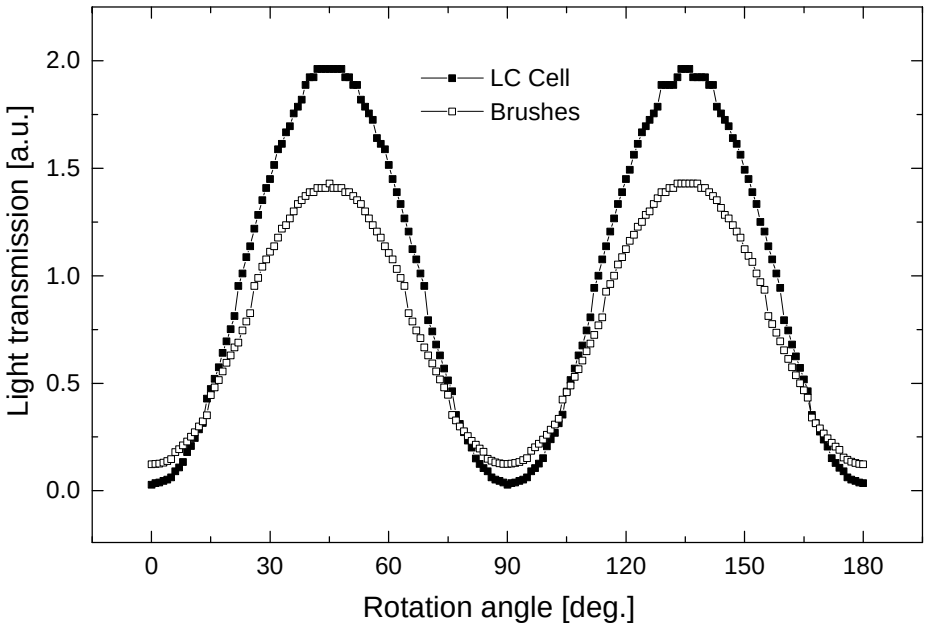

Fig. 6-5: *Light transmission of an LCP brush monodomain (open squares) and an LC cell filled with ZLI-1052 (solid squares) as a function of the rotation angle of the sample stage.*

The spacers between the substrates of the LC cell have a thickness of 23 µm. The nematic ZLI-1052 layer is therefore 23 µm thick or even thicker (cf. the thickness in Fig. 6-8). The thickness of the LC brushes is about 65 nm. In spite of the thickness difference with three orders of magnitude, both curves show very similar transmission-rotation behaviors and have the same period of 90° (Fig. 6-5). The similarities between the standard LC cell and the brush monodomain in the periodic transmission behaviors, together with the accordant microscope observations on the nematic textures, strongly suggests the presence of the homogeneous parallel alignment of the mesogenic units of the LC polymer brushes grown on the rubbed glass substrates.

Preparation of LC cells

LC cells are liquid crystals (usually nematics) sandwiched between two glass substrates, the surfaces of which are usually treated and act as the alignment layers to orient the LC molecules in between. Generally, the two substrates are glued together with thin spacers

between them. The liquid nematic is subsequently driven into the gap between the substrates by capillary force.

In this work polyethylen terephthalate (PET) films (Goodfollow, England) was used as the spacers. The thickness of the films was 23 µm. The two substrates were a little shifted in respect to each other so that a step was introduced on the cell edge for later filling of the nematic LC. After gluing, a drop of the nematic LC, in this work ZLI-1052, was placed on the edge step and the liquid was automatically sucked into the cell by capillary forces. The cell was equilibrated over night at room temperature, sometimes at elevated temperatures to accelerate the process. For the measurements carried out in this work, the two edges of the cells were not sealed.

The treatment of the substrate surface is a key factor to bring about uniform orientation of the nematic bulk with a desired tilt angle. The treated side of the substrate was placed towards the inside, in order to be in contact with the nematic bulk. When rubbed substrates were used, they were so placed that the rubbing direction was anti-parallel to each other.

We used UV Adhesive Type 651-B (Bohle, Haan, Germany) as the glue. This kind of adhesive was specially tested and selected because in some experiments the glued cells had to withstand solvent exposure (e.g. trans-decalin) at elevated temperatures for many hours [Benm00]. The thermal stability of the glue was tested in the following solvents, separately, by heating the glued cells in that solvent at 85°C over night and subsequently at 100°C for 11 hours:

a) dibutylphthalate (purum, Fluka),
b) glycerin (water free, or 85%, Fluka),
c) paraffin (purum, Fluka),
d) trans-decalin (purum, Aldrich),
e) silicon oil.

Examination of the glued cells after the heating tests showed the glue survived the heating procedures in all the five solvents listed above. It is concluded that this kind of glue for the glass substrates is not only thermally stable, but also resistant to many organic solvents.

Crystal Rotation Setup (CRS) for the measurement of tilt angle

The Crystal Rotation Setup (CRS), developed by Scheffer and Nehring [Sche76], provides a technique to accurately determine pretilt angles of a nematic LC in contact with an alignment layer (e.g. in cases of LC cells). The principles can be briefly summarized as follows.

The incident angle ψ of a laser light is changed successively by rotating the sample, and the intensity of the light transmitted through the cell and the two crossed polarizers placed before and after the cell is measured as the function of the angle ψ. Figure 6-6 gives a schematic sketch of the LC cell and the incident angle.

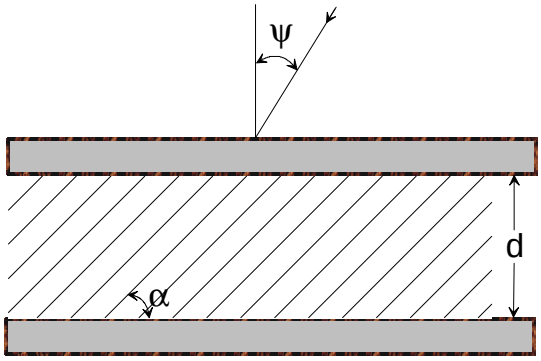

Fig. 6-6: *Cross section of a liquid crystal cell showing the tilt angle of the nematic molecules a, the incident angle y, and the cell thickness d. In a crystal rotation setup (CRS), there are a polarizer and an analyzer which are placed, with a crossed position, in the light pathway before and after the LC cell.*

The relative phase shift between the vertically and the horizontally polarized light δ(ψ) is a function of the tilt angle α of the nematic molecules, the incident angle ψ of the laser beam and the cell thickness *d*. It can be expressed as:

$$d(y) = 2p\frac{d}{l}\left[\frac{1}{c^2}(a^2-b^2)\sin a\cos a\sin y + \frac{1}{c}\left(1-\frac{a^2b^2}{c^2}\sin^2 y\right)^{1/2} - \frac{1}{b}\left(1-b^2\sin^2 y\right)^{1/2}\right] \qquad \textbf{(6-1)}$$

with

$$a = \frac{1}{n_e}$$

$$b = \frac{1}{n_o}$$

and

$$c^2 = a^2 \cos^2 a + b^2 \sin^2 a$$

λ is the wavelength of the incident radiation (A He-Ne laser was used in this work, therefore, λ = 623.8 nm.), n_o and n_e are the ordinary and extraordinary indices of refraction of the nematic ZLI-1052, respectively (see Fig. 1-1). The transmitted light intensity T(ψ) is given by:

$$T(y) = \frac{1}{2}\sin^2\left[\frac{1}{2}d(y)\right] \qquad \textbf{(6-2)}$$

A combination of the equations (6-1) and (6-2) gives the relationship between the incident angle ψ and the transmitted light intensity through the polarizer-sample-analyzer system T(ψ). The experimental data points are fitted with this equation, where the pretilt angle α and the cell thickness *d* are the fit parameters.

LC cells from monodomain brush substrates

LC cells were made from brush-monodomain substrates, that is, the substrates had been rubbed, immobilized and grown with polymer brushes to obtain the monodomain textures. The cells were filled with ZLI-1052. Figure 6-7 shows pictures of the texture observations with the polarizing microscope and Figure 6-8 gives the results of the Crystal Rotation Setup (CRS) measurements together with the pretilt angle and the cell thickness values achieved from the theoretical fitting on the experimental data.

Much less defects were observed in the texture of the brush-monodomain cell (Fig. 6-7), compared to the pure brush monodomain (see Fig. 6-4). The cell showed similar light transmission-rotation behaviors both in the nematic texture (see Fig. 6-4) and in the quantitative 90° period (see Fig. 6-5) as the samples of the brush monodomain thin film and the standard cell from rubbed substrates.

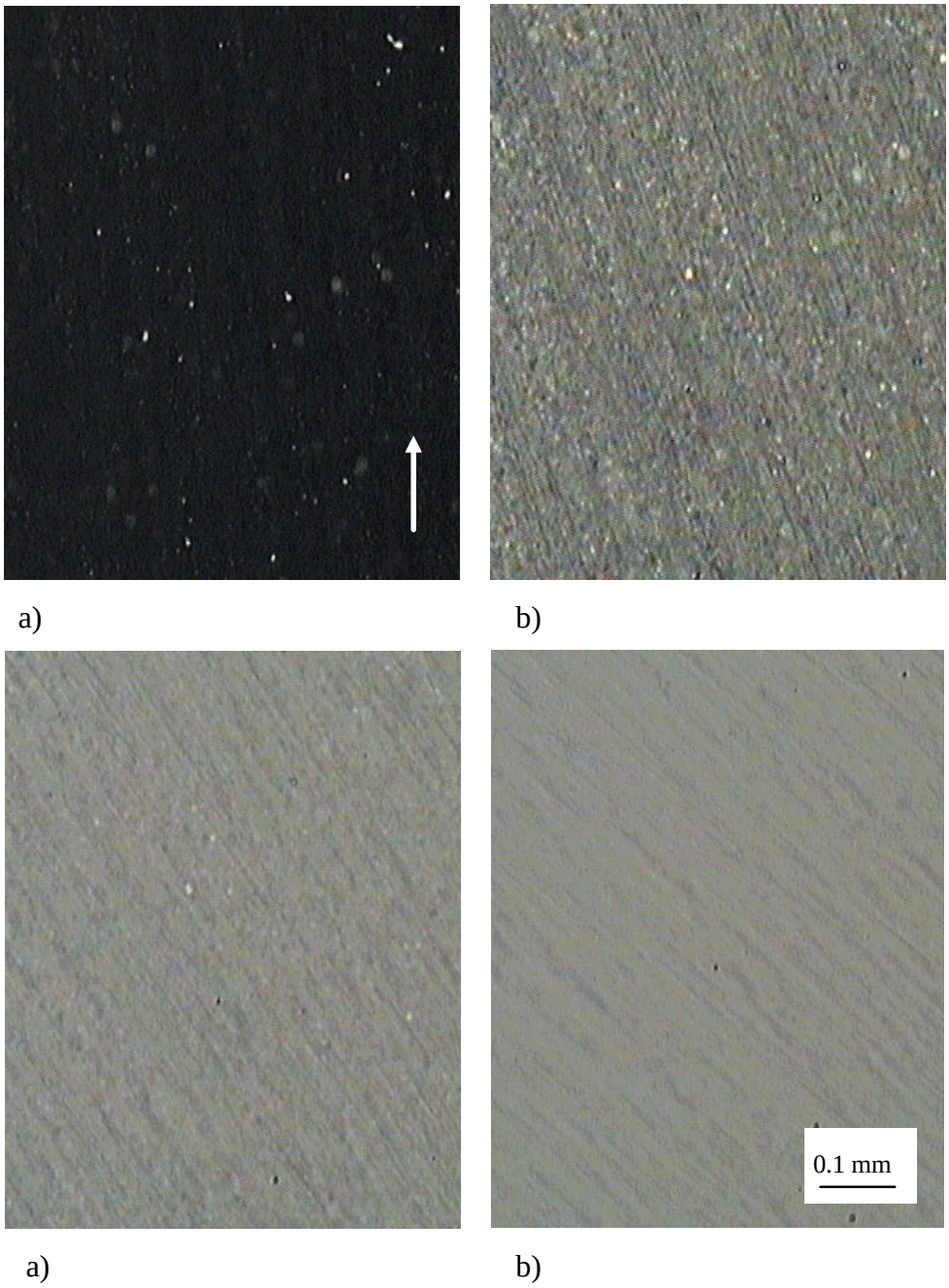

Fig. 6-7: *Textures of the LC cell made from two substrates covered with homogeneously aligned PM6 brushes observed under the polarizing microscope. The sample was rotated at the angles of a)0°, b)15°, c)30°, and d)45°. The rubbing direction is shown by the arrow.*

The experimental points from the CRS measurements are distributed symmetrically around 0° (Fig. 6-8). The fitting based on the combination of Equations (6-1) and (6-2) resulted in the cell thickness and the pretilt angle of 38.15 µm and 0°, respectively. The cell thickness is somewhat larger than the original thickness of the spacer film (= 23 µm), which could be attributed to the gluing procedure and is quite common in

preparing LC cells. At this point, there is no pretilt (*a = 0°).* The symmetry of the experimental data points show clearly a regular planar alignment is present in the LC cell.

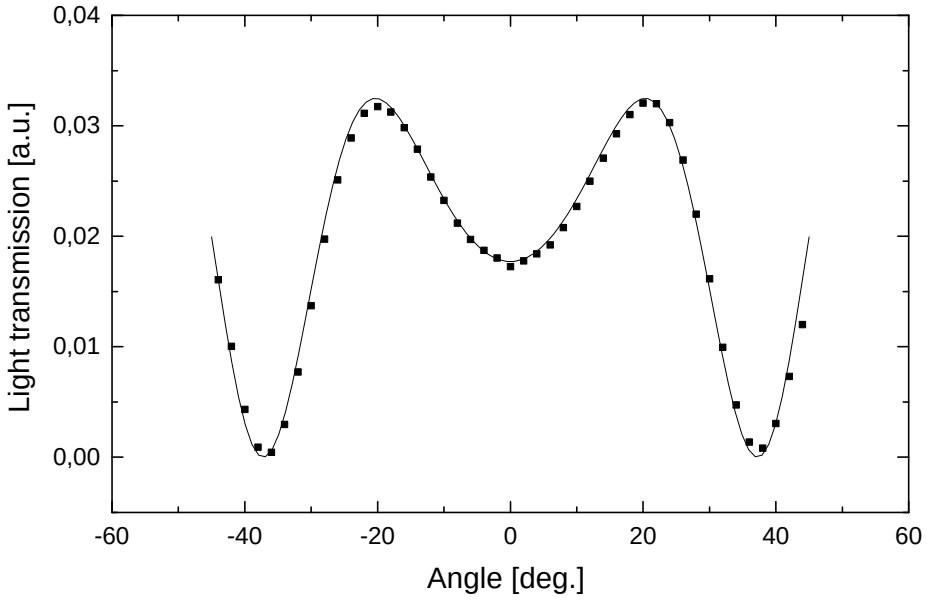

Fig. 6-8: *Crystal Rotation Setup (CRS) measurement (solid squares) of the LC cell made from two substrates both coated with homogeneously aligned LC polymer brushes and filled with ZLI-1052. The fitting (solid line) gave the cell thickness of d = 38.15 µm, and the pretilt angle of a = 0°.*

The periodical transmission-rotation behavior of the LC brush monodomains suggests homogeneous alignments of the mesogenic groups in the polymer films. CSR measurements and fittings in Fig. 6-8 show that the nematic molecules, aligned by the brush monodomains, are planar oriented in the bulk. Clearly, the mesogenic groups in the polymer side chains are not only able to arrange themselves uniformly into a monodomain in the brushes, this uniform arrangement is also capable of being homogeneously transferred into the adjoined LMW nematic molecules which in turn affect the orientation of the bulk nematic. As a result, the LC cell has achieved the homogeneous planar alignment.

In view of these findings it can be seen that the rubbing process previous to the initiator modification and the brush growth is an effective way to align the LC units in the side chains homogeneously to get polymer brushes with monodomain textures. The LC units in the brushes, when they are uniform aligned, are capable to transfer this alignment to

the adjacent nematic molecules which in turn orient the nematic bulk. Therefore, LC brush monodomain can be used as alignment layer to obtain planar orientation for LMW nematics.

6.4 Mechanism of the Homogeneous Alignment

Investigation on alignment mechanism

We have discussed that LC polymer brushes grown on pre-rubbed substrates show monodomain textures. It is of great interest to investigate the mechanism of the homogeneous alignment. As discussed in §1.2.3, there are three types of alignment mechanisms for the anchoring of LC molecules on rubbed surfaces. They are: the induced crystallization of the polymer chains on the surface, the formation of grooves, and the transfer of fibers from the rubbing material to the surface. The first mechanism (concerning induced crystallization of polymer chains) applies only to glass substrates that are coated with polymer films, not to the bare glass surfaces studied here. Therefore, we concentrated on the latter two mechanisms to discriminate which one, formation of grooves or transfer of fibrils, determines the homogeneous alignment of the mesogenic side chains.

To distinguish whether it is the formation of grooves or the transfer of fibrils which plays the essential role, the idea was to remove the organic fibers that might have been transferred to the substrate during the rubbing process, and then grow the LC brushes on such substrates to see if the monodomain property will retain. When, after removal of the fibers, the brushes do not exhibit the monodomain textures any more, it could then be concluded that the fibers should be the reason in introducing the homogeneous alignment.

Oxidative etching and UV irradiation were used to carry out the elimination of the fibrils before the brush growth. For oxidative etching, the rubbed substrate was treated with Piranha solution. Piranha solution is a mixture of concentrated sulfuric acid and hydrogen peroxide (H_2O_2) with a volume ratio of 4:1. It is a very oxidative liquid that etches away organic substances like Nylon fibers.

An alternative approach for the removal of transferred polymer fibers was to eliminate them by photo-ablation with UV light from a low pressure mercury lamp. The irradiation energy of the UV illumination is stronger than the chemical bonds in organic materials. The transferred fibers can be decomposed and ablated away by the UV light

through breaking up the chemical bonds and thus cutting the molecules into small pieces.

Pre-treatments of the substrates

The substrates were rubbed as the way described in §6.3. For the Piranha treatment, the rubbed substrates were immersed in 10 ml hydrogen peroxide and 40 ml concentrated sulfuric acid was carefully added portion by portion in to the reaction vessel and the reaction was carried out for 15 minutes. The process was repeated three times and the substrate were finally rinsed with water, and dried. A total reaction time of 45 minutes ensured that all fibers, fibrils or other organic substances that might have been transferred to the substrate surfaces were removed.

For the UV illuminations, a UV source with the Model 6000 Pen-Ray lamp (L.O.T-Oriel, Darmstadt) was used. The lamp was placed 0.5 cm above the rubbed surface of the substrates, and irradiation was carried out in two catalogues of different strength: the weak irradiation means that the treating time was 10 minutes with a low driving current at 10 mA; while the strong irradiation means that the substrates were treated with a high driving current at 17 mA for longer time (30 minutes). After these pre-treatments, the substrates were subjected to immobilization with the azo initiator and the brushes growth as before.

Figure 6-9 shows microscopic pictures of the substrate surfaces after various pre-treatments. The glass substrate surface after the rubbing process showed many defects under the microscope (Fig. 6-9a). After subsequent Piranha treatment of the rubbed substrate, all the defects were gone and a smooth surface was observed (Fig. 6-9b). The spot on the upper-left corner of the picture was a small piece of tissue purposely placed on the substrate in order to focus properly on the surface. From the cleanness of the sample surface after the Piranha treatment it can be seen that all the organic material was etched away by the oxidative solution. The microscopic observation of the substrates showed that most of the small defect centers that existed on the rubbed substrates were still on the surface after the subsequent UV treatment (Fig. 6-9c).

a) b) c)

Fig. 6-9: *Pre-treated glass substrates observed under microscope: (a) after rubbing with a velvet cloth; (b) after rubbing and subsequent Piranha treatment; (c) after rubbing and subsequent UV illumination. The arrow shows the rubbing direction.*

Growth of LC brushes on the pre-treated substrates

After the pre-treatment of the glass substrates as illustrated in the last subsection, a layer of the azo-initiator was immobilized on the surface and the LC polymer brushes were grown. The nematic textures of the brushes were investigated with the polarizing microscope to see if the monodomain characters have been preserved after the pre-treatments of the substrates (Fig. 6-10).

The first two pictures (Figs. 6-10a, and 6-10b) exhibit the texture of the LC brushes prepared on substrates that were etched with Piranha solution after the rubbing process. In contrast to the brushes grown on rubbed, but otherwise untreated substrates, a multi-domain texture was again obtained. The brightness of the texture did not depend on the rotation of the sample, proving the absence of a preferred orientation and the loss of the monodomain textures.

For the photo-ablation, the textures of the LC brushes depended on the strength of the treatment (Figs. 6-10b, -10c, -10d, and 10e). After a weak irradiation (10 mA for 10 min.), where the presumed polymer fibrils would supposedly be only partially destroyed, the final LC brush showed an increase in the defect density while the overall orientation is pertained (Figs. 6-10c and 6-10d). A periodical variation in the light transmission was still noticed by rotating the sample, indicating the existence of a preferred orientation. If, however, a longer irradiation time (30 min.) and an increased light intensity (17 mA driving current) was used, the alignment along the rubbing

direction was lost completely. The final LC brushes exhibited characteristic polydomain textures (Figs. 6-10e and 6-10f).

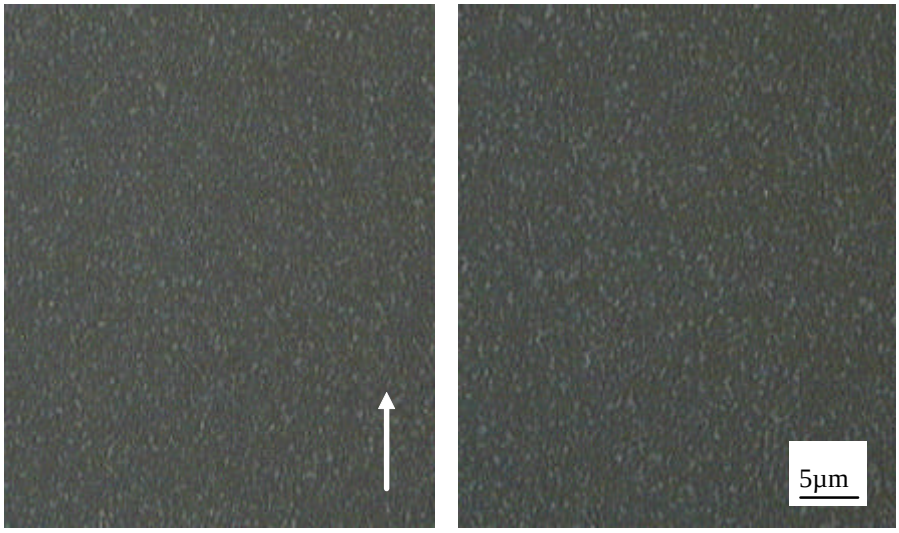

a) b)

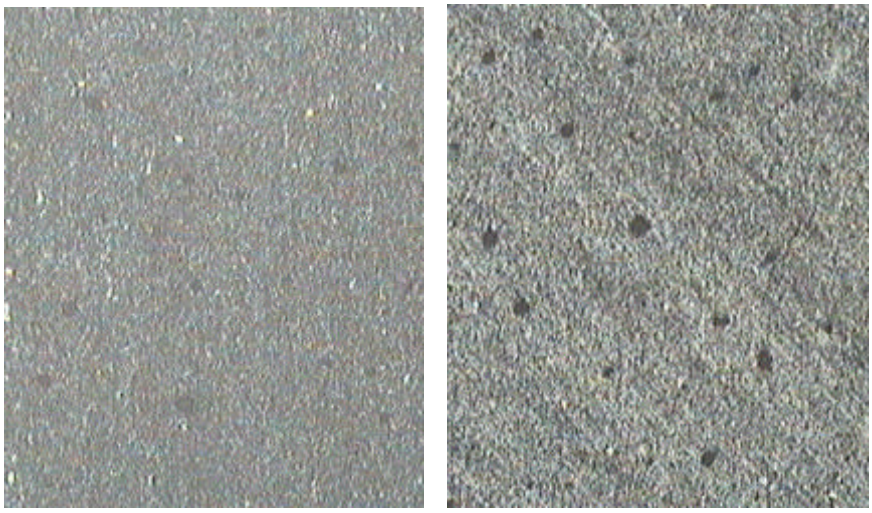

c) d)

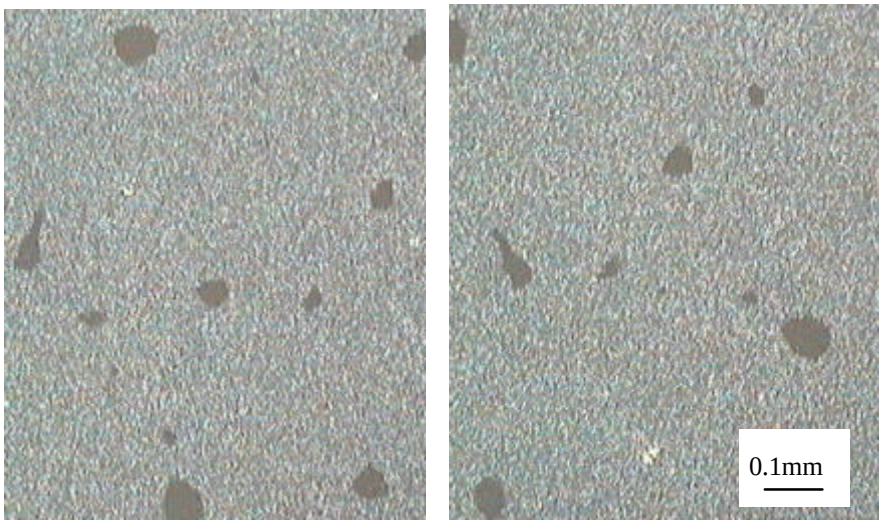

e) f)

Fig. 6-10: *LC textures observed under the polarizing microscope from brushes grown on pre-treated glass substrates. Preceding to the immobilization and the brushes growth, all the substrates were rubbed and then treated with the Piranha solution (a) 0°, (b) 45°; with a low intensity UV irradiation (c) 0°, (d) 45°; or with a high intensity UV irradiation (e) 0°, (f) 45°. The rubbing direction shown by the arrow is the same for all the substrates.*

The alignment mechanism

In conclusion, the monodomain characters, observed for LC brushes prepared on rubbed substrates, do not retain for the LC brushes when the rubbed substrates are etched with Piranha solution. These monodomain characters are partially pertained when the rubbed substrates are treated with a weak irradiation; moreover, they are entirely lost when the substrate are irradiated strongly. Generally, the UV treatment is less harmful to the glass surface than the oxidative etching by Piranha solution. Both processes are able to remove Nylon fibers that could be transferred to the substrate surface. However, the two methods have different effects on the grooves on the surface. While the oxidative etching might roughen grooves that might have been existed and thereby remove scratches in the glass, this would not be possible with the UV light.

The disappearance of alignment upon aggressive surface treatment proves that transferred Nylon fibrils - as opposed to small scratches in the glass substrate - are the alignment agent. The transferred fibers are elongated and oriented along the rubbing direction and the mesogenic units are then aligned along these fibers to form a parallel alignment. We find it remarkable that the transferred Nylon chains, firstly, did not prevent immobilization of the initiator and chain growth, and secondly, even imparted their orientation onto the brushes [Peng00].

6.5 Combination of Surface Treatments with Conflicting Anchoring Behaviors

Planar and homeotropic orientations

The conventional methods adopted in practice to introduce planar and homeotropic alignments of nematic molecules are rubbing and surfactant-covering of the substrate surface, respectively. It would be interesting to know what would happen to the orientation of the nematic molecules if both of these two conflicting procedures are applied to the same substrate. The rubbing procedure was done using the velvet cloth as the rubbing material, while the surfactant parameter was varied by selecting one of the several different surfactants to tune the interactions with the substrate. Figure 6-11 gives the chemical structures of these surfactant molecules.

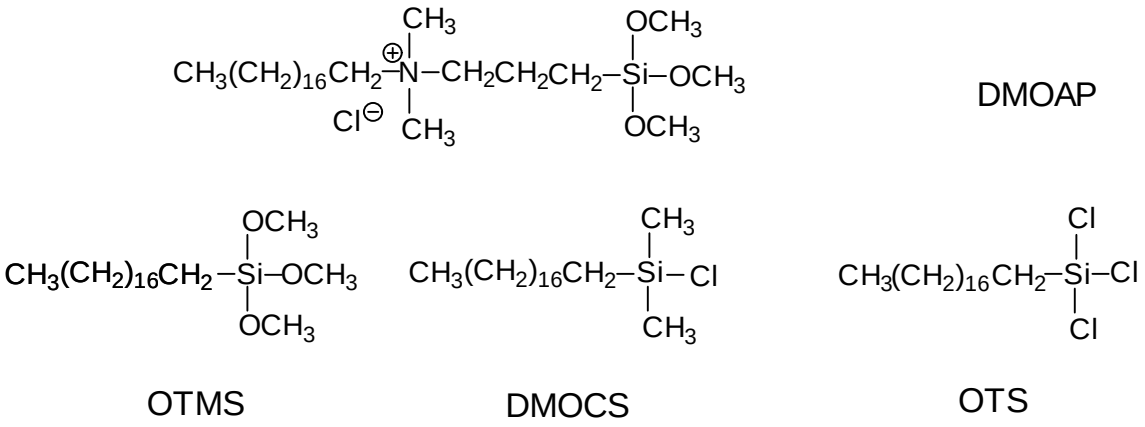

Fig. 6-11: *Amphiphilic chemicals with a hydrophilic head and a hydrophobic tail for substrate surface treatment, applied together with the rubbing procedure, to investigate the orientation of nematic liquid crystals. The comprehensive chemical names are in the text.*

Figure 6-11 shows four amphiphilic molecules (surfactants) used for the homeotropic orientation of nematic LC and for the combined treatments with the rubbing process. All of the four chemicals have the same alkyl chain as the hydrophobic tail, namely the octadecyl group, while the hydrophilic heads are different. DMOAP (dimethyl-octadecyl-[3-(trimethoxysilyl)-propyl] ammonium chloride) is one of the commonly used surfactants for the homeotropic anchoring in LC cells [Cogn82]. The other three were chosen based on the chemical structure of DMOAP. OTMS (octadecyltrimethoxy-silane) has all the groups as DMOAP except the quaternary ammonium group in the middle of the molecule. DMOCS (dimethyloctadecyl-chlorosilane) and OTS (octadecyltrichlorosilane) have one or three chlorosilane end groups, respectively,

through which the molecules can be immobilized on the substrate surface the same way as the initiator ADCS molecules do.

Combined procedures for surface treatments

The substrates were first rubbed and then the surfactant molecules were covalently linked to the rubbed surface of the substrate. The procedures could not be reversed because the rubbing procedure could wipe out the surfactant molecules that are coated on the surface. For the surface coverage with DMOAP and OTMS molecules which have methanoxyl as the anchoring group, a 1% ethanol solution was spin-coated on the rubbed substrates which were subsequently heated at 80°C for 30 minutes to achieve the anchoring reaction between the methanoxyl groups and the hydroxy groups on the substrate. For the coverage of the surfactants with chlorosilane groups (i.e. DMOCS and OTS) the molecules were immobilized on the surface in the same way like the ADCS-modification procedure, which was carried out in a water-free toluene solution under inert atmosphere at room temperature overnight.

The substrates whose surface were treated both with the rubbing procedure and with the coating of surfactant molecules were used for the preparation of LC cell which were then filled with ZLI-1052. CRS measurements were carried out on these cells and the experimental data points were fitted to give the cell thickness d and the tilt angle α. For comparison, equivalent cells were also made from substrates without the rubbing, that is, the substrate were only treated with the surfactants, a standard method to produce hometropic alignment. Figures. 6-12, 6-13, and 6-14 show the results.

All the surfactant-treated substrates (without the rubbing) induced homeotropic alignments for the LMW nematic LC ZLI-1052 (Figs. 6-12a, 6-13a, and 6-14a). However, the assembly of these amphiphilic molecules on rubbed substrates gave interesting alignments for the bulk nematics. The rubbing-DMOAP treatment resulted again in a homeotropic alignment (Fig. 6-12b), similar to the one without the rubbing procedure (Fig. 6-12a). The rubbing-DMOCS combination (Fig. 6-14b) and the rubbing-OTS combination (not shown) gave a planar orientation. Whereas the rubbing-OTMS association produced an orientation between the two extreme alignments with a pretilt angle of 97° (Fig. 6-13b).

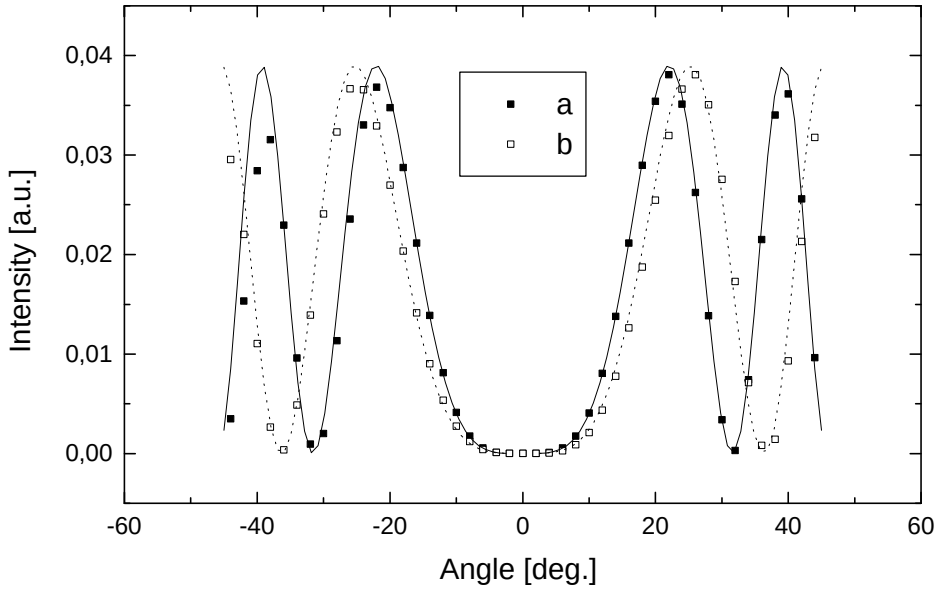

Fig. 6-12: *CRS measurements (points) and theoretical fittings (curves) of ZLI-1052 cells. The substrates were covered with DMOAP (a, ■), or first rubbed and then covered with DMOAP (b, □). The cell thickness d, and the tilt angle a from the theoretical fittings are: a) d = 39.0 µm, a = 90°; b) d = 30.0 µm, a = 90°.*

Although a quantitative investigate is not possible based on these data, a qualitative comparison between the anchoring “strength” of the surface treatments was possible on the basis of the above experimental findings. The substrates coated with DMOAP surfactant are “stronger” in anchoring the nematic molecules to the perpendicular position than the rubbed surfaces which favor a parallel position, because the combined rubbing-DMOAP process resulted in a hometropic alignment (Fig. 6-12). In the cases of DMOCS and OTS, the final alignment from the associated treatments was planar, indicating that the rubbed surfaces have more anchoring “power” than the surfactants assembled on the substrates (Fig. 6-14). As for the rubbing-OTMS combination, an in-between example is observed (Fig. 6-13).

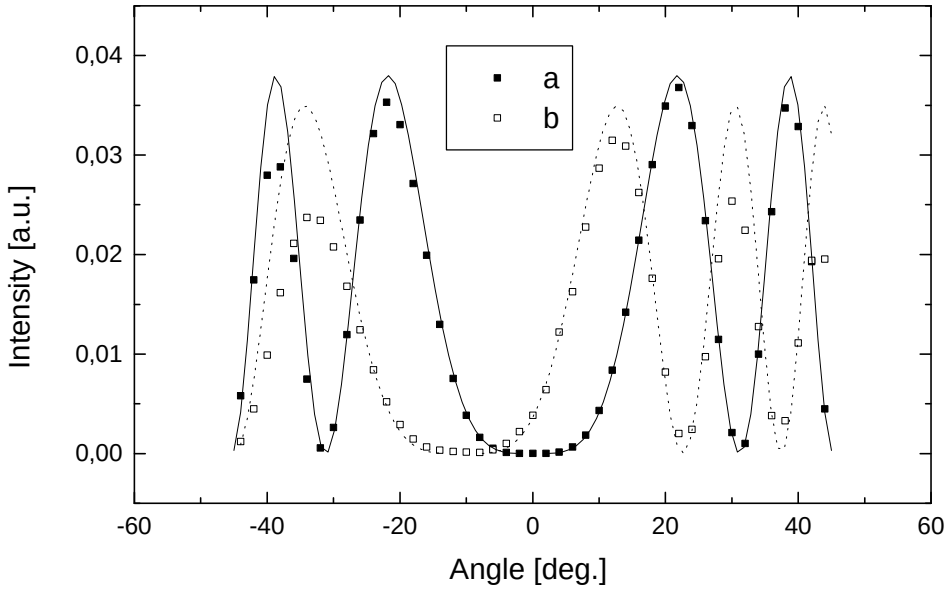

Fig. 6-13: *CRS measurements (points) and theoretical fittings (curves) of ZLI-1052 cells. The substrates were covered with OTMS (a, ■), or first rubbed and then covered with OTMS (b, □). The cell thickness d, and the tilt angle α from the theoretical fittings are: a) d = 40.0 µm, α = 90°; b) d = 35.0 µm, α = 97°.*

Observation of the alignment of the LMW nematic LC anchored by the substrate surfaces with combination of conflicting orientation treatments would give information about the alignment of the mesogenic units in LC brushes prepared on substrates treated the same way.

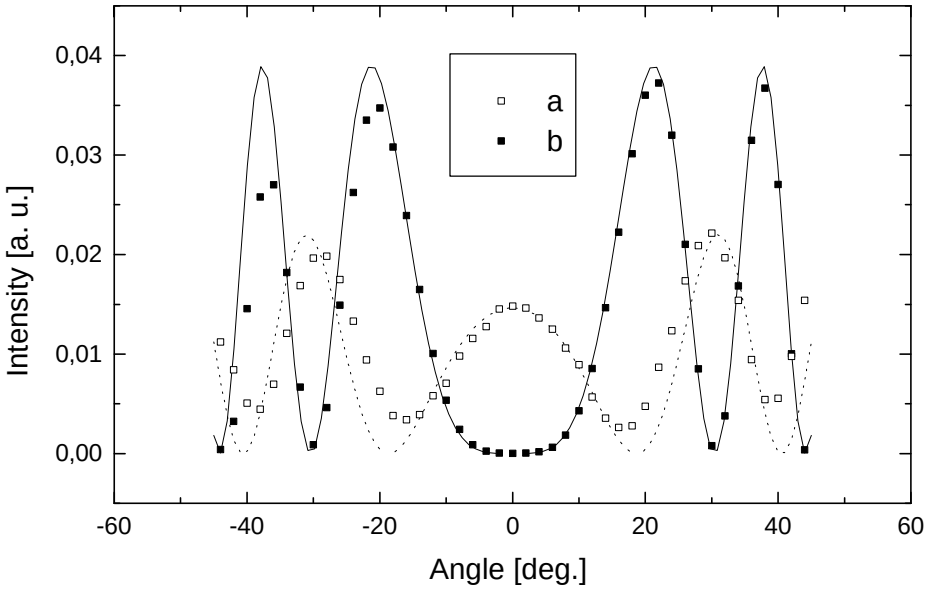

Fig. 6-14: *CRS measurements (points) and theoretical fittings (curves) of ZLI-1052 cells. The substrates were covered with DMOCS (a, ■), or first rubbed and then covered with DMOCS (b, □). The cell thickness d, and the tilt angle a from the theoretical fittings are: a) d = 42.0 µm, a = 90°; b) d = 58.1 µm, a = 0°.*

6.6 Biaxial LC Polymer Brushes

Uniaxiality and biaxiality

For a molecule or a substance, there are three refractive indices along the three principle directions (Fig. 6-15). When two of the refractive indices are the same, the molecule or the substance is called uniaxial, which is quite common for many liquid crystals (see §1.1 and Fig. 1-1). When all the three indices have different values, the molecule or the substance is defined as biaxial [Wahl79]. Conventionally, the three refractive indices are written according to their values in the order of n_α, n_β, and n_γ, with n_α having the largest value (Fig. 6-15).

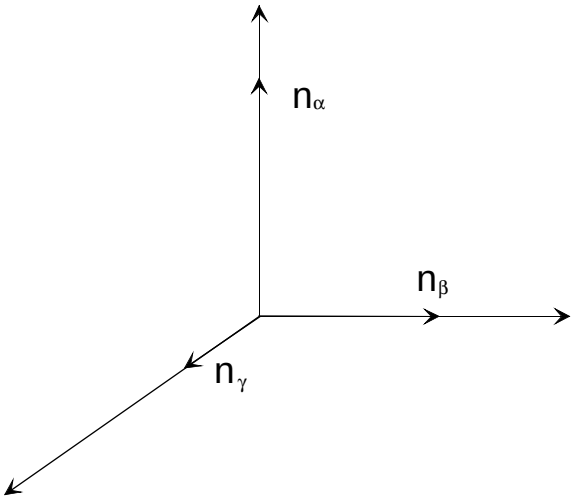

Fig. 6-15: *The three principle axes and the corresponding three refractive indices along them. Conventionally, the three refractive indices are expressed as* $n_a > n_b > n_g$.

The existence of a biaxial nematic phase for thermotropic liquid crystals was theoretically predicted by Freiser [Frei70]. Sixteen years later, Finkelmann and co-workers successfully synthesized and observed, for the first time, the optical biaxial phase behavior of a nematic side chain LC polymer whose mesogenic groups are laterally attached to the main chain [Hess86] (Fig 6-16).

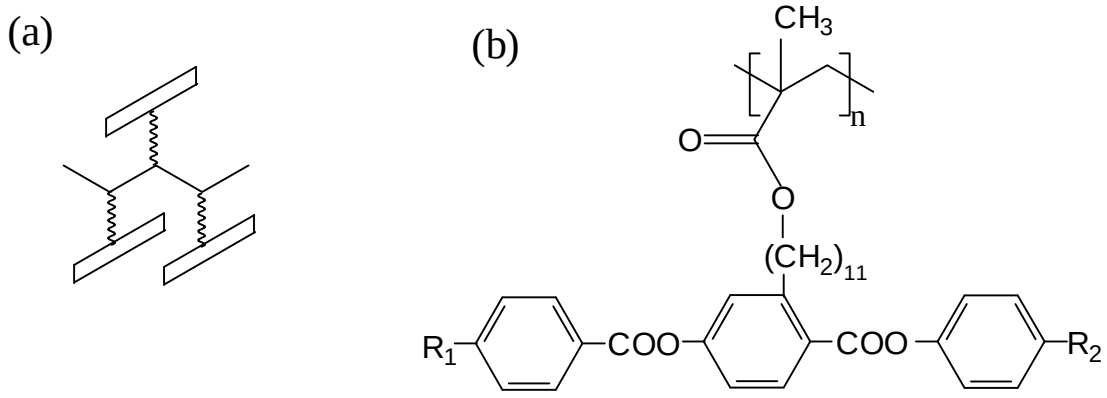

Fig. 6-16: *Liquid crystalline side chain polymers with the mesogenic groups laterally attached to the polymer backbones. (a) a schematic illustration of the situation; (b) a concrete example which shows biaxial behavior. The end groups* R_1 *and* R_2 *in (b) are* OCH_3, OC_4H_9, OC_6H_{13} *and CN [Hess85].*

The LC polymer (Fig. 6-16b) was sandwiched between two glass slides with a spacer having the thickness of 50 µm. The orientation was achieved by exposing the sample to a very strong magnetic field (7 Tesla) near the nematic-isotropic temperature of the LC polymer. Rotating the orientated sample under a conoscopic microscope revealed a cross at the 0° position and a maximum splitting of the two isogyres at the 45° position (referential pictures see Fig. 6-17), which suggests the presence of the characteristic behavior of biaxial substances [Wahl79, Noël98]. The authors attributed the formation of the biaxial phase to a hindered rotation around the long axes of the mesogenic moieties, which is achieved by connecting these mesogenic moieties laterally to the polymer backbones.

Preparation of biaxial LC brushes

In our side chain LC polymer systems the mesogenic units are terminally, not laterally, attached to the polymer backbones (see Fig. 1-2b). Nevertheless, biaxial behavior has also been observed from these LC polymer brush samples when the brushes were grown on specially treated substrates, i.e., the substrates had been rubbed and then covered with a layer of surfactant molecules.

The pre-treatment of a substrate surface was done in two steps: firstly, the substrate was rubbed with the velvet cloth, and secondly, it is modified with a toluene solution containing a mixture of the initiator ADCS and the surfactant DMOCS. The immobilization process was much the same as the standard procedure where ADCS was used alone. The surfactant molecules (DMOCS) also have chlorosilane end groups like those of ADCS. These two kinds of molecules can therefore be immobilized on the surface under the same conditions. The percentage of the surface covered by the surfactant could be controlled by the ADCS-DMOCS ratio in the toluene solution. After the immobilization, brushes were grown as usual on the substrates, the polymerization time (15 h) being kept the same for all samples.

Figure 6-17 shows the conoscopic images of LC polymer brushes prepared on rubbed glass substrate that had been modified with an ADCS solution diluted with DMOCS (molar ration, DMOCS : ADCS = 2:1). The polymerization was carried out at 60°C under vacuum in M6-toluene solution (M6 = 0.485 mole/L) for 15 hours. After the reaction, the samples were extracted with toluene overnight. The thickness of the brushes is around 70 nm (see §6.3).

Observation under the polarizing and conoscopic microscope

Under the polarizing microscope, the LC brushes prepared on rubbed-surfactant substrates exhibit similar nematic textures and rotation properties as the brushes grown

on rubbed substrates. Both of them show monodomain characters (cf. Figs. 6-4 and 6-5). When a condenser lens was put into the light path (thereby forming a conoscopic microscope), different images appeared (Fig. 6-17).

Under the conoscopic microscope, a clear cross was observed at the 0° position where the rubbing direction (shown by the arrow) was parallel to the direction of the polarizer (Fig. 6-17a). As the sample is rotated away from the 0° position the cross splits into two symmetric pieces, each of which is called an isogyre (Fig. 6-17b). The two split isogyres shift off-center continually with the rotation of the sample until the maximum is reached at the position of 45° (Fig. 6-17c). Further rotation of the sample stage causes the two isogyres turn back towards the center (Fig. 6-17d) until they combine to form a cross again (Fig. 6-17e). The splitting and recombination of the two isogyres with the rotation of the sample is the characteristic evidence of the presence of a biaxial substance [Wahl79, Noël98].

Subsequent rotation breaks the cross into two isogyres once more, but this time in a direction which is perpendicular to the one as shown in Fig 6-17b (Fig. 6-17f). The same behavior was observed as the sample was further rotated, all in the new direction (Figs. 6-17g, 6-17h). At 180°, the two isogyres merge into a cross again at the original location (Fig. 6-17i).

The information obtained from the conoscopic microscope strongly suggested that the brush samples are biaxial. To our knowledge, this was the first time that a well-defined biaxial nematic phase behavior of the side chain LC polymer brushes with the mesogenic units terminally attached to the polymer backbone was observed. The biaxiality is the result of the specific pre-treatment of the substrate surface and the subsequent arrangement of the mesogenic units on it. While LC brushes grown on pre-rubbed substrates show a monodomain character and are uniaxial, the covering of a layer of surfactant molecules after the rubbing procedure makes the LC polymer brushes showing monodomain texture and being biaxial. Although the thickness of these brush films is less than 100 nm (ca. 70 nm, cf. the thickness of the polymer layer in ref. [Hess85] was 50 μm), the biaxial behaviors under the conoscopic microscope (splitting and combination of the two isogyres) could be readily observed.

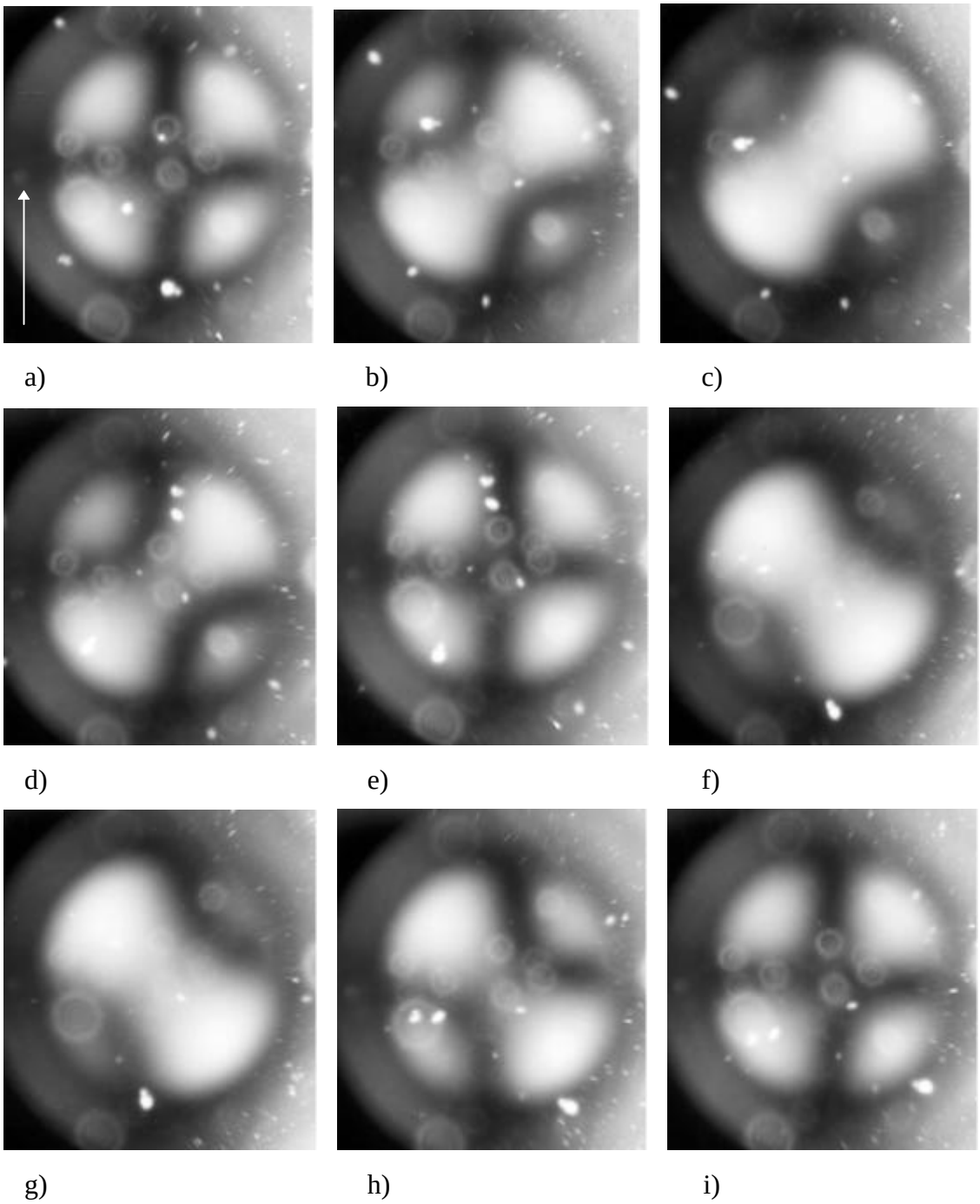

Fig. 6-17: *Conoscopic microscope images of PM6 brushes grown on rubbed substrate covered with DMOCS molecules. The magnification of the microscope is 200 x. The arrow indicates the rubbing direction. The relative angle of the sample with respect to the crossed polarizers are: 0° (a), 15° (b), 45° (c), 60° (d), 90° (e), 120° (f), 135° (g), 165° (h), and 180° (i). The splitting and recombination of the two isogyres by rotating the sample suggests clearly the presence of the biaxial behavior of the sample.*

Hybrid LC cells from substrates with biaxial brushes

In a hybrid LC cell the surfaces of the two substrate for the cell exhibit different properties. In this work hybrid LC cells were prepared, where one of the substrates had been modified with the biaxial LC polymer brushes and the other was a glass substrate that had been rubbed. These two substrate should have different anchoring properties for the nematic ZLI-1052 molecules. The rubbed glass surface, as a standard process, is expected to induce a planar orientation. Theoretically, a tilt alignment of the adjoining nematic molecules by the other substrate is predicted, which is the result of the combined effects of the polymer chain stretching and the substrate fraction unoccupied by the polymer chains (§2.1). The combined anchoring effect of the two substrates would give rise to a tilt alignment of the bulk nematic.

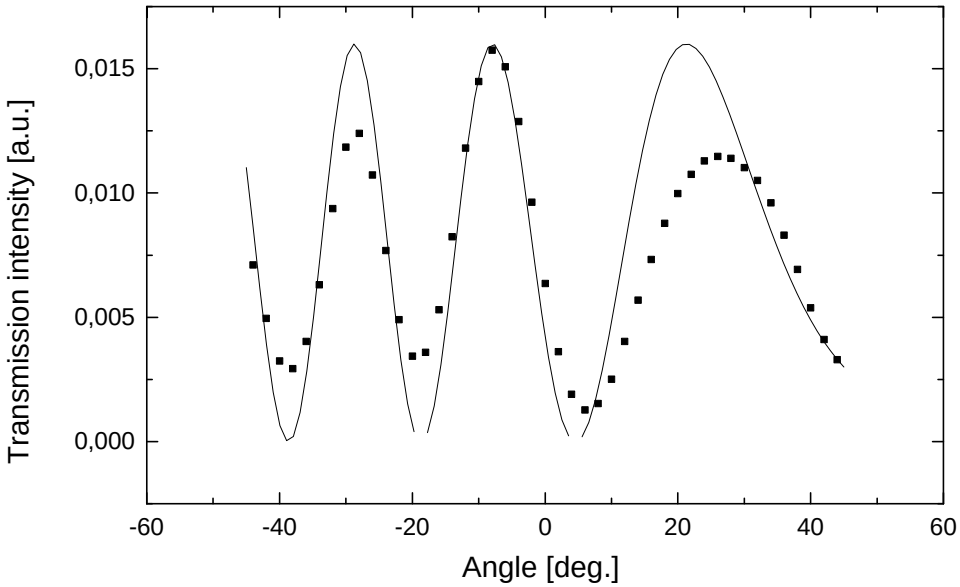

Fig. 6-18: *CRS measurement on a ZLI-1052 hybrid cell. One of the substrates was covered with the biaxial LC polymer brushes grown on rubbed-surfactant surface, and the other one was just rubbed. The theoretical curve gives a cell thickness d = 27.7 µm, and a tilt angle a = -15.5°. The tilt alignment of the nematic bulk comes from anchoring behavior at the interface of the biaxial LC brush layer.*

Crystal Rotation Setup (CRS) measurements on these hybrid LC cells supported the theoretical expectations (Fig. 6-18). The data obtained from these measurements carried out on different locations throughout the surfaces of the cells gave similar results (Fig. 6-18 shows only one set of them). The thickness obtained from these experimental results fluctuated between 27 and 30 µm (average: 28.7 µm), and pretilt angles between -14.5° and -17.5° (average: -15.6°) were found.

The profile at the brush/nematic interface on the LC cells could be imagined just as the situation illustrated in Fig. 2-1. The polymer brushes carrying the mesogenic units are attached on the substrate that is covered with the surfactant molecules. The rubbing process previous to the brush growth creates an anisotropy, according to which the LC units are homogeneously aligned to a monodomain texture. The combination of the anchoring effects by the substrate surface occupied by the surfactant molecules and by the stretching of the polymer chains results in a tilt alignment of the LMW nematics molecules in the bulk.

The pretilt angle data in Fig. 6-18 give preliminary results on the investigation of the biaxial LC polymer brushes as alignment layer for LMW nematics to obtain alignment with adjustable pretilt angles. Further work would include systematic variation of the DMOCS : ADCS ratio in the immobilization step and the achievements of the pretilt angle - ratio curves. For further investigation on the LC polymer brushes as alignment layers, the center of the work should be on the question how the tilt angle can be controlled by parameters such as the surfactant to initiator ratio.

7 Experimental

7.1 Chemical Reagents, Substrates and Equipment

7.1.1 Solvents and Other Chemical Reagents

Acetone (tech.)

Acetone (p.a. Riedel-de Haën)

Acrylic acid (purum, Fluka)

Purification: filtered from Aluminum oxide S; distilled from Cu(I)Cl under reduced pressure.

4,4'-azobis (4-cyanopentanoic acid) (purum, Aldrich)

4,4´-azobis(isobuytronile) (p.a. Fluka)

Purification: recrystallized from methanol.

Benzophenone (purum, Fluka)

tert.-Butyl-methylether (tech.)

2,6-*di*-*tert*.-Butyl-4-methylphenol (for synthesis, Merck-Schuchardt)

Calcium chloride (purum, Merck)

6-Chloro-1-hexanol (pract. ≥ 95%, Fluka)

Chloroform (purum, Fluka)

Dichlormethane (p.a., Riedel de Haën)

Dimethylchlorosilane (purum, Fluka)

Purification: freshly distilled under inert gas, b.p. 36°C.

Dimethylformamide (for analysis, Fisher Chemicals)

Dimethyloctadecyl [3-(trimethoxysilyl) propyl] ammonium chloride (pract. ≥50%, Fluka)

Ethanol (tech.)

Ethanol absolute (p.a., Riedel-de Haën)

Ethyl acetate (p.a., Fluka)

n-Hexane (p.a., Riedel-de Haën)

p-*n*-hexanoxy benzoic acid (purum, Fluka)

p-*n*-heptanoxy-phenol (purum, Fluka)

Hydrochloric acid (min. 37%, analytical reagent, Riedel-de Haën)

Hydrogen peroxide (35%, Riedel-de Haën)

Hydroquinone (purum, Fluka)

Hydroquinone monomethyl ether (purum, Fluka)

Hydroxybenzoic acid (purum, Fluka)

Lithium aluminium hydride (p. a., Merck)

Magnesium sulfate (purum, Fluka)

Methacrylic acid (purum, Fluka)

> *Purification: filtered from Aluminum oxide S; distilled from Cu(I)Cl under reduced pressure (boiling point: 60.5°C).*

Methanol (tech.)

Methanol (p.a., Riedel-de Haën)

p-Methoxyphenol (purum, Fluka)

Metyl-tert.-buthylether (tech.)

n-Octadecyltrichlorsilane (tech., Lancaster)

Potassium hydroxide (pellets, analytical reagent, Riedel-de Haën)

Potassium iodide (purum, Fluka)

Petroleum ether low boiling (p.a. Fluka)

Phosphorous pentachloride (purum, Fluka)

2-Proanol (tech.)

2-Propanol (purum, Riedel-de Haën)

Sand (p.a. 40-200 mesh, Fluka)

Silicagel (blue drying pearls, Kali-Chemie AG)

Sodium

Sodium hydrogen carbonate (powder, R.G. Riedel-de Haën)

Sodium sulfate (powder, R.G. Riedel-de Haën)

Sulfuric acid (95 - 97%, analytical reagent, Riedel-de Haën)

Tetrahydrofuran (tech.)

Tetrahydrofuran (purum, Fluka)

Purification: freshly distilled from Na-K mixture under inert gas.

Thionyl chloride (R. G., Aldrich)

Toluene (tech.)

Toluene (p.a., Riedel-de Haën)

Purification/drying: distilled from sodium under inert gas.

4-Toluene sulfonic acid (purum, Fluka)

Triethylamine (purum, Riedel-de Haën)

Purification/drying: refluxed over $LiAlH_4$ overnight and distilled off under inert gas.

7.1.2 Substrates and the Pre-treatment

Glass substrates

For glass substrates we used BK-7 (Schott) with the original size of 2.5 cm x 7.6 cm. The glass slides were cut into four pieces of identical size (2.5 cm x 1.9 cm). The substrates were cleaned by sofonication in 2% Hellmanex solution with a ultrasonic setup Sonorex RK510H (Bandelin) at 30°C for 15 minutes, 5 times washed with tap water, then 10 to 15 times with milli-Q water. This procedure was repeated twice and, finally, the substrates were washed twice with absolute ethanol and kept in absolute ethanol.

Substrates for Surface Plasmon Spectroscopy

The cleaned glass substrates were coated with a silver layer (ca. 50 nm, purity 99.99%) and a SiO_x layer (ca. 30 nm) using a Balzers BA-250E coating system.

Substrates for FTIR spectroscopy

Silicon wafers (Aurel), both sides of which had been polished, were used as the substrates for FTIR spectroscopy. The thickness was 1 mm. The wafers were modified with the initiator and polymerized in the same reaction vessel together with other glass substrates. Both side of the wafers were coated with the LC polymer brushes with a total thickness of about 100 nm. For spin-coated IR substrates, only one side of the substrates was covered with the LC polymer and the thickness was around 100 nm.

Rubbing of glass substrates

To rub a glass surface, a dried substrate was put face down on a piece of velvet cloth (Yoshikawa YA-20-R). The substrate was drawn over the velvet by hand while a gentle vertical pressure was exerted on it. This was usually repeated three times so that the whole rubbing length reached ca. 65 cm. Fibers that are loosely absorbed on the surface were blown away in a stream of air.

7.1.3 Methods

NMR spectroscopy

The ^{1}H- and ^{13}C-NMR spectra were recorded with a Bruker Avance250 (250 MHz) and an AMX300 (300 MHz) FT-NMR spectrometer at room temperature. The signals were calibrated to the residual proton signal of the solvent. The multiplicity of the peaks are donated as follows:

s = singlet, d = doublet, dd = double doublet, t = triplet, q = quadruplet, m = multiplet, b = broad.

FTIR spectroscopy

The FTIR spectra of the polymer brushes and the spin-coated polymers and monomers on Si-substrates were obtained on an FTIR-Spectrometer Magna-IR 850-II (Nicolet). The resolution was 4 cm^{-1} with 750 scans for each measurement. The background of the blank Si-substrate was taken previous to each measurement.

Surface plasmon spectroscopy

The light source for the measurement was a 5 mW He-Ne-Laser (Uniphase) with a wave length of 632.8 nm. The laser beam was moduled with a mechanical chopper. The polarization direction and the light intensity was regulated by two polarizers. The light came then to the surface of a 90° prism (BK7 glass, Schott), on the base of which a glass substrate with a thin layer on it (see, Fig. 3-12) was fixed with a sample holder. The incidental angle of the light on the prism was regulated by a goniometer, on which the sample holder was fixed. The reflected light was focused with a lens to a photodiode and the light intensity was measured by a lock-in amplifier (Modell 5208, EG&G) and saved in the PC. The programs for the measurement and data treatment had been developed at MPI-P.

Thermal measurement

DSC and TGA measurements were done using a Mettler Toledo STAR^e system. For each measurement, between 4 to 8 mg of the sample were used. The heating rate was 10°C/min. The samples for the measurements were analyzed directly after the synthesis without any previous thermal history.

Optical microscopy

The microscope used was an Axiophot (Zeiss) equipped with a camera and crossed polarizers. The ocular magnification was 10x and a 100x objective was used for the nematic texture observation of the LC polymer brushes. Pictures were taken with the camera. A Linkam TH-600 thermal stage was used to control the temperature, to an accuracy of ±0.1°C. For measurements with varying temperature a long distance objective LD50, together with the thermal stage, was used.

7.2 Synthesis of the Monomers

The synthesis of the monomers (M6 and A6) was carried out according to the literature [Fink78, Port81, Port82] with some improvements in the purification of the raw products.

7.2.1 Synthesis of the Methacrylate Monomer

Step 1: 4-(6-hydroxy)-hexanoxybenzoic acid

The 4-(6-hydroxy)-hexanoxybenzoic acid was etherified based on the Williams reaction. 101.5 g (0.735 mol) 4-hydroxybenzoic acid was suspended in 350 ml ethanol in a 2 liter three-neck flask with magnetic stirrer. A solution of 103 g (1.84 mol) potassium hydroxide dissolved in 200ml water was added to the flask, resulting in a clear solution. After addition of a spatula of potassium iodide, the solution was heated under reflux and 110.4 g (0.808 mol) 6-chloro-1-hexanol was added drop-wise while stirring. The mixture was refluxed over night. In the course of the reaction potassium chloride was formed which precipitated from the solution.

After the reaction, the solvent was distilled off. The remaining solid was dissolved in ca. 1000 ml water and extracted three times with 300 ml *tert.*-butyl-methylether. Half concentrated HCl was added to the aqueous solution after the extraction until the solution became acidic and no more precipitation formed. The solid was separated and

washed with water. After drying, the raw product was recrystallized from ethanol several times.

Yield: 96.0 g (0.403 mol, 54.8%), *Lit.* [Port81]: 64%.

^{1}H-NMR (acetone-d6, δ in ppm): 7.92 (d, 2H in $C_6\underline{H}_4$), 7.02 (d, 2H in $C_6\underline{H}_4$), 4.10 (t, 2H, $OC\underline{H}_2$), 3.56 (t, 2H, $HOC\underline{H}_2$), 2.08 (q, 4H in $CH_2(C\underline{H}_2)_4CH_2$), 1.51 (q, 4H in $CH_2(C\underline{H}_2)_4CH_2$).

Step 2: 4-[6-(2-methyl-propenoyloxy)-hexanoxy]-benzoic acid

The substituted benzoic acid was prepared by azoetropic esterification. 31.83 g (0.134 mol) 4-(6-hydroxy)-hexanoxybenzoic acid, 75 ml (1.09 mol) methacrylic acid, 4 g 4-toluene sulfonic acid, 4 g hydrochinon, and 75 ml chloroform were added to a 500 ml flask equipped with a Dean-Strack setup and refluxed over night. About 2 ml water was collected in the Dean-Strack setup. After cooling, the solution was dissolved in 450 ml *tert.*-butyl-methylether and washed five times with 200 ml of warm water (35°C). The organic phase was dried over sodium sulfate and half of the solvent was distilled off. The concentrated solution was cooled in a freezer (-20°C) overnight and the product precipitated. The raw product was recrystallized from 2-propanol.

Yield: 26.1 g (0.085 mol, 63.6%).

^{1}H-NMR (acetone-d6, δ in ppm): 7.94 (d, 2H in $C_6\underline{H}_4$), 7.00 (d, 2H in $C_6\underline{H}_4$), 6.03 (s, 1H in $C\underline{H}_2$=C), 5.59 (s, 1H in $C\underline{H}_2$=C), 4.09 (t, 2H, $OC\underline{H}_2$), 4.08 (t, 2H, $OC\underline{H}_2$), 1.88 - 1.69 (m, 8H in $CH_2(C\underline{H}_2)_4CH_2$), 1.50 (s, 3H in $C\underline{H}_3$C=).

Step 3: 4-[6-(2-methylpropenoyloxy)-hexanoxy]-benzoic acid-4'-methoxyphenyl ester (M6)

4-[6-(2-Methyl-propenoyloxy)-hexanoxy]-benzoic acid was first turned into the corresponding acid chloride and then reacted with 4-methoxyphenol to get the monomer M6. 25.62 g (0.084 mol) 4-[6-(2-methyl-allyloyloxy)-hexanoxy]-benzoic acid and 29 ml thionyl chloride were put in a 100 ml round flask with a drying tube. 5 drops of dimethylformamide as catalyst, and a spatula of 1,6-*di*-*tert*-butyl-*p*-kresol as inhibitor were added to the flask. The mixtures was stirred at room temperature for several hours until a clear solution was obtained. The system was slightly heated to 45°C for 1.5 hours to complete the reaction. The excess thionyl chloride was then removed in vacuum.

The remaining solid was dissolved in 50 ml absolute tetrahydrofuran and cooled with a ice-salt mixture under inert gas. 10.42 g (0.084 mol) 4-methoxyphenol, 15 ml dried

triethylamine were dissolved in 100 ml absolute tetrahydrofuran. The mixture was added drop-wise to the cooled solution under stirring. After stirring overnight at room temperature, the solution was dissolved in 1000 ml dichloromethane and washed six times with 400 ml warm water (ca. 35°C) and dried over sodium sulfate. After removal of the solvent, the raw product was purified by column chromatography. In stead of dichloromethane as reported in the literature [Port81], we used a solvent pair as the eluent which composed of *n*-hexane and ethyl acetate at a volume ratio of 10:3. The silica gel to raw product quota was 80:1 by weight. The product was finally recrystallized from 2-propanol.

Yield: 20.1 g (0.049 mol, 57.9%).

Melting point: 54 - 55.5 °C, *Lit.* [Fink78]: 47°C.

^{1}H-NMR ($CDCl_3$, δ in ppm): 8.11 (d, 2H in $C_6\underline{H}_4$), 7.10 (d, 2H in $C_6\underline{H}_4$), 6.96 (dd, 4H in $C_6\underline{H}_4$-COO-$C_6\underline{H}_4$), 6.08 (s, 1H in $C\underline{H}_2$=C), 5.55 (s, 1H in $C\underline{H}_2$=C), 4.14 (t, 2H in $OC\underline{H}_2$), 4.06 (t, 2H in $OC\underline{H}_2$), 3.82 (s, 3H in CH_2=$CC\underline{H}_3$), 1.93 (s, 3H in $OC\underline{H}_3$), 1.85 (q, 2H in $CH_2(C\underline{H}_2)_4CH_2$), 1.72 (q, 2H in $CH_2(C\underline{H}_2)_4CH_2$), 1.53 (m, 4H in $CH_2(C\underline{H}_2)_4CH_2$).

^{13}C-NMR (CD_2Cl_2, δ in ppm): 18.39; 26.01; 26.12; 28.91; 29.35; 55.91; 64.88; 68.59; 114.63; 114.72; 122.13; 122.90; 125.01; 132.39; 137.13; 145.01; 157.68; 163.86; 165.49; 167.61.

7.2.2 Synthesis of the Acrylate Monomer

The synthesis of the acrylate monomer A6 was similar to that of the methacrylate analog M6 which has been described in §7.2.1. Therefore, only the used amounts of the related chemicals, the yields and characterizations of each step are documented in the following.

Step 1: 4-(6-hydroxy)-hexanoxybenzoic acid

The same as §7.2.1 Step 1.

Step 2: 4-(6-propenoyloxy)-hexanoxybenzoic acid

33.9 g (0.142 mol) 4-(6-hydroxy)-hexanoxybenzoic acid and 75 ml (1.086 mol) acrylic acid were used.

Yield: 21.1 g (0.072 mol, 50.8%), *Lit.* [Port81]: 62%.

Phase behavior (°C): c 87 n 108 i, *Lit.* [Port81]: c 85 n 104 i.

^{1}H-NMR ($CDCl_3$, δ in ppm): 8.01 (d, 2H in $C_6\underline{H}_4$), 6.92 (d, 2H in $C_6\underline{H}_4$), 6.42 - 5.53 (m, 3H in $C\underline{H}_2$=C$\underline{H}$), 4.16 (t, 2H, O$C\underline{H}_2$), 4.01 (t, 2H, O$C\underline{H}_2$), 1.81 - 1.47 (m, 8H in $CH_2(C\underline{H}_2)_4CH_2$).

Step 3: 4-(6-propenoyloxy)-hexanoxybenzoic acid -(4'-methoxyphenyl ester (A6)

23.58 g (0.084 mol) 4-(6-propenoyloxy)-hexanoxybenzoic acid, 25 ml thionyl chloride, and 10.01 g (0.081 mol) 4-methoxyphenol were used for the reactions. The raw product was purified by column chromatography using *n*-hexane : ethyl acetate = 5:2 as eluent and finally recrystalization twice from ethanol.

Yield: 18.6 g (0.047 mol, 57.9%), *Lit.* [Port81]: 44%.

Melting point: 55 - 57 °C, *Lit.* [Port81]: 63°C; [Horv85]: c 48 n 54 i.

^{1}H-NMR ($CDCl_3$, δ in ppm): 8.01 (d, 2H in $C_6\underline{H}_4$), 7.01 (d, 2H in $C_6\underline{H}_4$), 6.85 (dd, 4H in $C_6\underline{H}_4$-COO-$C_6\underline{H}_4$), 6.35 (d, 1H in $C\underline{H}_2$=CH), 6.10 (m, 1H in CH_2=C$\underline{H}$), 5.72 (d, 1H in CH_2=C$\underline{H}$), 4.08 (t, 2H in O$C\underline{H}_2$), 3.98 (t, 2H in O$C\underline{H}_2$), 3.88 (t, 3H in CH_2=C$C\underline{H}_3$), 1.93 (s, 3H in O$C\underline{H}_3$), 1.85 (q, 2H in $CH_2(C\underline{H}_2)_4CH_2$), 1.72 (q, 2H in $CH_2(C\underline{H}_2)_4CH_2$), 1.53 (m, 4H in $CH_2(C\underline{H}_2)_4CH_2$).

7.3 Synthesis of the LC Polymers

7.3.1 Synthesis of the Methacrylate Polymer

Radical polymerization in solution

The polymers with side chain LC units were prepared by radical polymerization in solution with various monomer and initiator concentrations, and different polymerization time. The following is the steps for the preparation of the polymer PM6-6 as an example. 1.31 g (3.18 mmol) M6 and 18.0 mg (0.11 mmol) AIBN were dissolved in 10 ml absolute toluene in a 40 ml Schlenk tube to form a solution with a monomer concentration [M] = 0.318 mol/L and an initiator concentration of [I] = 3.45 mol%. The amounts of the monomer and initiator were varied in different polymerization to obtain different molecular weights. Argon gas was passed through the Schlenk tube for 10 to 15 minutes to get a oxygen-free condition. In cases when the initiator concentrations were very low, the solution was degassed through three freeze-

thaw cycles to remove oxygen. After degassing, the solution was polymerized at 60 °C for 8 to 24 hours.

Purification of the polymers

After reaction, the viscosity of the solution has clearly increased. To separate the polymer from the monomer the solution was dropped into 300 ml *n*-hexane under heavy stirring. The polymer precipitated while the un-reacted monomer stayed in the solution. After separation the polymer was dissolved again in 15 ml dichloromethane and precipitated into 300 ml methanol and stirred overnight. Finally the polymer powder was filtered off and dried in vacuum. The preparation conditions, yields and molecular weights of all the LC polymers are listed in Tables 3-1 and 3-2 in §3.3.

^{1}H-NMR of the polymer PM6-2 ($CDCl_3$, δ in ppm): 8.10 (d, 2H in $C_6\underline{H}_4$), 6.84 - 7.09 (m, 6H in $C_6\underline{H}_4$-COO-$C_6\underline{H}_4$), 3.82 - 4.04 (m, 4H in $OC\underline{H}_2(CH_2)_4C\underline{H}_2O$), 3.75 (s, 3H in $OC\underline{H}_3$), 1.62 (s, 3H in CH_2-$CC\underline{H}_3$), 1.45 - 1.90 (m, 8H in $CH_2(C\underline{H}_2)_4CH_2$).

^{13}C-NMR of the polymer PM6-2 (CD_2Cl_2, δ in ppm): 17 (b); 19 (b); 26.13; 26.36; 28.53; 29.46; 45.3 (b), 55.93; 65.30; 68.61; 114.66; 114.75; 122.22; 122.93; 132.45; 145.01; 157.70; 163.82; 165.42; 178 (b)

7.3.2 Synthesis of the Acrylate LC Polymer

The acrylate LC polymer was synthesized and purified the same way as the methacrylate analogs, i.e., radical polymerization in toluene and purified by precipitation. For the preparation of PA6-1, 2.6 g (6.53 mmol) A6, 10.7 mg (0.065 mmol) AIBN were dissolved in 25 ml absolute toluene in a 40 ml Schlenk tube. Argon gas was passed through the tube for 15 minutes. The solution was polymerized at 60°C for 20 hours. After the reaction, the unreacted monomer was seperated from the polymer by precipitating the viscous solution into 400 ml *n*-hexane, repeated by 20 ml THF and 400 ml methanol and stirred overnight. The polymer was finally isolated and dried in vacuum.

Yield: 1.80 g (4.52 mmol, 69%), *Lit.* [Port81]: 64%.

^{1}H-NMR ($CDCl_3$, δ in ppm): 8.03 (d, 2H in $C_6\underline{H}_4$), 7.02 - 6.85 (m, 6H in $C_6\underline{H}_4$-COO-$C_6\underline{H}_4$), 3.92 - 3.73 (m, 4H in $OC\underline{H}_2(CH_2)_4C\underline{H}_2O$), 3.73 (s, 3H in $OC\underline{H}_3$), 1.73 - 1.42 (m, 8H in $CH_2(C\underline{H}_2)_4CH_2$).

7.4 Synthesis of the Azo-initiator

The syntheses were carried out according to a method developed by Prucker [Pruc95, Pruc98].

Step 1: 4,4'-azobis (4-cyanopentanoic acid chloride)

Under inert gas and in a 1000 ml round-bottom flask, 148 g (0.70 mol) phosphorous pentachloride was dispersed in 400 ml dichloromethane and cooled to 4°C. 56 g (0.2 mol) 4,4'-azobis (4-cyanopentanoic acid) was added to the system in small portion. The flask was packed with aluminum foil to avoid light exposure and the suspension was stirred at room temperature overnight. After the reaction, the excess solid was filtered and the filtrate was concentrated to about 100 ml, causing more phosphorous pentachloride to precipitation. Under inert gas the solution was filtered into 300 ml cold *n*-hexane (6°C), and the product precipitated. The solution was stirred for one hour and the product was separated and dried in vacuum.

Yield: 45.4 g (0.143 mol, 71.6%), *Lit.* [Schi98]: 84%.

^{1}H-NMR (acetone-d6, δ in ppm): 3.30 (t, 2 x 2H in $CH_2C\underline{H}_2CO$), 2.58 (t, 2 x 2H in $CH_2C\underline{H}_2CO$), 1.75 (s, 2 x 3H in $C\underline{H}_3$)

Step 2: 4,4'-azobis (4-cyanopentanoic acid)-allyl ester

Under inert gas and in 1000 ml flask, 45.4 g (0.143 mol) 4,4'-azobis (4-cyanopentanoic acid chloride) was dissolved in 500 ml dichloromethane and cooled with an ice-salt bath to 4°C. 19.6 ml (0.29 mol) allyl alcohol and 50 ml (0.36 mol) dried triethylamine were dissolved in ca. 30 ml dichloromethane and the mixture was dropped into the cooled solution, causing the mixture to warm up to ca. 40°C. The system was stirred at room temperature overnight. Triethylamine chloride precipitated during the course of the reaction and was filtered off. The filtrate was washed twice with 300 ml 2N sulfuric acid, followed by 2x 300 ml half-saturated sodium hydrogen carbonate solution and 2x 300 ml water or saturated magnesium sulfate solution. After drying the organic phase with magnesium sulfate, the solvent was distilled off and the product was dried in vacuum.

Yield: 35.9 g (0.10 mol, 69.7%), *Lit.* [Schi98]: 84.7%.

^{1}H-NMR ($CDCl_3$, δ in ppm): 5.80 (m, 2 x 2H in $C\underline{H}_2$=CH), 5.25 (t, 2 x 1H in CH_2=C$\underline{H}$), 4.58 (d, 2 x 2H in O$C\underline{H}_2$), 2.48 (m, 2 x 4H in $C\underline{H}_2C\underline{H}_2$), 1.66 (s, 3H in $C\underline{H}_3$), 1.72 (s, 3H in $C\underline{H}_3$).

Step 3: 4,4'-azobis-[4-cyanopentanoic acid-(3'-chlorodimethylsilyl) propyl ester] (ADCS)

In a 500 ml round flask under inert gas, 35.9 g (0.10 mol) 4,4'-azobis (4-cyanopentanoic acid)-allyl ester was suspended in 150 ml (1.38 mol) dimethylchlorosilane. 120 mg hexachloroplatin (IV) acid was added and the system was refluxed at 36°C for 6 hours. The solid dissolved during the reaction and a homogeneous solution was formed. After cooling the solution, 4 g sodium sulfate was added into the system. The solid was filtered and the excess solvent was removed in vacuo overnight. The product was kept in a sealed bottle in a freezer.

Yield: 47.7 g (86.8 mmol, 86.8%), *Lit.* [Schi98]: 87.7%.

^{1}H-NMR ($CDCl_3$, δ in ppm): 3.26 (m, 2 x 4H in $C\underline{H}_2C\underline{H}_2$), 2.48 (m, 2 x 6H in $C\underline{H}_2C\underline{H}_2C\underline{H}_2$), 2.04 (s, 2 x 3H in $CC\underline{H}_3$), 1.80 (s, 2 x 6H in $Si(C\underline{H}_3)_2$).

7.5 Synthesis of LC Polymer Brushes

For a detailed description of the procedures, the reader is referred to the literature [Pruc95, Pruc98]. The synthesis consists of two steps: firstly, a layer of the initiator molecules is immobilized on substrate surface, and subsequently, the polymerization is carried out at elevated temperature.

Immobilization of the Azo-initiator

In a 40 ml Schlenk tube with two BK7 glass substrates under inert gas, ca. 20 - 25 ml absolute toluene, 2 ml initiator solution (0.46 g ADCS dissolved in 30 ml absolute toluene) and 2 ml dried triethylamine were added. The tube was sealed kept at room temperature overnight. After the reaction, the substrates were carefully washed with toluene, methanol and acetone and dried in vacuum.

Polymerization on the Substrate

In a 10 ml narrow Schlenk tube with two azo-modified substrates under inert gas, 3 to 5 ml of the monomer dissolved in toluene at the desired concentration were added. The

tube was sealed and degassed by three to five freeze-thaw cycles. The tube was then placed in a thermostat to carry out the polymerization at 60°C for the desired time. After the reaction, the substrates were extracted with toluene in a Soxhlett setup for ca. 15 hours.

7.6 Synthesis of the Nematic 6PB7

In a 100 ml round bottom flask equipped with drying tubes and magnetic stirrer, 16.6 g (0.075 mol) *p*-*n*-hexanoxy benzoic acid and 30 ml thionyl chloride were added and stirred at room temperature for 2 hour, then at 45°C for another hour. After the reaction, the excess thionyl chloride was removed in vacuum.

The remaining solid was dissolved in 50 ml of dry tetrahydrofuran, 18 ml dry triethylamine were added and the system was cooled with an ice-salt bath. 15.57 g (0.075 mol) *p*-*n*-heptanoxy-phenol were dissolved in 100 ml dry tetrahydrofuran and the solution was dropped slowly to the cooled mixture. The system was stirred at room temperature overnight.

After reaction, the solution was dissolved in 1000 ml dichloromethane and washed three times with 350 ml warm water (35°C). After drying with sodium sulfate, the solvent was evaporated. The raw product was purified by column chromatography with (ethyl acetate : *n*-hexane = 2:5) as the eluent and finally recystallized twice from 2-propanol.

Yield: 23.7 g (0.057 mol, 76.6%).

Phase behavior (°C): c 55 n 86 i, *Lit.* [Mete73]: c 55 n 88 i.

^{1}H-NMR ($CDCl_3$, δ in ppm): 8.02 (d, 2H in $C_6\underline{H}_4$), 6.82 (m, 6H in $C_6\underline{H}_4COOC_6\underline{H}_4$), 3.96 (t, 2H in $OC\underline{H}_2$), 3.90 (t, 2H in $OC\underline{H}_2$), 1.70 - 0.90 (m, 24H in $(C\underline{H}_2)_4C\underline{H}_3$, and $(C\underline{H}_2)_5C\underline{H}_3$).

8 Summary

Polymer brushes (polymer chains which are terminally attached to the substrate surface with chemical bonds) with liquid crystalline (LC) side chains, the so-called LC polymer “brushes”, were synthesized on planar glass substrates and their nematic textures were investigated. The LC polymers consist of an acrylate or a methacrylate main chain and a phenyl benzoate group as the mesogenic unit which is connected to the main chain via a flexible alkyl spacer composed of six CH_2 units. The material exhibit nematic LC state at temperatures higher than the glass temperature of the polymer.

The LC polymers were prepared by radical polymerization of the corresponding monomers in toluene. The molecular weight was controlled by the monomer and initiator concentrations. The preparation of the LC polymer brushes was carried out according to the “grafting from” technique: a self-assembled monolayer of azo-initiators was firstly immobilized on the substrate. Subsequently, radicals were generated via thermal decomposition of the initiator molecules and a radical polymerization on the surface was started in the presence of the vinyl monomers, which resulted in a layer of polymer chains chemically attached to the surface through the rest of the initiator molecules. LC polymer brushes with a thickness from a few nm to 230 nm were synthesized by varying the monomer concentration and the polymerization time.

All compounds (monomers, polymers, and brushes) were thoroughly characterized by NMR, IR spectroscopy, and thermal methods (DSC, TGA). The thickness of the LC polymer thin films (spin-coated films or brushes) was measured with Surface Plasmon Spectroscopy (SPS).

The LC polymer brushes were thick enough to allow for direct observation of the nematic textures with a polarizing microscope. The LC polymer brushes grown on untreated glass substrates exhibited irregular textures (“polydomains”). The domain size is in the range of some micrometers and depends only weakly on the brush thickness. Spin-coated films from the same LC polymer exhibit similar nematic textures as those of the terminally attached polymer samples. In accordance with previous studies we find that the domain size of the spin-coated films grows with time upon thermal annealing of the samples.

The investigations on the texture-temperature relationship of the LC brushes revealed that the brushes exhibit a surface memory effect, that is, the identical texture reappears after the LC brush sample has experienced a thermal isotropization or a solvent treatment, at which the nematic LC state has been completely destroyed. The surface memory effect is attributed to a strong anchoring of the orientation of the mesogenic units to heterogeneities at the substrate surface. The exact nature of the surface heterogeneities is unknown. Trivial explanations such as surface roughness or chemical heterogeneity can be ruled out as spin-coated films generated from the same LC polymers exhibit a completely different behavior. The size of the domains and the surface memory effect depend solely on the brush nature of the polymer molecules. Although this may be interesting from a theoretical point of view, such a strong coupling of the LC orientation to certain defects is not desired for practical applications. Aligned LC layers should show as few domains as possible since domain boundaries decrease the contrast in LC displays.

It was also noticed that the dark thick lines that surround a nematic domain disappear at a temperature just below the N-I transition, which might be a consequence of an anchoring transition at the film-air interface. The N-I transition temperature of LC polymer brushes was 2 – 3 °C higher than that of spin-coated films. The increase in the transition temperature may be attributed to the chain stretching of the polymer backbones which stabilizes the nematic phase.

Phase diagrams of the LC polymer and a low molecular weight (LMW) nematic with similar chemical structure (ZLI-1052) showed that the two substances are partially miscible. At room temperature there is, however, a miscibility gap for polymer contents less than 50% in spite of the fact that ZLI-1052 has the same mesogenic unit as the LC polymers. Based on the phase diagrams, a maximum swelling of the LC polymer brushes by the LMW nematic to twice the dry thickness is expected.

The domain size increased several times after the LC brushes were swollen with the nematic ZLI-1052. The texture of the swollen brushes can be transferred to the adjacent LMW nematic phase, that is, the brush and the nematic bulk exhibit the same texture. The surface memory effect was observed for the swollen brushes as well, i.e., thermal isotropization does not change the textures of the swollen brushes.

Rubbing the glass substrate with a piece of velvet cloth prior to the surface modification with the initiator and the brush growth is an effective procedure to generate an in-plane anisotropy on the substrate which gives rise to the formation of homogenous alignment

of the mesogenic units in the LC polymer side chains. Monodomain textures were obtained for LC brushes grown on the rubbed substrates.

The mechanism of the homogeneous alignment was investigated. Grooves formed by rubbing or transfer of fibrils to the substrate surface are possible candidates. The rubbed substrates were treated with Piranha solution or UV light and the brushes were then grown. Both treatments are able to remove textile fibrils that might be transferred to the surface. The monodomain character is completely lost for brushes which are grown on rubbed substrates after subsequent Piranha treatment, which is a first indication that the alignment is induced by fibrils generated during the rubbing. A weakly irradiated substrate loses the monodomain character partly and a strongly irradiated substrate loses the character completely. Since photo-ablation is a rather gentle process, geometrical grooves would not be damaged. It can be concluded that the mechanism for the alignment is based on the transfer of the Nylon fibers, not on the formation of grooves.

LC cells filled with ZLI-1052 were prepared from substrates that were modified with brush monodomains. Crystal Rotation Setup (CRS) measurements carried out on the cells revealed that the LMW nematic molecules are uniformly aligned in the bulk (tilt angle $\alpha = 0°$). The LC polymer brush monodomains induce homogeneous planar orientation in LMW nematics. They can be used as alignment layers

Rubbing the substrate and covering of the surface with a thin layer of surfactant molecules are two conventional methods to induce planar and homeotropic alignments, respectively. In a series of experiments the surfactant dimethyloctadecylchlorosilane was mixed with the azo-initiator used for the brush generation on rubbed substrates. LC polymer brushes grown on such a substrate exhibited biaxial optical properties, that is, the three refractive indices along the three principle axes have different values. Hybrid LC cells made from a substrate modified with biaxial brushes and a rubbed glass substrate show an orientation with a tilt angle of $\alpha = -15.6°$).

This work shows that LC brushes grown on rubbed surfaces fulfill the important criteria for alignment layers. They can form macroscopic monodomains and they are able to transfer this orientation into the adjacent LMW nematics. First results indicate that by diluting the brush with molecules which are also covalently bound to the surface but induce a different orientation, a system is obtained in which the two conflicting alignment mechanisms to generate a tilted alignment. Such a cell is interesting from a technological point of view. In order to allow for an application of the alignment layers into a potential product, subsequent work should focus on the questions how easy and in which range the tilt angle can be controlled.

Literature

[Alex77] S. Alexander, *J. Phys. (Paris),* **38** (1977), 997; **38** (1977)983

[Arno60] H. Arnold, H. Sackmann, *Z. phys. Chem.,* **213** (1960), 137; **213** (1960), 145

[Aust94] E. F. Aust, S. Ito, M. Sawodny, W. Knoll, *Trends in Polymer Science,* **2** (1994), 313

[Baha90] B. Bahadur,ed., *Liquid Crystals and Uses,* World Scientific, Singapore**,** 1990

[Benm99] F. Benmouna, B. Peng, J. Rühe, D. Johannsmann, *Liq. Cryst.,* **26** (1999), 1655

[Benm00] F. Benmouna, B. Peng, J. Gapinski, A. Patkowski, J. Rühe, D. Johannsmann, *Phys. Rev. E,* submitted (2000)

[Bent85] H. Benthack-Thoms, H. Finkelmann, *Makromol. Chem.,* **186** (1985), 1895

[Berr73] D. W. Berrman, *Mol. Cryst. Liq. Cryst.,* **23** (1973), 215

[Bies99] M. Biesalski, *Dissertation,* Johannes Gutenberg-Universität Mainz, 1999

[Bill84] F. W. Billmeyer, Jr., *Textbook of Polymer Science*, 3rd edition, Wiley-Interscience, 1984

[Böef89] C. Böeffel, H. W. Spiess, in McArdle ed., *Side Chain Liquid Crystal Polymers, Ch.8,* Blackie, 1989

[Bove91] G. Boven, R. Folkersma, G. Challa, A. J. Schouten, *Polymer,* **32** (1991), 50

[Chan92] S. Chandrasekhar, *Liquid Crystals, 2nd ed.,* Cambridge University Press, 1992

[Chen89] W. Chen, M. B. Feller, Y. R. Shen, *Phys. Rev. Lett.,* **63** (1989), 2665

[Chie98] E. Chiellini, M. Laus, in D. Demus, J. Goodby, G. W. Gray, H. W. Spiess, V. Vill, eds., *Handbook of Liquid Crystals, Vol.3, Ch.2,* Wiley-VCH, 1998

[Clar85] N. A. Clark, *Phys. Rev. Lett.,* **55** (1985), 292

[Cogn82] J. Cognard, *Mol. Cryst. Liq. Cryst.,* **Suppl. 1** (1982), 1

[Coll97] P. J. Collings, M. Hird, *Introduction to Liquid Crystals,* Taylor & Francis, London, 1997

[deGe75] P. G. De Gennes, *C. R. Acad. Sci. Paris*, **281** (1975), 101

[deGe76] P. G. de Gennes, *J. Phys. (Paris)*, **37** (1976), 1443

[deGe80] P. G. de Gennes, *Macromolecules*, **13** (1980), 1069

[deGe93] P. G. De Gennes, J. Prost, *The Physics of Liquid Crystals*, Oxford University Press, 1993

[Demu98] D. Demus, J. Goodby, G. W. Gray, H. W. Spiess, V. Vill, eds., *Handbook of Liquid Crystals, Vol.3*, Wiley-VCH, 1998

[Faet91] S. Faetti, in I. Khoo, F. Simoni, eds. *Physics of Liquid Crystalline Materials*, Gordon & Breach, 1991

[Fink78] H. Finkelmann, H. Ringsdorf, J. H. Wendorff, *Makromol. Chem.*, **179** (1978), 273

[Fink82] H. Finkelmann, H.-J. Kock, G. Rehage, *Mol. Cryst. Liq. Cryst.*, **89** (1982), 23

[Fink84] H. Finkelmann, G. Rehage, *Adv. Polym. Sci.*, **60/61** (1984), 99

[Frei70] M. J. Freiser, *Phys. Rev. Lett.*, **24** (1970), 1041

[Gray89] G. W. Gray, in C. B. McArdle ed., *Side Chain Liquid Crystal Polymers, Ch.4*, Blackie, 1989

[Grei98] A. Greiner, H. W. Schmidt, in D. Demus, J. Goodby, G. W. Gray, H. W. Spiess, V. Vill, eds., *Handbook of Liquid Crystals, Vol.3, Ch.1*, Wiley-VCH, 1998

[Habi98] J. Habicht, *Dissertation*, Johannes Gutenberg-Unversität Mainz, 1998

[Halp93] A. Halperin, D. R. M. Williams, *Europhys. Lett.*, **21** (1993), 575

[Halp94] A. Halperin, D. R. M. Williams, *J. Physics: Condens. Matter*, **A297** (1994), 6

[Hess86] F. Hessel, H. Finkelmann, *Polym. Bull.*, **15** (1986), 349

[Horv85] J. Horváth, K. Nyitrai, F. Cser, Gy. Hardy, *Eur. Polym. J.*, **21** (1985), 251

[Jérô91] B. Jérôme, *Rep. Prog. Phys.*, **54** (1991), 391

[Jérô98] B. Jérôme, in *Handbook of Liquid Crystals, Vol. 1, Chapter 10*, D. Demus, J. Goodby, G. W. Gray, H. W. Spiess, V. Vill, eds., Wiley-VCH, 1998

[Kann93] R. M. Kannan, J. A. Korfield, N. Schwenk, C. Boeffel, *Macromolecules*, **26** (1993), 2050

[Kelk80] H. Kelker, R. Hatz, *Handbook of Liquid Crystals*, Verlag Chemie, 1980, and references therein.

[Knol91] W. Knoll, *MRS Bulletin*, **16** (1991), 28

[Kost82] S. G. Kostromin, R. V. Talroze, V. P. Shibaev, N. A. Platé, *Makromol. Chem. Rapid Commun.*, **3** (1982), 803

[Laib75] R. Laible, K. Hamann, *Angew. Makromol. Chem.*, **48** (1975), 97

[Lest95] G. Lester, J. Hanmer, H. Coles, *Mol. Cryst. Liq. Cryst.*, **262** (1995), 149

[Mark85] H. F. Mark, N. M. Bikales, C. G. Overberger, G. Menges, *Encyclopedia of Polymer Science and Engineering, Vol.1,* 2nd Ed. Wiley-Interscience, 1985

[Maug11] C. Mauguin, *Bull. Soc. Fr. Min.*, **34** (1911), 71

[McAr89] C. B. McArdle ed., *Side Chain Liquid Crystal Polymers*, Blackie, 1989

[Mete73] J. P. van Meter, B. H. Klanderman, *Mol. Cryst. Liq. Cryst.*, **22** (1973), 271

[Mura93] M. Murakami, H. Fujii, *Mol. Cryst. Liq. Cryst.*, **225** (1993), 259

[Mura00] H. Murata, J. Rühe, submitted for publication.

[Nehr72] J. Nehring, A. Saupe, *J. Chem. Soc., Faraday Trans.-II,* **68** (1972), 1

[Neöl98] C. Neöl, in *Handbook of Liquid Crystals, Vol. 3, p.93,* D. Demus, J. Goodby, G. W. Gray, H. W. Spiess, V. Vill, eds., Wiley-VCH, 1998

[Neub80] M. E. Neubert, L. T. Carlino, D. L. Fishel, R. M. D'Sidocky, *Mol. Cryst. Liq. Cryst.*, **59** (1980), 253

[Odia91] G. Odian, *Principles of Polymerization*, 3rd ed., Wiley, (1991), Chapter3.

[Peng99] B. Peng, D. Johannsmann, J. Rühe, *Macromolecules*, **32** (1999), 6759

[Peng00] B. Peng, J. Rühe, D. Johannsmann, *Adv. Mater.*, accepted (2000)

[Perc89] V. Percec, C. Pugh, in C. B. McArdle, ed., *Side chain liquid crystal polymers, Chapter 3*, Blackie, Glasgow, 1989

[Perc89] V. Percec, D. Tomazos, C. Pugh, *Macromolecules*, **22** (1989), 3259

[Pett00] M. C. Petty, in T. H. Richardson ed. *Functional Organic and Polymeric Materials, Ch. 2*, John Wiley, 2000

[Port82] M. Portgall, H. Ringsdorf, R. Zentel, *Makromol. Chem.*, **183** (1982), 2311

[Pruc95] O. Prucker, *Ph. D. thesis*, Universität Bayreuth, 1995

[Pruc98] O. Prucker, J. Rühe, *Macromolecules*, **31** (1998), 592; **31** (1998), 602

[Raja96] V. N. Raja, D. S. S. Rao, S. W. Kang, J. C. Lee, S. S. Lee, S. H. Jin, *Liq. Cryst.*, **20** (1996), 41; *Mol. Cryst. Liq. Cryst.*, **287** (1996), 169

[Rühe94] J. Rühe, *Nachr. Chem. Tech. Lab.*, **42** (1994), 1237

[Rühe00] J. Rühe, W. Knoll, in C. Cifferni ed., *Supramolecular Chemistry,* in press.

[Rysc76] G. Ryschenkow, M. Kleman, *J. Chem. Phys.,* **64** (1976), 404

[Schä89] J. Schätzle, W. Kaufhold, H. Finkelmann, *Makromol. Chem.,* **190** (1989), 3269

[Sche77] T. J. Scheffer, J. Nehring, *J. Appl. Phys.,* **48** (1977), 1783

[Schi95] M. Schimmel, *Diplomarbeit,* Universität Bayreuth, 1995

[Schi98] M. Schimmel, *Dissertation,* Johannes Gutenberg-Universität Maniz, 1998

[Shib84] V. P. Shibaev, N. A. Platé, *Adv. Polym. Sci.,* **60/61** (1984), 173

[Shiw90] T. Shiwaku, A. Nakai, H. Hasegawa, T. Hashimoto, *Macromolecules,* **23** (1990), 1590

[Skor93] S. S. Skorokhodov, in N. A. Platé , eds., *Liquid Crystal Polymers, Ch.5,* Plenum, 1993

[Teix93] P. I. C. Teixia, T. J. Slucken, D. E. Sullivan, *Liq. Cryst.,* **14** (1993), 1243

[Thom85] E. L. Thomas, B. A. Wood, *Faraday Discuss. Chem. Soc.,* **79** (1985), 229

[Uchi92] T. Uchida, H. Seki, in *Liquid Crystals: Application and Uses, Vol. 3, Chapter 5,* B. Bahadur ed., World Scientific, 1992

[Wahl79] E. Wahlstrom, *Optical Crystallography*, 5th edition, John Wiley and Sons, 1979

[Will96] D. R. M. Williams, A. Halperin, *Prog. Polym Sci.,* **21** (1996), 1089

[Witt91] J. C. Wittmann, P. Smith, *Nature*, **352** (1991), 414

[Witt96] M. M. Wittebrood, D. H. Luijendijk, S. Stallinga, T. Rasing, I. Musevic, *Phys. Rev.,* **A54** (1996), 5232

[Wood86] B. A. Wood, E. L. Thomas, *Nature,* **324** (1986), 655

[Yoko88] H. Yokoyama, *Mol. Cryst. Liq. Cryst.,* **165** (1988), 265

[Zent84] R. Zentel, H. Ringsdorf, *Makromol. Chem., Rapid Commun.,* **5** (1984), 393

Danksagungen

An dieser Stelle möchte ich allen meinen aufrichtigen Dank aussprechen, die durch ihre Unterstützung oder Anregungen zur Durchführung und zum Gelingen dieser Arbeit beigetragen haben:

Herrn Prof. Dr. Wolfgang Knoll für die herzliche Aufnahme in seine internationale Arbeitsgruppe, die Möglichkeit, dieses faszinierende Thema am MPI für Polymerforschung bearbeiten und für mich ein ganz neues Land und ganz neue Kulturen kennenlernen zu können.

Herrn Prof. Dr. Jürgen Rühe für seine hervorragende fachliche und freundschaftliche Betreuung, die ausgiebigen fachlichen Diskussionen zu jeder Tages- und Nachtzeit und seine sorgfältige Durchsicht des Manuskripts. Ohne seine immer neuen Ideen und zahllosen Anregungen wäre diese Arbeit nicht möglich gewesen.

Herrn Dr. habil. Diethelm Johannsmann für seine immer „offene“ Bürotür für Diskussionen und Anregungen. Seine Stets Interesse und seine Ideen waren ein Grundstock für diese Arbeit.

Herrn Dr. Oswald „Ossi“ Prucker für seine Diskussion an Seminaren, seine Breitschaft für fachliche Fragen und seine sorgfältige Durchsehen des Manuskripts.

Teresa Siepchen gilt ein besonderer Dank für ihre großartige Unterstützung in der Laborarbeit und zahllose Messungen. Von den vielen hilfreichen Händen möchte ich stellvertretend Gretl Dworschak und Martina Knecht dankend erwähnen.

Farida Benmouna für die fruchtbare Zusammenarbeit bei der Untersuchung zu Übergangstemperaturen verschiedener Mischungen von LC Polymeren-Nematen.

Für die schöne Atmosphäre im Büro, die Breitschaft für meine vielen Fragen und die Diskussionen über Computer Programme, die deutsche Sprache sowie die für mich sehr fremd europäischen Kulturen möchte ich Stephan Krämer, Max Kreiter, Christoph Spößler, Marc Hamdorf und José Luis Hernández-López danken.

Torsten Stöhr, Hironobu Murata und Stefen Schiller für die schöne Atmosphäre im Labor und die Diskussionen über zahlreiche chemische Reaktionen und Spektren.

Thomas Lehmann, Jörg Habicht, Marcus Bisalski, Martin Schimmel, Ulrike Hees, Martin Gelbert und Alex Laschitsch für die fruchtbare Diskussionen an Seminaren und die Hilfe an Bedienung von Geräten.

Die Kollegen, die mit mir in der Inter-Bar bzw. in Kneipen der Mainzer-City waren. An diesen Abenden, übers Bier, habe ich nicht nur mein gesprochenes Deutsch bzw. Englisch viel verbessert, auch vieles über die Kultur, die Sitten und Gebräuche kennengelernt.

Allen aktuellen und ehemaligen „Knollies“ möchte ich ein „Xiexie“ aussprechen: für die tolle Atmosphäre, die stets Hilfs- und Diskussionsbereitschaft und die vielen nette Erinnerungen während meiner Promotionszeit.

Mein ganz besonderer Dank gilt meinen Eltern für die liebevolle moralische Unterstützung während der Promotion und während des gesamten Studiums.

Schließlich danke ich ganz besonderes meiner Frau Liping Luo und meinem Kind Youlin für die Hilfe und Unterstützung.